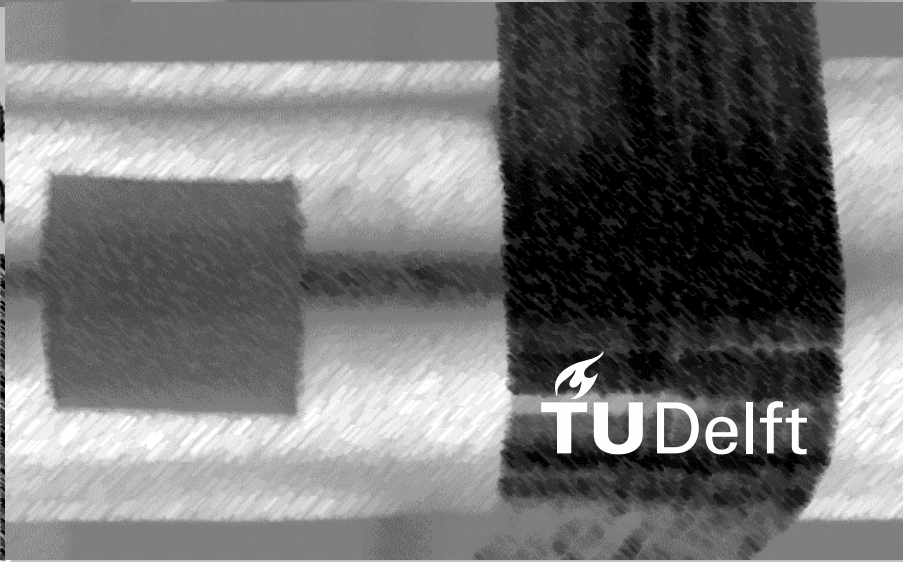
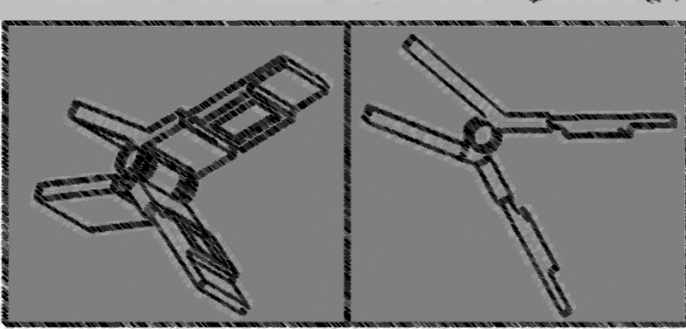
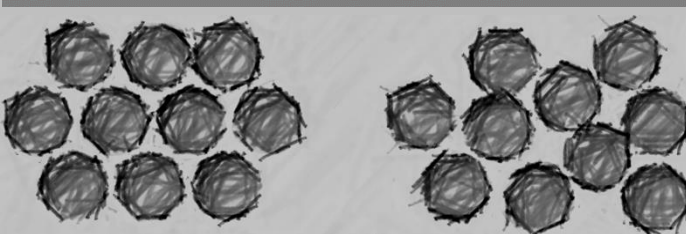
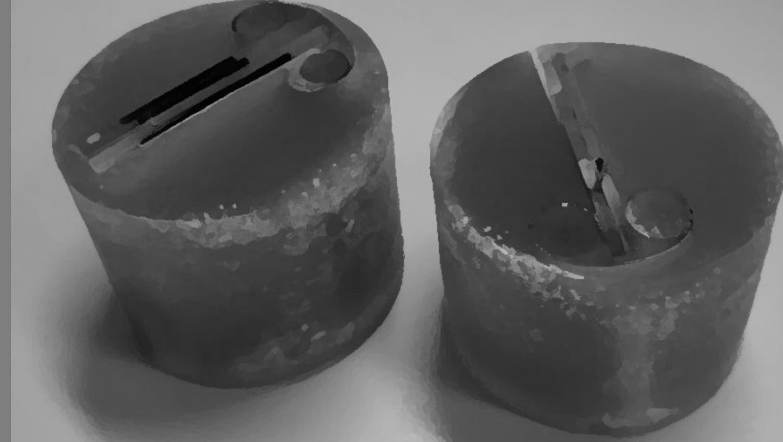
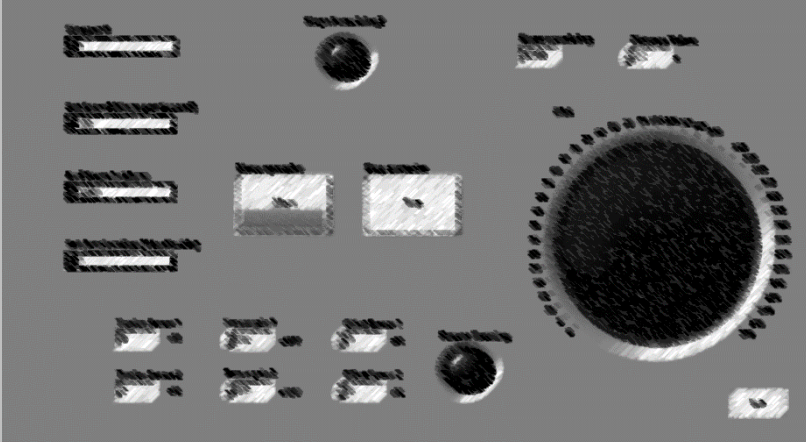


# MICROSTRUCTURE FORMATION IN TOW SPREADING

Palak Singh



# Microstructure Formation In Tow Spreading

Palak Singh

Student number: 5115191

in partial fulfilment of the requirements for the degree of

**Master of Science**

in Aerospace Engineering

at the Delft University of Technology,  
to be defended publicly on Wednesday, 17.11.21 at 13:00.

An electronic version of the thesis is available at <http://repository.tudelft.nl/>.

DELFT UNIVERSITY OF TECHNOLOGY  
FACULTY OF AEROSPACE ENGINEERING  
DEPARTMENT OF AEROSPACE STRUCTURES AND MATERIALS

**GRADUATION COMMITTEE**

Date: 17 November 2021

Chair holder: \_\_\_\_\_

Prof. Clemens Dransfeld

Committee members: \_\_\_\_\_

Prof. Clemens Dransfeld

\_\_\_\_\_

Dr. Bilim Atli-Veltin

\_\_\_\_\_

Dr. Baris Caglar

\_\_\_\_\_

Dr. Daniel Peeters

\_\_\_\_\_

Dr. Wilko Happach

I HAVE NO IDEA WHAT I'M SUPPOSED TO DO. I ONLY KNOW WHAT I CAN DO.

-CAPTAIN JAMES T. KIRK

# ACKNOWLEDGEMENTS

---

This report summarises the past year of work done for my master of science thesis. This thesis gave me an opportunity to show and implement some valuable learnings obtained during my time at TU Delft. A significant portion of my research was done during the Covid 19 pandemic and while the whole experience was new and challenging, I feel I come out of it a stronger and more independent woman.

This project was far from a one-man job and I was fortunate to have an excellent support system around me. I would like to express an immense amount of gratitude to my supervisors Clemens Dransfeld, Bilim Atli-Veltin and Baris Caglar for their patience, their ideas and their constant support while I navigated through the challenges of my research. I would also like to thank Marianne de Knecht-Overduin for all her help and for being so kind when I made mistakes. A big thank you to Alexander Uithol, Berthil Grashof, Fred Bosch, Durga Mainali, Victor Horbowiec and all the other staff of the DASML lab. A special mention to Alexander for his constant encouragement during my thesis and great conversations about politics, food and the Dutch culture.

Furthermore, I am grateful to my family for their unconditional support and their constant reminders that I was loved and missed. I want to thank Huub (primadonna) Urselmann, Yerik Singh, Gisela Rosado Bailon, Arshdeep Singh Brar, Irene Solbes Ferri, Ranjan Gaur, and all the other wonderful friends I made for always helping and cheering me on. I owe all of you a big bear hug. A big thank you to Dr. Parvez Imam for being the most chill adult I know and to his daughters for brightening up my days during a rather difficult phase. Lastly, I would like to thank Martijn and Poppie for being the best part of my day, every day.

*Palak Singh*

*Delft, November 2021*



Tow spreading is a process of flattening fibre tows into thinner and wider tapes that increases resin impregnation, lowers void content in impregnated tows and produces lightweight composites with improved mechanical performance. There are several techniques to spread fibre bundles ranging from using induced forces through mechanical elements to using air jets, vibrations and corona discharges.

The majority of tow spreading technology however is owned by companies in the form of intellectual property and patents thus limiting the scientific understanding of the process. This aspect leaves tow spreading open as a field of research for exploration and investigation. While some previous studies focused on understanding the behaviour of tow spreading, the applicability of these studies has so far been limited in their experimental apparatus. These studies identified the gap that exists between the sophisticated industrial technology and the research setups providing an incentive to further develop an experimental facility that generates a deeper understanding of the current industrial practices in tow spreading.

The objective of this study was divided into three parts: i) to develop a reliable and controllable mechanical tow spreader, ii) gain a better understanding of the influence of spreading parameters on spreading behaviour through experimental investigation and iii) developing a technique to generate spread tow specimens for microstructural investigation.

In this research, a mechanical tow spreader was developed that utilizes cylindrical spreader bars to facilitate the spreading of fibres. The spreader consists of three main units: the unwinding unit, the spreading unit and the winding unit. The unwinding unit consists of the material spool attached to a mechanical brake which generates pretension in the fibre tow. The spreading unit consists of topocrom coated spreader bars that are the main components responsible for the spreading of fibres. The winding unit consists of an empty spool for winding the fibre tow. The tow spreader's performance was evaluated by observing whether the spreading output was controllable and repeatable. The material used for studying the spreader was Toray T700SC 24k 50C.

Development of the tow spreader was followed by an experimental analysis where different input parameters were isolated to check for their influence on spreading behaviour. A sample size of 5 spreader runs was used and the spreading width was captured through a camera. It was found that tension, spreader bar orientation, heat and speed have the biggest influence on the spreading behaviour. An increase in pretension (218 to 318 cN) induced by the mechanical brake increased the final tension (2100 to 2900 cN) in the tow but it did not appear to influence the spreading behaviour of the fibres. When testing the effect of each spreader bar on the amount of spread, it was found that *five* spreader bars were sufficient to achieve spreading stability. Another relationship was observed between the wrap angles of the tow with the bar and the spreading behaviour. An increase in wrap angles (252 to 732°) led to an increase in spreading width (9 to 14 mm). A friction study on the interaction between spreader bars and tow was done by adopting the Coulomb friction model and the coefficient of friction distribution was observed between 0.2-0.25. Three spreader bars were heated up to a temperature of 125°C that led to an increment in spreading width from 14 mm to 18.5 mm. Lastly, the winding speed was tested for its influence on spreading width and it is found that with

an increase in winding speed (60 to 240 RPM), the spreading width increased by a small amount (14.3 to 15.8 mm).

Following the experimental analysis, a microstructural investigation of spread tow followed. Five spread tow samples were generated by using a 3d printed mould that clips onto the tow in spreader on-site and was observed under a confocal microscope. The microstructural investigation of spread tow allowed for visualisation of fibre distribution evolution as the tow becomes wider and thinner. Image processing of cross-sectional photographs of the spread tow samples yielded detailed heatmaps of fibre distribution. From this, it was found that that the unspread tow is approximately elliptical but as it is spread and flattened, it transforms into a rectangular shape of increasingly sparse and uniform fibre distribution.

In conclusion, this study creates research questions and directions for further experimentation to understand the influence of spreader parameters on spreading and the interdependency of these parameters on each other. Additionally, with a technique to develop samples for microstructural investigation; an opportunity to observe the changes in spreading behaviour on fibre level is created which implies that the spreading behaviour that was previously observed on a mesostructural level in the current research can now be investigated on a microstructural level too.





# TABLE OF CONTENTS

---

LIST OF FIGURES .....	xii
LIST OF TABLES .....	xvi
<b>1 Introduction .....</b>	<b>1</b>
1.1 Background .....	1
1.2 State of the art .....	4
1.2.1. Tow spreading techniques.....	4
1.2.2. Mechanics of fibre tows .....	17
1.2.3. Spreading on a microstructural level.....	19
1.2.4. Analysis of spreading parameters.....	21
1.3 Research questions and thesis objective .....	28
1.3.1. Research questions .....	29
1.3.2. Thesis objective .....	32
<b>2 Methodology .....</b>	<b>33</b>
2.1 Development of a tow spreader.....	33
2.1.1 The base design of the spreader .....	33
2.1.2. Upgraded setup, its validation and flow of operation .....	34
2.1.3. Flow of operation .....	39
2.2 Experiment methodology.....	41
2.3 Microstructure specimen generation.....	43
2.3.1 Sample quality assessment.....	43
2.3.2. Embedding techniques for sample generation.....	44
2.3.3. Selected embedding technique.....	47
<b>3 Experimental analysis of spreading parameters .....</b>	<b>49</b>
3.1 Parameters evaluated .....	49
3.2 Repeatability.....	50
3.3 Unwinding unit .....	51
3.3.1 Translation of pretension from the mechanical brake settings.....	51
3.3.2. Tension variation along the length of the material spool .....	52
3.3.3. Influence of pretension on spreading behaviour .....	53
3.4. Spreading unit .....	55
3.4.1. Influence of number of bars on spreading behaviour .....	55
3.4.2. Rotating and fixed bars.....	57

3.4.3.	Influence of wrap angle on spreading behaviour .....	57
3.4.4.	Determining the coefficient of friction between tow and spreader bars .....	60
3.4.5.	Influence of length between spreader bars on spreading behaviour .....	65
3.4.6.	Influence of heat on spreading behaviour .....	66
3.5.	Winding unit .....	71
3.6.	Statistical analysis .....	72
3.7.	Summary .....	75
4	Microstructural analysis of spread tow specimens .....	76
4.1.	Evaluation of specimen's image quality .....	76
4.2.	Setup for spreading visualisation .....	78
4.3.	Spread tow microstructure .....	79
5	Conclusions .....	83
6	Recommendations for future work .....	85
A.	Tow spreader components/external tools and their specifications .....	87
B.	Spreader troubleshooting key points .....	88
C.	R squared values of individual parameters .....	92
D.	Fibre distribution plots for each sample .....	99
E.	Post-processing codes in python .....	105
F.	Raw data and processing files .....	117
	References .....	118



# LIST OF FIGURES

---

Figure 1.1: Composite formation [1] .....	1
Figure 1.2: Types of composite reinforcements [3].....	2
Figure 1.3: Role of fibre length on composite performance [2] .....	2
Figure 1.4: Fibre tow being spread [4].....	2
Figure 1.5: Tensile performance of spread tow [8] .....	3
Figure 1.6: Spreading of tow into a flat profile [10].....	4
Figure 1.7: Air flow through fibres during spreading [10] .....	5
Figure 1.8: Spreading of tow through suction [13].....	5
Figure 1.9: Spreading with vibrating bars [16].....	6
Figure 1.10: Spreader using speaker pulsations [20].....	8
Figure 1.11: Spreading through electrostatic energy [23].....	9
Figure 1.12: Example of a spreader bar configuration [28].....	11
Figure 1.13: Profile of convex roller for spreading via fanning effect [32] .....	13
Figure 1.14: Convex profile vs straight profile action on the degree of spreading .....	13
Figure 1.15: A rotatable wheel with a multibar configuration [34].....	14
Figure 1.16: Expandable wheel schematic with elastic rods/tapes [36].....	15
Figure 1.17: Carbon fibre on a) Microscale b) Mesoscale c) Macroscale [38].....	17
Figure 1.18: Ideal fibre lattice vs real packing .....	19
Figure 1.19: Amir’s representation of two fibres in tow at different heights [4] .....	20
Figure 1.20: Irfan’s representation of fibres in tow at different heights [26] .....	20
Figure 1.21: Side view of Wilson’s experimental setup [26].....	21
Figure 1.22: The fibre tow is fixed at O and goes over the spreader bar O’x which is visualised as a thin blade. PP’ is a random single fibre in the tow. [27].....	22
Figure 1.23: Geometric parameters in Amir’s study [29] .....	25
Figure 1.24: Interaction flowchart of parameters in mechanical tow spreading .....	26

Figure 2.1: Approach for developing the tow spreader.....	34
Figure 2.2: Developed tow spreader design .....	34
Figure 2.3: Unwinding unit with mechanical brake [48] and fibre spool.....	35
Figure 2.4: Spreading unit with spreader bars, positioning pieces [48] tension meters [49].....	35
Figure 2.5: Spreader bar arrangement .....	36
Figure 2.6: Construction of heated spreader bar .....	36
Figure 2.7: Winding unit of the tow spreader.....	37
Figure 2.8: Colour blocking 5 <sup>th</sup> spreader bar for tow width calculation .....	38
Figure 2.9: LabVIEW program for tow spreader .....	39
Figure 2.10: Operational flow of the tow spreader .....	40
Figure 2.11: Drawing of mould for capturing tow in resin.....	47
Figure 2.12: 3d printed mould and sample generated .....	47
Figure 2.13: Clarity of microstructural image .....	48
Figure 2.14: Locations for microstructure samples captured .....	48
Figure 3.1: A general categorisation of spreader parameters tested.....	49
Figure 3.2: Repeatability of results .....	50
Figure 3.3: Induced pretension in tow via a mechanical brake .....	51
Figure 3.4: Fibre unwinding from the spool is passed through a thread positioning piece .....	52
Figure 3.5: Pretension variation along the length of the spool .....	53
Figure 3.6: a): Influence of pretension on spreading b): Spread width-tension distribution for pretension .....	53
Figure 3.7: Representation of spreading unit .....	55
Figure 3.8: Setup for testing the influence of the number of bars .....	55
Figure 3.9: Spreading relationship with the number of bars.....	56
Figure 3.10: Tension output with fixed and rotating bars .....	57
Figure 3.11: Representation of wrap angles in spreader bars [50] .....	57
Figure 3.12: a) Bars orientation 1 b) Bars orientation 2 c) Bars orientation 3.....	58

Figure 3.13: a) Influence of wrap angles on spreading b) Spread width-Tension distribution for wrap angles .....	59
Figure 3.14: Analysis of friction in the tow during spreading .....	60
Figure 3.15: Schematic of a belt wrapped over a cylinder .....	60
Figure 3.16: Schematic of a very small slice of belt over the rod .....	61
Figure 3.17: Schematic of a spreading unit to calculate tension ratios.....	61
Figure 3.18: Influence of input parameters on coefficient of friction .....	63
Figure 3.19: Influence of length between bars on spread width.....	65
Figure 3.20: Schematics of number of heated bars placement in spreading unit (heated bar = yellow) .....	67
Figure 3.21: Influence of number of heated bars on spreading .....	67
Figure 3.22: Influence of temperature on spreading width .....	68
Figure 3.23: Schematics of different arrangements of heated bars in the spreading unit .....	70
Figure 3.24: Influence of arrangement of heated bars on spreading.....	70
Figure 3.25: a) Influence of winding speed on spreading b) Spread width- tension distribution for winding speed .....	71
Figure 4.1: Fibres in ideal state (homogeneous and straight) (left) and real state (inhomogeneous and tortuous) (right) [55] .....	76
Figure 4.2: Close up of a microscopic image of tow sample.....	77
Figure 4.3: a) Fibre distribution plot (top) b) Image displaying tow microstructure (middle) .....	77
Figure 4.4: a) Original image displaying tow microstructure b) Threshold binary image c) Close up of the binary image .....	78
Figure 4.5: Evolution of spreading visualised through fibre distribution .....	79
Figure 4.6: Heatmap and histogram of a) Unspread tow – 8 mm b) Spread tow – 14.2 mm .....	81
Figure B.1: Cyclic unwinding of tow from the material spool.....	88
Figure B.2: Schematic of tow interaction with thread positioning piece .....	89
Figure B.3: Tension meter(s) accuracy check.....	90
Figure B.4: Signal output from the laser sensor .....	90
Figure D.1: 8 mm unspread tow microstructure .....	100

Figure D.2: 10 mm spread tow microstructure.....	101
Figure D.3: 12.5 mm spread tow microstructure.....	102
Figure D.4: 13.5 mm spread tow microstructure.....	103
Figure D.5: 14.2 mm spread tow microstructure.....	104



## LIST OF TABLES

---

Table 1: Comparative analysis of different spreading elements .....	16
Table 2: A summary of results in Irfan’s study.....	24
Table 3: Baseline input parameters of tow spreader .....	41
Table 4: Experiment approach for evaluation of input parameters .....	42
Table 5: List of embedding techniques evaluated for microstructural sample generation.....	46
Table 6: R square for input spreading parameters for 25 data sets (left) and 125 data sets (right) ....	72
Table 7: Coefficients of input parameters for 25 data sets (left) and 125 data sets (right) .....	73
Table 8: R square data for each input spreading parameter .....	74
Table 9: Specifications of spreader components.....	87
Table 10: R square values of individual parameters .....	94
Table 11: Input data for regression analysis with 25 data sets.....	95
Table 12: Input data for regression analysis with 125 data sets.....	98



# 1 Introduction

---

In this chapter, a brief introduction to the process of tow spreading is presented along with its advantages in composite structures, its industrial applications and the necessity it creates for a scientific investigation. This is followed by the state of the art comprising of the current spreading techniques with a focus on mechanical spreading, a description of mechanics of fibres tows during the spreading process, their interaction on a microstructural level and an analysis of the spreading parameters. In the end, the research objective of this thesis is defined based on the research questions that highlight the scope of this study.

## 1.1 BACKGROUND

A composite comprises two or more materials that are used in combination to produce properties in a structure otherwise difficult to obtain with a single homogeneous material. Structural composites consist of reinforcements embedded in a matrix (Figure 1.1) where the reinforcements (fibres) are the main source of stiffness and strength and the matrix binds them together while supplying good shear properties. In recent years, lightweight composites have become increasingly popular in several industries for the benefits they offer such as high strength to weight ratio, cost efficiency, tailorable properties and superior mechanical performance.

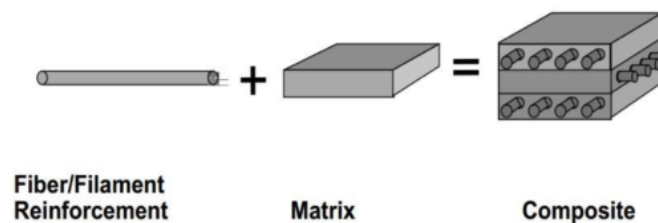


Figure 1.1: Composite formation [1]

Several types of reinforcements are available in the industry and they can be broadly classified into particles, discontinuous fibres, continuous unidirectional fibres and textiles (Figure 1.2). Selection of the appropriate reinforcement is done on basis of the properties they offer. Figure 1.3 shows such different qualities as a function of the length of the fibres. As the fibre length increases, the modulus, strength and impact performance of the fibres can be expected to increase but the processibility decreases. This means that for continuous fibres, the mechanical performance is higher but they are more complex to process as opposed to discontinuous fibres that have a significantly smaller length [2].

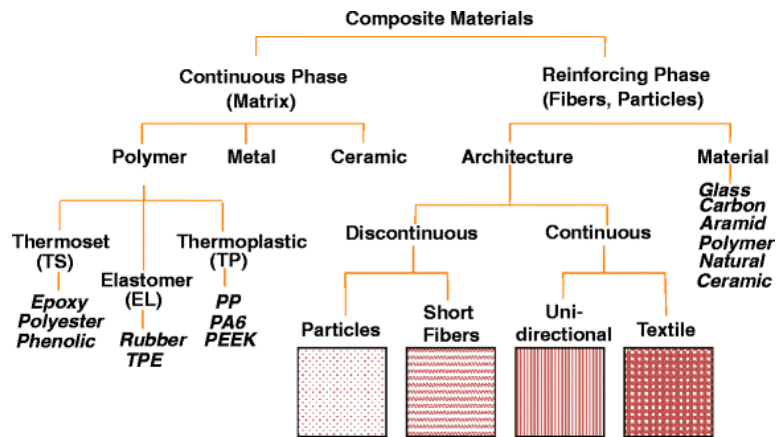


Figure 1.2: Types of composite reinforcements [3]

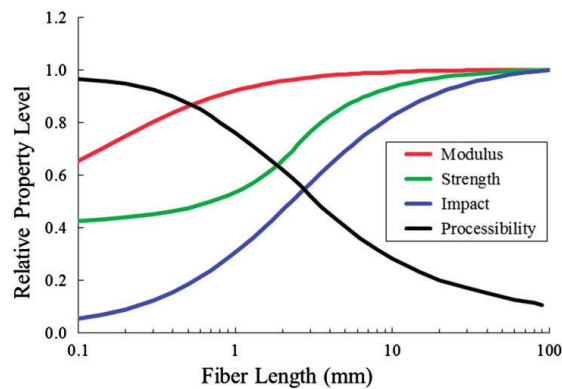


Figure 1.3: Role of fibre length on composite performance [2]

This demonstrates that continuous fibres in comparison to its competitors are a well-suited reinforcement option for structures demanding high mechanical performance. This mechanical performance, however, can further be improved by turning continuous fibres tows into ‘spread tapes’ by the method of tow spreading. Tow spreading is a process in which the filaments in a fibre tow are spread to create wider and thinner tapes and by consequence have a lower aerial weight (Figure 1.4). Areal weight in this context is defined as the weight of the tow per unit area.



Figure 1.4: Fibre tow being spread [4]

Woven fabrics made of spread tow were found to have improved impregnation, lower void content and reduced resin-rich areas in composites [5] compared to unspread tow fabrics. In terms of mechanical performance, Kim and Soni [6] researched the failure of composites made of thin and thick plies and concluded that thin plies had a higher threshold of delamination compared to thick ply composites. Another study done by Shin et al. [7] stated that the spread tow composites were more resistant to microcracks, delamination and damage. Furthermore, an investigation conducted by Morii et al. [8] on the performance of spread UHMWPE tow in comparison to unspread UHMWPE tow revealed that spread tows were found to have better tensile performance (Figure 1.5).

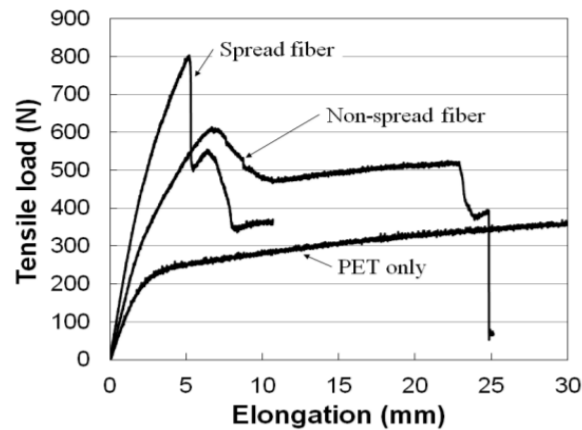


Figure 1.5: Tensile performance of spread tow [8]

Despite several studies showing the certain benefits of using spread tows; there are, however, limited studies centered around the process of tow spreading itself. A significant amount of the information and research on the development of tow spreading is owned by the companies providing this product as intellectual property or in the form of patents. This aspect leaves tow spreading open as a field of research for exploration and investigation. While some previous studies focused on understanding the process of tow spreading, the applicability of these studies has so far been limited in their experimental apparatus. These studies identified the gap that exists between the sophisticated industrial technology and the research setups hence providing an incentive to further develop an experimental facility that generates a deeper understanding of the current industrial practices in tow spreading.

This report presents the research conducted within the scope of the thesis. Chapter one introduces the field of tow spreading along with its significance followed by a literature study that analyses the past industrial and academic developments. Based on the findings of the literature study, the thesis objective is presented along with its research questions and corresponding goals. It is followed by chapter two that presents the details and functioning of the developed tow spreader, the methodology to conduct an experimental analysis on the spreading parameters and the concept of capturing spread tow for microstructural investigation. With an established methodology, chapter three presents the results of the experimental analysis of spreading parameters. Chapter four then presents the results of the microstructural investigation to visualise how the tow structure evolves during the spreading process. Based on the information in the aforementioned chapters, chapter five draws conclusions on the findings of this research and lastly, chapter six proposes recommendations for further optimization and investigation of the spreader and tow spreading behaviour.

## 1.2 STATE OF THE ART

Spread tow technology is defined as the practice of spreading fibre tows into wider and flatter tapes for further applications and uses in manufacturing lightweight composite structures (Figure 1.6). The state of art presented below begins with providing some insight into different spreading techniques. These techniques are classified based on the terminology proposed by Gizik et al. [9] as active or non-contact techniques and passive or contact techniques, as will be explained further in this chapter. It is followed by a special focus on mechanical tow spreading, which is a passive technique. An attempt has been made to describe the mechanics involved in a tow spreading process, influences acting on the spreading behaviour at a microstructural level and parameters that control the degree of spread.

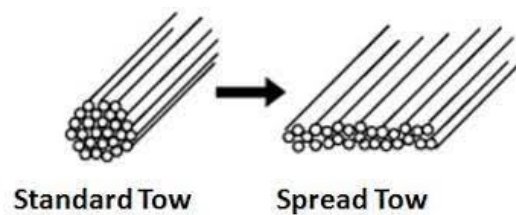


Figure 1.6: Spreading of tow into a flat profile [10]

### 1.2.1. Tow spreading techniques

Through the several patents and methods of spreading developed, Gizik et al. [9] analyzed the core techniques of spreading the fibres and broadly classified them into active methods, passive methods or a combination. Active methods are non-contact methods that use energy such as air, acoustic vibrations, electrostatic in a non-contact manner to aid the process of spreading whereas passive methods use mechanical forces induced in tow via contact. Active methods work without inducing high forces in the fibre tow as opposed to passive methods that need forces to enable spreading. Thus, active methods have a lower amount of fibre damage in their spreading process as was claimed by several patents that used an active spreading method. In this study, the focus has been given to passive techniques to narrow down the survey while deciding on adopting the most suitable spreading technique relevant to this thesis. The active techniques are described briefly for the sake of completeness in this study and to have an overall picture of the tow spreading developments.

#### A. Active methods

##### Pneumatic spreading

Pneumatic spreading is a method that uses gas or air to spread the fibre bundles. An airflow passing through the tow helps the fibres bundles spread without inducing high forces thus being a technique that causes a significantly lower amount of damage to the fibres as compared to mechanical spreading.

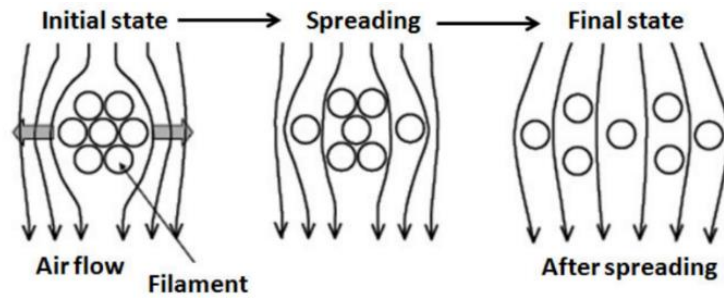


Figure 1.7: Air flow through fibres during spreading [10]

In figure 1.7 given above, the air flow wraps around the filament bundle such that the pressure above the fibre bundle is higher than the pressure on either side of it such that a force develops in the width direction thus loosening the fibres in the process. The pressure difference is caused due to difference in velocity generated in the centre and side of the tows [10] (Bernoulli's principle: static pressure + dynamic pressure = total pressure). As the flow of air continues and the fibres get looser, airflow passes through the spaces between the fibres during the spreading stage (given in figure 1.7), and the pressure differences created are such that the pressure on the centre of the fibres is highest, followed by the pressure in the spaces between them and having the lowest pressure on their sides. The widthwise forces thus continue to the point of spread where stability is achieved (the final state in figure 1.7). A pneumatic airflow spreading method was developed by Harmoni industry co. ltd. along with the Industrial Technology Centre in Fukui to spread a fibre tow from 5mm to 25mm increasing the width by 400%.

Three methods of pneumatic spreading are investigated in this review that use venturi profile, compressed air and vacuum to facilitate the spreading process. Each method is very different from the other in terms of design but ultimately uses air to deform the fibre tow using aerodynamic forces. Ames et al. [11] and Chung et al. [12] in their design of a fibre spreader and prepreg forming device respectively incorporate a spreading station that utilises compressed air/gas blown in a transverse direction to the direction of the tow such that the fibres spread. The pressure of blowing air is a key parameter in action and the flow should be controlled such that an even spreading/thickness is obtained along the width. Chung et al. spread 15 tows of 6k carbon fibres fed together to produce a sheet of 88.9mm.

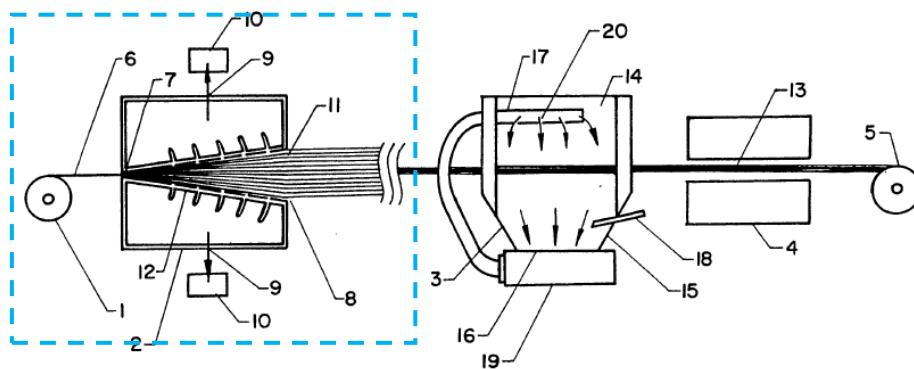


Figure 1.8: Spreading of tow through suction [13]

Suction or blowing of air by vacuum generation is another technique to spread the fibre bundles as developed by Baucom et al. [13] (Figure 1.8) and Kawabe et al. [14] for their spreading sections in their respective patents. Baucom designed an expansion unit for spreading where two walls inclined away from each other had holes in them that were meant to generate vacuum and suction the air from between the plates to develop lateral forces. The tow when subjected to the air being sucked out from the holes in the side walls were exposed to these lateral aerodynamic forces thus leading to their expansion in width. Kawabe on the other hand designed a suction cavity that would generate a vacuum and pull the air into the bottom of this cavity. The tow during the spreading process is overfed into the system such that it gets sucked into the cavity with a controlled amount of bend and this bending portion is the area of the tow that is spread at a single instance. The tow by the process of being overfed and bent down into the suction cavity is continuously spread in this design. Kawabe's spreading achievement was to flatten 12k carbon fibre of approximately 6mm initial width to 18mm which was an increment of 200%.

Finally, Daniels [15] invented a unique spreading technique that subjected the tow to lengthwise airflow instead of a cross-sectional airflow like in other designs. Her two-part spreader system used venturi profiles to first, spread the fibre tows and second, straighten them. The first venturi termed a preblower has the tow and air pass through a venturi slot after passing which the air flowing in the same direction as the tow expands expanding the fibres with it. The spread tow then passed through the second spreader where the air blows against the direction of motion of the tow generating forces that straighten the fibres along their length.

### Vibration spreading

A spreader bar may be subjected to vibrations over which a fibre tow passes for spreading. Based on its intensity, it can be used to spread the fibre tows without a large amount of tension building up or friction in the fibres thus preventing a significant amount of fibre damage as opposed to mechanical spreader bars despite having a similar operation. In the case of spreading, the vibrations in effect are regular throughout the spreading duration in the spreading element to provide an even spreading through the length of the tow.

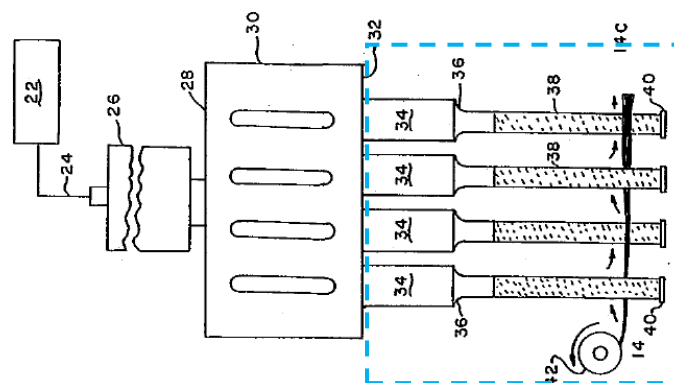


Figure 1.9: Spreading with vibrating bars [16]



Akase et al. [17] used a series of vibrating and non-vibrating spreader bars to enhance the effect of spreading through the vibrations and stabilise the amount of spread with intermediate non-vibrating spreader bars. They also deduced a suitable relation between the diameter size of the two bars and emphasized the importance of the distance between each bar to avoid any loss of spread width. Sager [16] (Figure 1.9) on the other hand developed a device with all the rods subjected to vibrations, unlike Akase who claimed multiple back-to-back use of vibrating rods will lead to the creation of fuzz in the fibre tows.

Yamamoto et al. [18] and Tanaka et al. [19] too followed similar footsteps in their inventions of creating an apparatus to spread the fibre tows. While Yamamoto had a simple design of freely rotating spreader bars subjected to vibration to spread the bundles, Tanaka's design was more complex and deployed the use of possibly vibrating spreader bars and a 'base body', a rotatable roller with small spreader bars in it that were periodically made to contact the fibre bundles and could have an option of being vibrated. An interesting aspect of Tanaka's spreading configuration was his emphasis on the position of rollers and base bodies in upstream or downstream contact with the tows and their direction of rotation. He also designed his rollers or base bodies to have projections along the periphery. In conclusion, while his use of vibration was straightforward, the geometry and arrangement of his spreading elements are to take notice of.

In each of the mentioned designs above, the control parameters of vibration were the same. One, the vibrations generated were in the longitudinal direction of the spreader bars. Two, each of the designs controlled the amount of vibration by controlling and adjusting the amount of frequency and amplitude input into the system. The vibrations caused the fibres to have intermittent contact with the vibrating surface with reduced friction, tension and shear forces; loosening of sizing present between filaments and thus by consequence allowing the tow to spread with minimal damage and interference.

### Acoustic spreading (Airborne vibrations)

Acoustic spreading means the deformation of fibre tows through vibrations carried in a gaseous medium/air. A sound is generated in a speaker or any other suitable device creates vibrations of a certain frequency and amplitude that are carried by the gaseous medium to transfer to the fibre bundles such that the tow loosens thus leading to a spreading effect.

Iyer et al. [20] patented a design (Figure 1.10) to spread the fibre bundles where he used a combination of spreader bars positioned over an acoustic vibration source, a speaker, to cause the fibres to spread. The arrangement of spreader bars is such that the tow wraps over and under them in a zig-zag fashion to enhance the spreading effect. As mentioned earlier, the spreader bars are stationed over a housing unit for a speaker. The operation of the spreading system is such that the pulsations from the acoustic source are generated at a predefined frequency and amplitude making the vibrations in the fibre tows regular and controlled. According to Iyer, the spreading amount is a direct product of the amount of tension in the fibre tow and the amplitude of vibrations it is subjected to within a certain limit. So, increasing the amplitude will increase the amount of spread to a certain point and lowering the tension in the fibres will have the same effect. However, too little tension can cause fibre damage due to the uncontrolled movement of individual fibres. He also preferred that the spreader bars rotate instead of being fixed to avoid fibre damage.

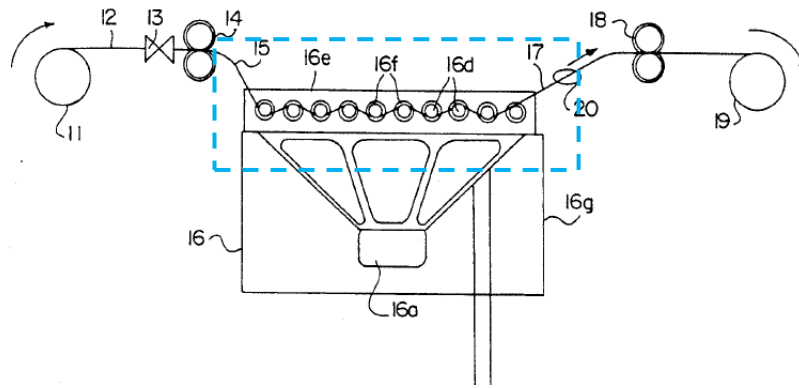


Figure 1.10: Spreader using speaker pulsations [20]

Hall [21] in his invention to spread graphite fibres had a different version for using acoustic energy to spread the fibre bundles. His design while using a speaker to generate pulsations was devoid of any physical elements to keep the fibre bundles in place except a positioning ring at the exit of the spreading system. The positioning ring was of a predetermined size which also constrained and controlled the width of spread tow. The principle of using acoustic energy to spread the fibre tows was similar for Iyer and Hall. Hall had the tow pass over the pulsating gaseous medium in a tangential direction to the horizontal plane of the speaker. The vibrations then interact with the fibres in the tow to separate them and this occurs when the vibrations in single filaments are equal to that of the source. His design realised the amount of spreading is controlled by three parameters. One, the tension in the fibre tow; lower tension allowed for lower frequency to be used to enable spreading. Two, the length of the tow over the pulsating gaseous medium termed by him as 'free span'; longer free span allowed for lower frequencies to spread the fibres. Last was the specifications of the vibration source itself which in this invention was a speaker with an attached amplifier.

Both inventions essentially emphasized the importance of low tension in the tows to be spread and frequency and amplitude of the pulsations created much like in the technique of spreading using vibrations in spreader bars. It can be assumed that the low tension in the fibre tows reduced the amount of friction that was present between the fibres and thus preventing them from getting damaged.

### Electrostatic spreading

Electrostatic spreading is a method in which the conductive fibres in tows are electrically charged to facilitate spreading. The fibres are usually charged such that they repel each other separating transversely and spreading in the process. Niina et al. [22] in their design to spread yarn bundles coat the fibres with water or any other solution to enable electrical conductivity through them. The conductive agent is sprayed onto the fibres by a compressed air jet and the amount of conductivity can be controlled by the pressure of the air jet, the type of nozzle, the distance between the nozzle and the fibres and the type of conductive material. The tow is then passed through an electrode to which a high voltage is supplied usually in the range of 5000V to 100000V. The charge in the fibres causes them to repel each other in the widthwise direction and the spreading takes place over the grounded spreader bars that are positioned after the electrode. The amount of spread in the tow can be controlled by the voltage that is supplied to the electrodes. According to Niina, their invention

allows for any fibres to be spread irrespective of their conducting ability. Niina's maximum spreading was to widen a 110 denier nylon 6 yarn to 150mm wide fabric.

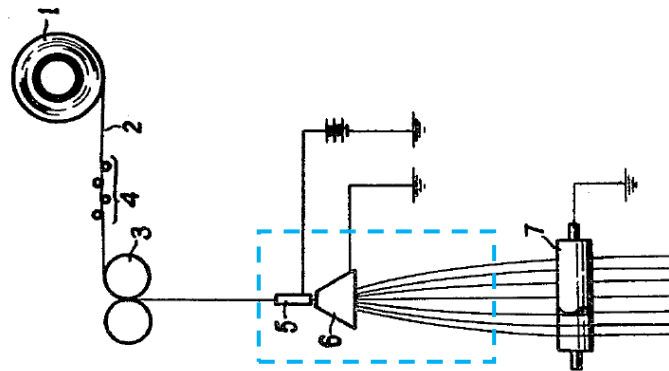


Figure 1.11: Spreading through electrostatic energy [23]

Uchiyama et al. [23] on the other hand used a two-part electrode system for spreading where potential was generated between two electrodes to separate the fibres in a tow (Figure 1.11). The first electrode is a small tube with a tiny passage for the tow to pass through into the second electrode which is a truncated cone geometry flaring outward in the direction of the tow. The two electrodes are also placed at a small distance from each other and care has to be taken to not let the spreading fibres touch the inner surface of the second electrode that is grounded. A minimum potential of 500 V applied to the first electrode was needed to spread the fibres in the tow. The charged fibres repel each other, are subjected to an electric field and spread toward the diverging conical second electrode due to attraction leading to an increase in the overall width. Uchiyama spread a 70 denier nylon 6 yarn to a width of 47mm.

Sternberg [24] used corona discharge electrodes as his option for spreading. He used a thin and flat sheet of an air jet to travel the fibres tow over a flat plate to spread the fibre bundles. The corona discharge electrodes were placed over a particular section of the flat plate and their position depended on the velocity of the air and the velocity of tow at each point along the length of the plate. The corona discharge electrodes are conical with a sharp tip that are arranged in a row along the length of the tow. Due to this arrangement, the fibres are charged through multiple electric fields generated by the discharge electrodes and leads to a higher amount of charge and thus spreading.

Another design using corona discharge electrodes was invented by Peritt et al. [25]. Their corona discharge device too contains a row of electrodes but instead of following the length of the tow, is placed perpendicular to it to ensure that no part of the fibre tow laterally is alienated or unexposed from the electric field generated by the discharge electrodes. They deduced that the amount of charge that was developed in the fibre tows was dominantly affected by the electric potential, the distance between the tow and the electrodes and the environment it is present in (humidity and air composition). The tow in the spreading station travels along with a conductive but grounded foil sheet underneath it such that the tension in the setup is bore by the foil instead of the fibre tow. The tow sticks to the foil due to electrostatic attraction. The system also has rollers present in a specific arrangement to guide the tow when needed. When exposed to the discharge electrodes, the foil is removed temporarily from the fibre with the help of a roller and reattached once the tow exits the electric field. But it is separated again because spreading cannot occur with the foil being adhered to

the fibre tow. The amount of spreading in this system can be controlled by adjusting/varying the position of the rollers that separate the foil from the tows and by varying the amount of net charge developed in the fibre bundles.

In conclusion, electrostatic spreading techniques out of all seems to be the least invasive in terms of force generation into the fibre bundles and by consequence causing minimal fibre damage. However, information in a lot of developments about the kind of fibres that can be used based on their conductivity is rather limited which may be the biggest drawback of this spreading technique.

## *B. Passive methods*

### Mechanical spreading

A mechanical tow spreader generally consists of an unwinding unit, a spreading unit with mechanical elements like cylindrical bars and a winding unit. It can also be used in combination with other energy-based spreading elements (active methods), can be integrated with a system for resin impregnation for the spread tow or have the winding unit replaced with a weaving unit to produce textiles and weaves.

The unwinding unit houses the unspread tow creels from which the fibre bundles are supplied as input to the spreading unit. Here, pre-tension can be induced in the fibre bundles and the rate of unwinding can be controlled. The spreading unit comprises spreading elements where forces are induced in the fibre bundles that facilitate the deformation of tows. This unit also can be used to control the amount of final tension present in the final flattened tows. Finally, the winding unit houses the empty creel in which the spread tow winding takes place.

For the tow spreader to qualify as smoothly functioning, the most important aspect is to have boundary conditions that are well understood and controllable such that no unpredictable behaviour is observed upon operation. Mechanical spreading has several mechanism options for spreading fibre bundles that have been developed over the years. Of all the spreading methods, spreading by mechanical means is the area of focus in this project to better understand the nature of spreading to its finest details. A mechanical spreader due to its simplified setup allows for relatively controllable boundary conditions, quantifiable parameters in tow spreading and a clear picture to understand the behavioural changes in carbon tows as they deform into wider and flatter tapes. Therefore, the following section in this study attempt to highlight and analyse the various elements of mechanical tow spreading as it is the chosen method of spreading for this study.

### Types of mechanical elements for spreading

This section describes some mechanical elements that have been used by the industry or past studies to spread the fibre tow via contact/passive method. Each element or multiple of them constitute the spreading sub-unit of a spreader system. The details about their geometry, the process of spreading and the motion of tow through the element are discussed through various developments that have occurred to date in the form of research or patents. Each element's key features, advantages or disadvantages in Table 1 are analysed and concluded towards the end of this section.

## Spreader bars

Spreader bars are long cylindrical rods that can be arranged in a specific configuration to facilitate the spreading process [26] (Figure 1.12). The first study on the spreading effect comprising a theoretical model with spreader bars was presented by Wilson [27] in his study which will be highlighted in section 1.2.4 of the review. The tow is wound around the spreader bars in tension to spread as it moves over them. The key aspects for the tow spreader to work effectively in this system are tension, the configuration of the bars and motion. Tension is a parameter that provides the necessary forces for the fibre bundles to spread; the height and distance between the spreader bars control the amount of tension that is built up in them as they move from one bar to another and motion allows for the tow to enter and pass through the spreading system and passively controls the degree of spread.

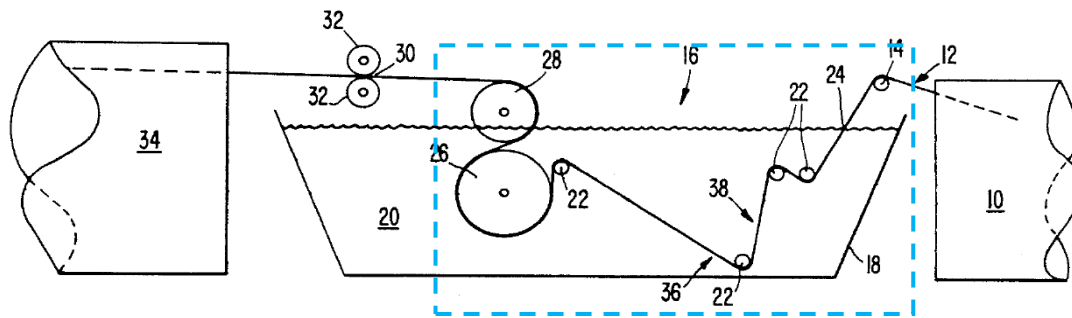


Figure 1.12: Example of a spreader bar configuration [28]

Spreader bars are an easily implementable tool for spreading with several parameters that can be used to control and study the nature of flattening of tows. However, multiple factors need to be experimented upon before designing the final spreading configuration. Their effects can have a significant impact on the final quality of tow deformation. Given below is a description of some parameters while choosing the spreader bars needed:

- *Influence of symmetry:* In an arrangement of spreader bars, symmetry or periodic arrangement is often observed as opposed to asymmetry. With a symmetrical (periodic) layout of the spreader, the modifications in the height and distance are easy to do while being able to control and predict the tension that each spreader bar generates (explained further in detail later in this section). It also allows for controllable boundary conditions during testing. The height and distance between the bars are what ultimately varies the contact angles between the tows and the bars. A symmetrical setup can be used to uniformly change the tension ratios between each bar as the tow passes through them. However, a non-symmetrical setup allows for tension spikes in specific areas for increased spreading locally if necessary and does not need the effort of moving every single bar in the configuration. This can be advantageous in systems where the spreading of fibre tows and their impregnation occur simultaneously like in the patented design by Calkins [28]. His setup of spreader bars was asymmetrical to allow for sharp angles the fibre tow undergoes in an impregnation bath.
- *Effect of surface roughness:* Some studies in the literature have tested the effect of surface roughness on the spreading of fibre bundles [29] [30]. It is an important aspect to consider because a) it can directly be responsible for the fibre damage that occurs during spreading and b) it controls the amount of friction that exists between tow and the spreader surface.

Thus, too much friction may lead to fibre damage due to rough interactions between the tow and the surface and too little of it may not provide the necessary amount of friction that could increase the tow's aspect ratio to its full potential without any damage done to it.

- *Effect of rotation of bars:* The spreader bars can be deployed as a static element for the tow to pass over or be allowed to rotate as has been tested by Irfan [20] in some of his models to inspect the spreading extent. While he didn't directly confirm the effect of rotation in the same configuration for spreading, his results did show a lower spread for rotatable bars as compared to fixed ones of a different configuration. In several experiments done in different studies, rotation of bars was adopted under the assumption that it allowed for reduced friction [29], reduced tension [30] and lower damage to the fibre as compared to static elements.
- *Variation in bar diameters for a single setup:* Variation in bar diameters within a single spreading system follows the same logic as that of symmetry. Based on local requirements as was the case for Calkins [28], he used larger diameter bars along with smaller ones in the resin bath to improve or better facilitate the impregnation of spread fibre tows as they reach their maximum spreading potential. It may be beneficial to look at the application of the spreader bar while opting for different sizes in bar diameters.

Spreader bars due to their simple design and implementation allow for a bigger design envelope with the multitude of arrangements and profiles of spreader bars that can be used. For instance, in a design developed by Guirman et al. [31], a spreader system takes a series of tows and spreads them using an air jet to produce a textile fabric. Before being subjected to the sharp flow of air, the fibre bundles are 'prespread' to flatten them initially before final spreading into a single sheet. This prespreading is achieved through spreader bars that instead of being a straight profile are bent/curved (banana shape) and the tow is placed over the convex part of the bars. The convex profile over which the tow passes widens the tow through a fanning effect. A detailed analysis of this is given in the following sections. In sum, there are several factors in a spreader bar system that can be varied and designed to develop or further optimize the process of spreading. It can be done so by creating different profiles of the bars themselves, testing different diameters and roughness of bars, using symmetrical/asymmetrical setup et cetera.

### *Convex bars*

Convex or spherical bars have a working principle similar to that of cylindrical spreader bars, the tow passes over the element and due to induced tension and acting friction and undergoes spreading. But the main difference between the two is the different geometry along the length of the element. For curved surfaces, spreading occurs through what could be described as a fanning effect. These mechanical elements were used in a spreader developed by Nakagawa et al. [32]. The claim for their increased effectiveness as compared to regular spreader bars was made by Marissen et al. [33] in a study that was done to develop an improved resin impregnation system for fibres. Figure 1.13 below shows the profile of a convex spreader bar.

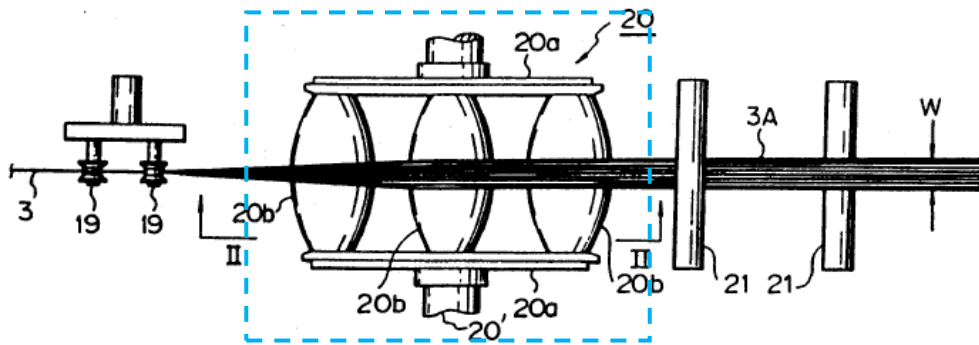


Figure 1.13: Profile of convex roller for spreading via fanning effect [32]

Nakagawa et al. [32] use a separating roller comprised of symmetrically arranged convex roller elements/rods to enable the spreading of fibre bundles (Figure 1.13). The separating roller rotates along the middle shaft to flatten the tows. The concept of a roller will be explained in the following section about the multibar wheel. The fibre bundles while going over the convex surface of the spreader element tend to adhere to the curved surface due to the normal force acting on them. The arc that forms the curvature of the convex profile is longer than the cylindrical bar for the same horizontal section (Figure 1.14) thus the fibres in the bundle tend to slide down the curvature as compared to the straight profile of the cylindrical spreader leading to a greater degree of spreading. This fanning effect where fibre bundles spread along the curve of the bar allows for the option of controlling the extent of spreading if needed by varying the angle of curvature. A bar with a higher curvature will lead to larger spreading as compared to one with a lower curvature.

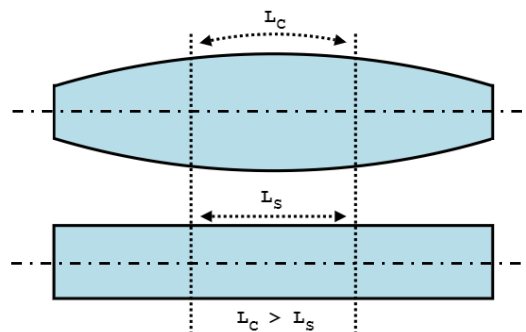


Figure 1.14: Convex profile vs straight profile action on the degree of spreading

### Multi-bar wheel

A multibar wheel spreading system was developed and patented by Nakagawa et al [8] and later adopted by Irfan et al [34] to facilitate the spreading of tows (see figure 1.13, 1.15) while stepping away from traditional spreader bar configurations. As can be seen in figure 1.15 below, a multibar wheel consists of multiple spreader bars attached between two discs at the same distance from the centre of the discs such that when the wheel rotates, the fibre bundle comes in contact intermittently the same way for each bar [32]. While Nakagawa used convex bars in his system instead of straight cylindrical ones like Irfan did, this goes to show that within the wheel itself are multiple potential options of spreader bar profiles that can be used for the optimization of the spreading process. An example of such would be a patented design developed by Krueger [35] where he used rows of spaced pins along the circumferencing the wheels to comb the fibre bundles into a flatter, spread tow. These pin rows were variable in spacing and positioning along the direction of the motion of tow. This allowed for the unspread tow to be spliced into smaller bundles and overall a wider tow.

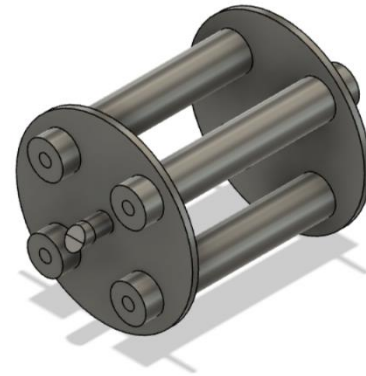


Figure 1.15: A rotatable wheel with a multibar configuration [34]

There appear to be some distinct benefits to using a technique such as this. Since the wheel's rotation is necessary as the tow must come in contact with each spreading element, the wheel also allows for the tow to move faster in the spreading system by adding possibly a component of rotational velocity to the running tow or in the least providing minimal resistance longitudinally against the speed of processing. Another important aspect to consider is reduced damage in fibres. Compared to its more traditional and simpler setup of spreader bars that induces high forces on tows and thus high fibre damage, the multibar wheel seems to offer improved performance due to its design and operational technique. The rotation of the wheel and intermittent contact of the tow with spreader bars reduces tension and by consequence friction between the tow and the bars thus preventing fibre damage. However, the technique is more complex to implement as compared to a simple spreader bar configuration and care must be taken to balance the speed of processing and the desired spreading width that is to be achieved in the process.

### Expandable wheel

An expandable wheel was developed by Lifke et al. [36] to spread the fibre tow by elastic expansion and contraction of the spreader elements between tow discs as the tow passes through it (Figure 1.16). The wheel comprises two outer discs between which elastic bars/tapes or compressible and expandable foam can be placed. The discs are angled to each other such that the point of the smallest distance between the discs has rods that will expand or stretch as the wheel does a rotation. This point of smallest distance is the position of entry for the tow to contact the spreading elements and as the wheel rotates, the rods stretch and the tow over them is forced to widen as well thus leading to spreading. The exit point of the now spread tow is the maximum distance between the two discs such that it is spread to the full potential of the wheel's expanding ability.



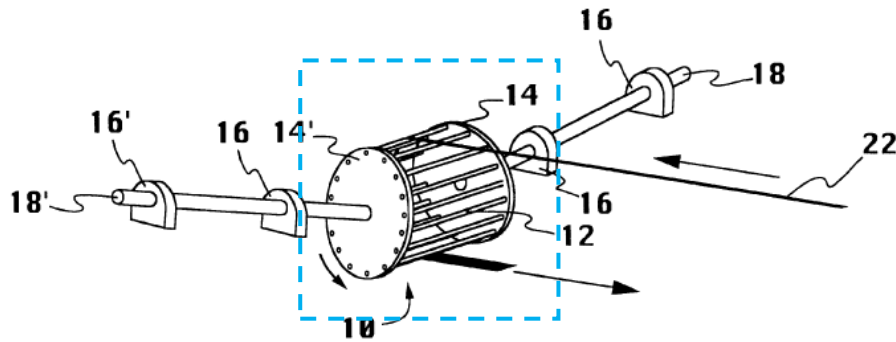


Figure 1.16: Expandable wheel schematic with elastic rods/tapes [36]

This unique design has an important benefit; the width of the tow can be controlled by varying the angle between the discs. A higher angle can lead to more spreading and a lower angle can limit the amount of spreading as desired. The fibre bundles as they come in contact with the elastic rods adhere to the surface due to tension and thus are forced to deform laterally when the rods do. One downside though to using this spreading element is the slip of fibres. At a high inclination of discs with each other, the spreading in an ideal case should also increase. This however could be complex to achieve if the fibres will be forced to separate overcome the lateral friction acting on them due to the rods and try to regain their original position via slipping back towards the centre line of the fibre tow. Nevertheless, this technique prevents fibre damage by inducing lower forces as compared to spreader bars due to its rotational movement. Lifke et al. used an untwisted carbon fibre tape of an initial width of 6.35mm and spread it by approximately 293% to a width of 25mm.

A similar concept was developed by Van Den Hoven [37] in 1981 before Lifke (the year 2000) to spread the fibre bundles into wider or narrower tows. He used a cylindrical rod that consisted of grooves that converged on one side and diverged on the other. Depending on the direction of rotation of the rod, the type of width whether reduced or increased could be achieved. The concept of spreading using this element is similar to that of regular spreader bars but the groves of varying overall width (from small to large) were used to guide and spread the filament bundles along their contours.

Spreading element	Features	Possible advantages	Possible disadvantages	For further reference
<b>Spreader bars</b>	<ul style="list-style-type: none"> <li>• Straight cylinders</li> <li>• Fixed/ Rotatable</li> <li>• Theoretical models available</li> </ul>	<ul style="list-style-type: none"> <li>• Simple design/easy integration in system</li> <li>• Controllable boundary conditions</li> <li>• Uniformity in fibre spread profile can be expected</li> </ul>	<ul style="list-style-type: none"> <li>• High fibre damage</li> <li>• Limited spreading compared to competitors</li> <li>• High tension expected in fixed bars</li> </ul>	[26] [28] [31] [46]
<b>Convex bars</b>	<ul style="list-style-type: none"> <li>• Curved profile</li> <li>• Adjustable curvature</li> <li>• Fixed/ Rotatable</li> </ul>	<ul style="list-style-type: none"> <li>• High degree of spreading</li> <li>• Width variation controlled by curvature variation</li> <li>• Simple design</li> </ul>	<ul style="list-style-type: none"> <li>• High fibre damage</li> <li>• Possible unbalanced sliding of tows in either direction</li> <li>• High tension expected in fixed bars</li> </ul>	[32] [35]
<b>Multi-bar wheel</b>	<ul style="list-style-type: none"> <li>• Symmetrical arrangement of spreading bars in a wheel</li> <li>• Rotation needed to spread</li> <li>• Adjustable number of bar elements in wheel</li> </ul>	<ul style="list-style-type: none"> <li>• High system speed possible</li> <li>• Low tension in system</li> <li>• Low fibre damage</li> <li>• Low intensity of loads acting on fibre tows</li> </ul>	<ul style="list-style-type: none"> <li>• Complicated system in comparison to competitors</li> <li>• Degree of spreading heavily dependent on rotation speed.</li> </ul>	[32] [34] [35]
<b>Expandable wheel</b>	<ul style="list-style-type: none"> <li>• Elastic expansion between discs</li> <li>• Tow spreads as elastic tapes between discs spread</li> <li>• Rotation needed to spread</li> </ul>	<ul style="list-style-type: none"> <li>• High system speed possible</li> <li>• Low tension in system</li> <li>• Low fibre damage</li> <li>• Highly controllable spreading width</li> </ul>	<ul style="list-style-type: none"> <li>• Possible uneven spreading due to forced lateral widening</li> <li>• Complicated system</li> </ul>	[36][37]

Table 1: Comparative analysis of different spreading elements

### 1.2.2. Mechanics of fibre tows

Understanding the relationship between micro-meso-macro scales of composites in terms of behavioural dependency may be valuable in controlling the properties of the final composite structure. It is known that the spreading of fibre tows allow for them to have improved mechanical properties and better absorption of resin and as of late, a crucial and beneficial technique to use before resin impregnation during composite production.

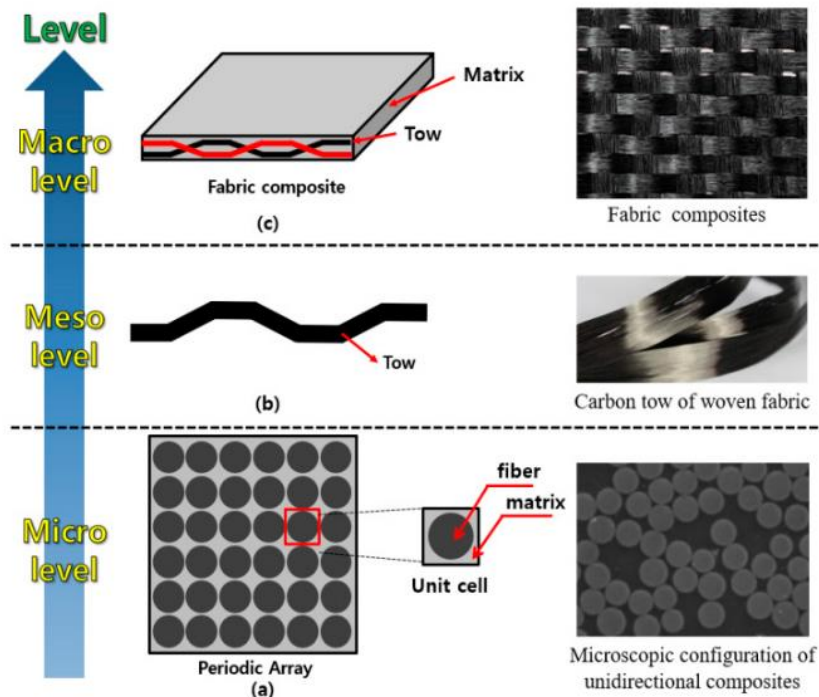


Figure 1.17: Carbon fibre on a) Microscale b) Mesoscale c) Macroscale [38]

While tow spreading is a phenomenon that is observed on a mesoscale, it is crucial to understand the behaviour of the fibres in the bundle while they spread. As can be observed in figure 1.17, on a micro-level, the resin and the fibre cells are distributed evenly in an ideal state, however, in reality, the microscopic images do not represent so. Moving to the mesoscale, in addition to the variations that are observed in 2D, other features such as fibre waviness and tortuosity along the length of the fibres come into play. Therefore, the consequence of these features on a macro scale is a deviation in the expected mechanical performance of the composite due to their non-ideal arrangement [39].

Tow spreading may be assumed to be controlled by the forces that act on it as the test parameters in tow spreading studies are mostly related to induced forces which will be explained on reading further. However, there are some other aspects that on the microscopic level also affect the extent or nature of spreading. These characteristics of fibres and their interactions could contribute towards what the final width and cross-sectional profile of the tow could look like. It may be thus advantageous for the sake of better understanding of tow spreading behaviour to have some insight on these factors. Given below are some of the characteristics that could affect tow spreading with a big or small influence:

- *Fibre-fibre friction*: The frictional interaction between fibres during spreading may influence the flattening of the tow due to the sliding movements fibres have with each other while changing their orientation. While the common relationship for friction force can be described

as  $F = \mu N$  (Amonton's law) where  $F$  is the frictional force,  $N$  is the normal force and  $\mu$  is the coefficient of friction. However, studies done by [40] realised that for fibres the law didn't apply as in certain case studies, the friction coefficient increased as the load went down. They thus developed a modification of the equation based on empirical data. The new equation  $F = \alpha N^n$  described the relationship between frictional force and normal force for fibres where  $\alpha$  and  $n$  were empirical constants dependent on the material. A quantifiable friction amount between fibres during the spreading process may thus derive a relationship between friction and the extent of spreading.

- *Inconsistency in filament diameters:* A certain amount of dispersity or difference in filament sizes is obtained during the production of fibres [41]. Irfan's analysis of fibre interaction stated above (Figure 16 (ii)) relied heavily on the forces each fibre exerted on its neighbours apart from the tension acting on it and described the concept of spreading as fibres falling into spaces below after overpowering the friction and reaction forces acting on them. This would be disrupted or made more complex if the fibres are not found to be of the same diameters. For instance, if a lighter fibre (smaller diameter) was being forced into a space between two heavier fibres, the friction and reaction forces to be overcome before it can slide between the two would be higher in comparison to the three fibres of the same size. This dispersity can therefore interfere with the spreading forces albeit on an extremely small level.
- *Sizing in the fibres:* Sizing is a thin and homogeneous protective coating applied on fibres to prevent them from getting damaged during usage, improve resin impregnation and adhesion to the matrix [42]. It holds the individual fibres together and prevents them from straying acting like glue and a lubricant. This can have some consequences such as increased friction [43] and additional forces, due to the sizing that try to bind the fibre and prevent it from spreading as it otherwise can.
- *The orientation of fibres as supplied in tows:* As mentioned earlier, fibre tow in an ideal state is visualised to have a crystal-like lattice, homogenous distribution and straight fibres. However, such is not the case and the fibres are in actuality inhomogeneous in packing arrangement with waviness along their length (see figure 1.18) [39]. This unpredictability in packing arrangement can also cause issues in the spreading behaviour of fibres. With a non-uniform distribution of fibres, it is also safe to assume that the movement of those fibres in the tow will be non-uniform too thus leading to uneven spread tows especially in heavy tows with a high number of filaments. This despite the advantages of using spread tow plies to improve the mechanical performance of composites may be perhaps a factor of a hindrance for further optimisation of composites.

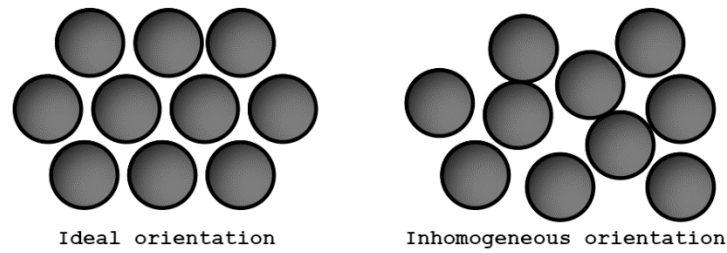


Figure 1.18: Ideal fibre lattice vs real packing

- Twisted filaments and entanglements:* In a study done by Suzuki et al. on the mechanics of fibre entanglement [44], attention was given to fibre bending over cylindrical rods and entanglements present in fibre sheets using nylon fibres for their testing. While this study was developed in the field of textiles, the motivation for the said study however was valuable to tow spreading. Their concern regarding fibre entanglements was that they affected the mechanical properties of the fibre such as tensile strength, bending strength and shear strength. For tows too it may be said that entanglements pose a problem not just with the overall mechanical performance of the continuous fibres but for the spreading process also. Twisted fibres and entanglements during spreading cause obstruction in the lateral displacement and subsequently desirable parallel arrangement of tows. If two fibres are entangled, they will tend to knot up and, in the process, create high local forces around that entanglement such that those fibres become more likely to damage as compared to the rest of the fibres in the bundle. Otherwise, if there are multiple filaments entangled with each other where the local forces may not cause damage, the consequence that can be expected in that particular area is reduced or limited spreading.

### 1.2.3. Spreading on a microstructural level

Interactions on fibre level, when subjected to tension, are responsible for the compaction behaviour of fibre tow, its cross-sectional shape [45] and deformations that lead to spreading. In a study done by Amir Davijani [29] to create a discrete element model for tow spreading, he conceptualised the effect of forces on two fibre filaments at different heights (layers) in a tow wrapped around a spreader bar (see figure 1.19). According to his analysis of the geometry of a spreader bar-tow interaction, the filaments with a bigger height ( $h_2 > h_1$ ) are expected to spread more due to a higher normal force acting on the filaments thus meaning that the top layers of fibres in tow have a higher tendency to spread as compared to the ones closer to the spreader bar. This was due to the fibres in the top layers having a higher tension force as a function of a larger strain than those closer to the bar that has less strain and thus less tension in comparison. Due to this incremental variation in tension from bottom to top layers, the normal force also increases therefore pushing the filaments down and forcing the tow to spread. He also realised the effect of the wrap angle of the tow around the bar and concluded that the increase in the spread was directly proportional to the increase in wrap angle. This particular observation of his agrees with the capstan equation stated in the section above when keeping tension as a spreading parameter in mind.

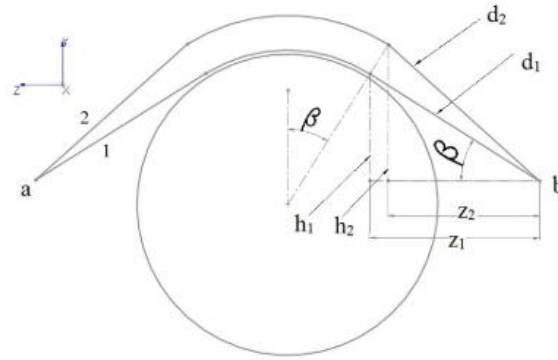


Figure 1.19: Amir's representation of two fibres in tow at different heights [4]

Amir's explanation may be limited by his experimental setup for spreading. In this experimental setup, he measures the effect of spreading over a single bar while the two bars on either side of it are designed to prevent the tow from spreading to constraint the boundary conditions. On the other hand, tow spreading using spreader bars commonly makes use of multiple bars in defined configurations around which the tow is wound thus making the boundary conditions very different from those described in his study. Thus, his theory needs to be extrapolated and analysed for a multi-spreader system to gain an understanding of the mechanics in that system.

Another analysis was done by Irfan et al. [26] on fibre interaction projects spreading as a function of bending moment of the fibre tow along with the tension acting on it. In Figure 1.20 (i), a fibre tow schematic containing three parallel rows of fibres on a surface is shown. The arrows define the interaction path each fibre has with the other and the contact surface. He described two coefficients of friction; one for the fibre-spreader bar interaction and the other for the friction present between the fibres (fibre-fibre interaction). Following this, Figure 1.20 (ii) shows a free body diagram of two fibres in contact with each other from a cross-section view.  $R_{EF}$  and  $R_{FE}$  are the reaction forces acting on the other fibre,  $w$  is the weight of the fibre with  $w\sin\theta$  being its tangential component and  $F_{EF}$  is the frictional force acting in the opposite direction in response to the tangential component. On applying the free body diagram to figure 1.20 (i), it was found that the reaction forces were the highest for fibres in contact with the surface and diminished with increasing height ( $R_{SH} > R_{HF} > R_{FE}$ ).

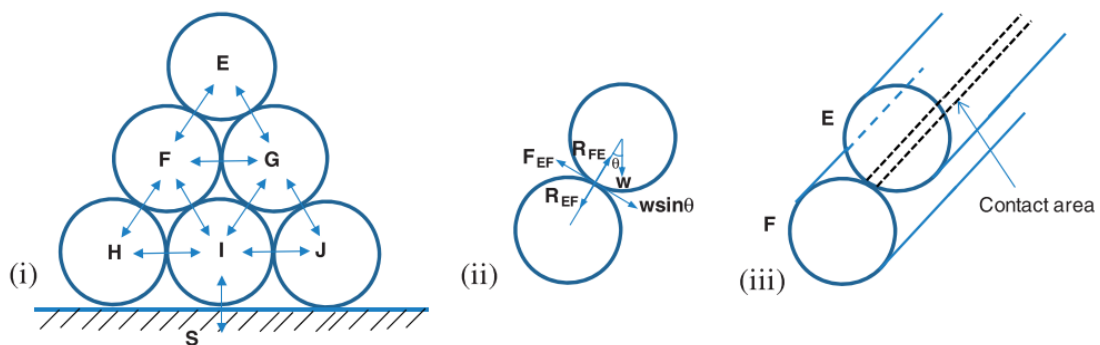


Figure 1.20: Irfan's representation of fibres in tow at different heights [26]

On application of tension in the fibre bundle, it was observed that tension forced the fibres to fall into the spaces between the fibres below through shuffling around by being supported from the surface of adjacent fibres. The reason for this slipping movement was the tangential component of weight

being large enough to overcome the frictional forces posing as a resistance factor. Irfan's study is not constrained by any imposed boundary conditions and seems rather feasible to adopt for checking this behaviour experimentally.

#### 1.2.4. Analysis of spreading parameters

With insight on theoretical and industrial background on tow spreading developments, it is also crucial to understand the spreading behaviour from an experimental perspective for which several research papers were analysed to spot common findings, understand different experimental setups for spreading and take note of the parameters that were experimented with. This section introduces two significant theoretical models proposed in past research done and further branches out to explore other literature that contributes to this study based on the experimental parameters that can be applied and tested in a practical setup. Figure 1.24, in the end, is used to summarise all the observed parameters and their relation to each other to conclude the analysis.

#### Wilson's model

An important development in the field of tow spreading was introduced in the form of a theoretical model by Wilson [27]. His study proposed the relationship between the width of the tape and the orientation of the first spreader bar. In figure 1.21 below, Wilson's experimental setup is described. He created a symmetrical spreading system where he passed a tow fixed on one end over two spreader bars and the free end of the tow was attached to a mass. The tow in this system was then subjected to certain tension cycles until equilibrium in spread width was obtained. The spread of the fibre bundles was observed over the first spreader bar hence his system was a single spreader bar system.

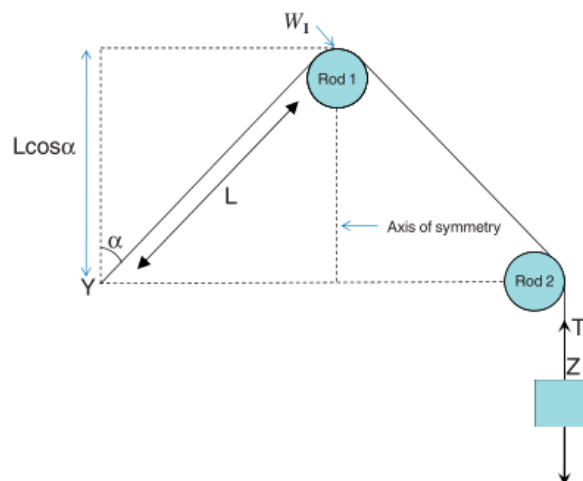


Figure 1.21: Side view of Wilson's experimental setup [26]

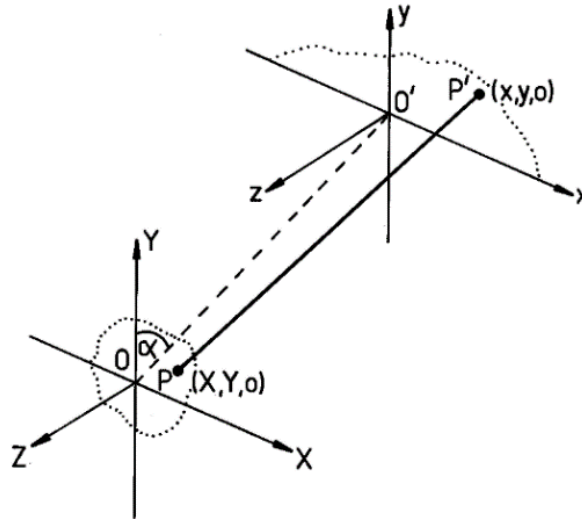


Figure 1.22: The fibre tow is fixed at O and goes over the spreader bar O'x which is visualised as a thin blade. PP' is a random single fibre in the tow. [27]

From figure 1.21 and 1.22, L is equal to OO' which is the distance between the fixed point and the spreader bar,  $\alpha$  is the angle between the tow and vertical axis y and T is the tension in the tow due to a certain mass Z. Wilson spread the tow by a series of to and fro motions until the spreading had reached an equilibrium stage. For his theoretical model, he developed the equation given below:

$$W_1 = (12AL\cos\alpha)^{1/3}$$

Where  $W_1$  is the width of the spread tow on the first spreader bar and A is the cross-section area of the fibre tow. Wilson treated the fibre tow as a continuum and not as a collection of individual filaments. His setup was simplified with certain assumptions he made while developing the equation. He assumed that each fibre in the tow bore the same amount of tension and friction played little role in the effect of spreading in the cross-section of the tow. He also assumed that fibres had no movement along their length and lastly, there were no entanglements or twists present in the fibre bundles. On comparing the results from the model with his experimental values, he found an error of 10-15% in width which he considered to be due to friction and entanglements. Additionally, he concluded that spreading is a consequence of spreader orientation independent of the tension in the fibre and the effect of additional spreader bars on spreading is minimal.

#### *Irfan's model and experimental analysis*

Irfan et al. [26] further develop Wilson's theoretical model for additional spreader bars. Since his motivation was to improve the quality of resin impregnation in fibre tows, he found it necessary to extend the original model to include more spreader bars as they allowed for a higher degree of spreading. Based on the same numerical model, he further continued to predict the thickness, width and contour of the fibre tow on a second bar. Validation of this extended model was done through tow spreading experiments of several bar configurations using different test parameters such as number and arrangements of spreader bars, rod diameter, tension release. His experimental setup



had followed Wilson’s path of experimenting where he and Wilson attached masses to the fibre tow and enabled spreading through back-and-forth motions.

Irfan made several conclusions through his experiments that described the influences that occur on tow spreading (see Table 2). Using the back-and-forth motions of the tow over two spreader bars or ‘tension cycles’, he realised that six tension cycles were needed to reach a spreading equilibrium state. His reasoning for the tow reaching an equilibrium state was that the fibres attain an almost stable arrangement in the spread tow and the inter fibre friction was too high to let any more spreading from occurring. Additionally, he also found that the amount of spreading beyond the first spreader bar was very small over the following ones which validated Wilson’s proposition about additional spreader bars. His next observation was concerning a ‘tension release process’. Tension release is a process where after the tension cycles are applied to the tow, two more cycles are applied, one with tension and one after the tension is released from the tow that caused deformation of fibre bundles. He observed that on releasing the tension from the spread tow, the tow spread more and he attributed it to the fact that since no more forces were acting on the fibre tow, its stable arrangement was lost and it could afford to spread even further. Interestingly, due to tension release, Irfan’s obtained maximum width exceeded Wilson’s spreading prediction by 30%.

<i>Influence parameter</i>	<i>Irfan’s findings</i>
Tow material	<ul style="list-style-type: none"> <li>• Variation in width and cross-section area along the length of tow (dependent on the position of tow in the creel) disrupts data of spreading.</li> <li>• There was a presence of twists in a tow (effect discussed in a later point).</li> <li>• Sizing in fibres due to their cohesion caused an unfavourable effect on spreading.</li> </ul>
Tension cycles	<ul style="list-style-type: none"> <li>• Six tension cycles were needed for spreading to be in equilibrium</li> <li>• First tension cycle increased the width by 80% followed by smaller increases.</li> <li>• Beyond six cycles, fibres were damaged.</li> </ul>
Presence of twists	<ul style="list-style-type: none"> <li>• Twists are of two types- whole twists along the length of the tow and twists between the fibres in the tow.</li> <li>• Twists are unfavourable when aiming for a high degree of spreading.</li> </ul>
Bar diameter	<ul style="list-style-type: none"> <li>• Smaller the diameter, the higher the degree of spreading.</li> <li>• Maximum permissible tension cycles for different diameters of bars were the same.</li> </ul>
$L \cdot \cos\alpha$ (from Wilson’s model)	<ul style="list-style-type: none"> <li>• Spreading increases as <math>L \cdot \cos\alpha</math> increases until the spreading reaches equilibrium.</li> <li>• Limited range of L for which its variation can have an impact on the degree of spreading.</li> <li>• Spreading increases with decreasing <math>\alpha</math> up to a certain value beyond which it will start decreasing due to its interaction with the adjacent bar (a certain minimal angle is needed for spreading to occur between two bars).</li> </ul>

Additional bars	<ul style="list-style-type: none"> <li>• First spreader bar causes a large amount of spreading but additional ones cause much less spreading.</li> <li>• Complies with Wilson’s argument of additional spreader bars.</li> </ul>
-----------------	--

Table 2: A summary of results in Irfan’s study

While both Wilson and Irfan’s theoretical models provide valuable insight into the parameters causing the tows to flatten, the error margin of their theoretical model to the experiments they performed are quite high. However, both of these studies laid a foundation for further experimentation, development and optimisation of mechanical spreading techniques. Several researchers have taken Wilson and Irfan’s models as their primary literature and tried to understand tow spreading under their experimental conditions and setup.

Another study based on Wilson’s model was by Tonejc et al. [46] to understand the geometric parameters that affect mechanical tow spreading. This study was composed of two parts; the first was an experimental setup similar to Wilson’s to use his theoretical model. This was done to predict the width of the tow being spread until it reaches an equilibrium stage. The second part involved setting up an automated spreader that would take tow directly from the material creel, spread it in the system while recording data on the degree of spread and wind it in an empty spool. The goal of this setup was to develop a data acquisition system for capturing the amount of spreading and it was done so through sensors that would capture the profile of the tow before and after tow deformation. The results from the first experimental setup showed that the obtained spreads in width were smaller than that of Wilson and Irfan and it was attributed to the difference in experimental setups. In this setup, acetal rollers instead of rods were used which would reduce the friction in the system significantly due to permissible rotation in the rollers. It was also concluded that a higher value of mass attached to the tow reduced the amount of spreading which is interesting because theoretically a higher amount of tension should lead to a higher degree of spreading but this needs to be verified diligently. The second experiment with an automated spreading system did not yield a high degree of spreading so focus was given to the laser sensors that captured a before and after spreading tow profile. While it does not contribute to analysing any ‘geometrical parameters’, the study did elaborate upon the tricks to capture good data points of the tow contour and how to post-process them.

Amir Davijani’s [29] experimental setup too was a simplified setup based on Wilson’s model where the spreading behaviour was captured over a single spreader bar. Since the goal of his thesis was to develop a discrete element model for spreading, his experiment was designed in such a manner that the boundary conditions were simple and easily controllable. He too subjected the fibre tow to tension cycles until an equilibrium state was achieved. Although for his experiment, the number of tension cycles necessary for spreading to stabilise were five instead of six as Irfan had found. The parameters he investigated in his study were tension in the tow, friction between the tow and the spreader bar, tow twists, fibre sizing and the geometrical variations of the tow with respect to the bar.

Amir found through his experimental data that tension did not affect the extent of spreading. He varied the amount of tension in the fibre bundles by varying the weight (200g-600g) hanging from it. His values of spread were similar although he does state that the result could differ from his conclusion if higher values of tension were used. He also concluded that friction had no impact on the spreading behaviour. He tested so by spraying the spreader bar with PTFE lubricant and graphite powder and

comparing it to regular spreading conditions. It was observed that the lubricant reduced the amount of spread which was probably because of the wet filaments adhering to each other and that graphite powder made no difference in the extent of spread. There was a margin of doubt regarding the friction test as it couldn't be understood whether the lubricant and powder made little difference to the spreading because the friction in the system was already too low or whether they played no role at all. Despite the slightly ambiguous results obtained during the investigation of tension and friction's influence on spreading, Amir did have solid conclusions about the tow twists, tow sizing and geometrical variations in the spreading system. It was noted that twists along the length of the fibre tow were highly unfavourable and inversely proportional to the final width obtained by the spreading process. This was the same conclusion in Irfan's study. He also found that unsized tows spread 26-33% more than sized tows. Finally, the results of geometric variations are explained in figure 1.23. It was found that as the height  $h$  increased, the amount of spread increased too. This was attributed to the increment in normal forces acting on the tow as the height in the system was increased. Additionally, the horizontal distance  $z$  on being decreased increased the amount of spread.

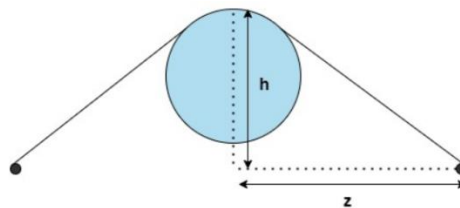


Figure 1.23: Geometric parameters in Amir's study [29]

A study by Gizik et al. [9] on spreading investigated the spreading behaviour of heavy carbon fibre tows (12k,24k,50k) using an industrial spreading machine. An aspect that stood out in this investigation was the usage of different types of fibre tows to study the dependency of spreading on the material quality itself which is a factor that hasn't been discussed before.

The test parameters in this study were tension in the tow, spreader speed, aspect ratios of the spread tow along the length of the tow from a single creel and threshold values of minimum attainable areal weight before fibre damage. It was found that the obtained aspect ratio with different tensions had no specific pattern for different fibre types but the machine speed shared a common behaviour for all tows; the higher the machine speed, the lower was the obtained width. This could be because the fibre tows did not have enough time in the spreading unit to attain their maximum possible width. Another important observation was the maximum attainable aspect ratio of each spread tow before fibre damage. It makes the development of a common spreading system for all fibre types all the more complex as each time a system may potentially have to be tailored according to the material quality of the fibre tow that requires spreading. Variation of spread aspect ratios along the length of a single type of fibre tow and variation of them across different creels adds another dimension to the obstructions that could occur when designing a controllable spreading setup especially because these aspects are not necessarily controllable themselves. In conclusion, Gizik et al. [9] highlighted the challenges of controlling the spreading behaviour of fibre tows and it showed that designing a smoothly operating spreader is not enough. For consistency to occur in tows with regards to spreading, understanding and monitoring the material and its responses itself is a complex process as it is largely dependent on the manufacturing conditions/techniques of the fibres.

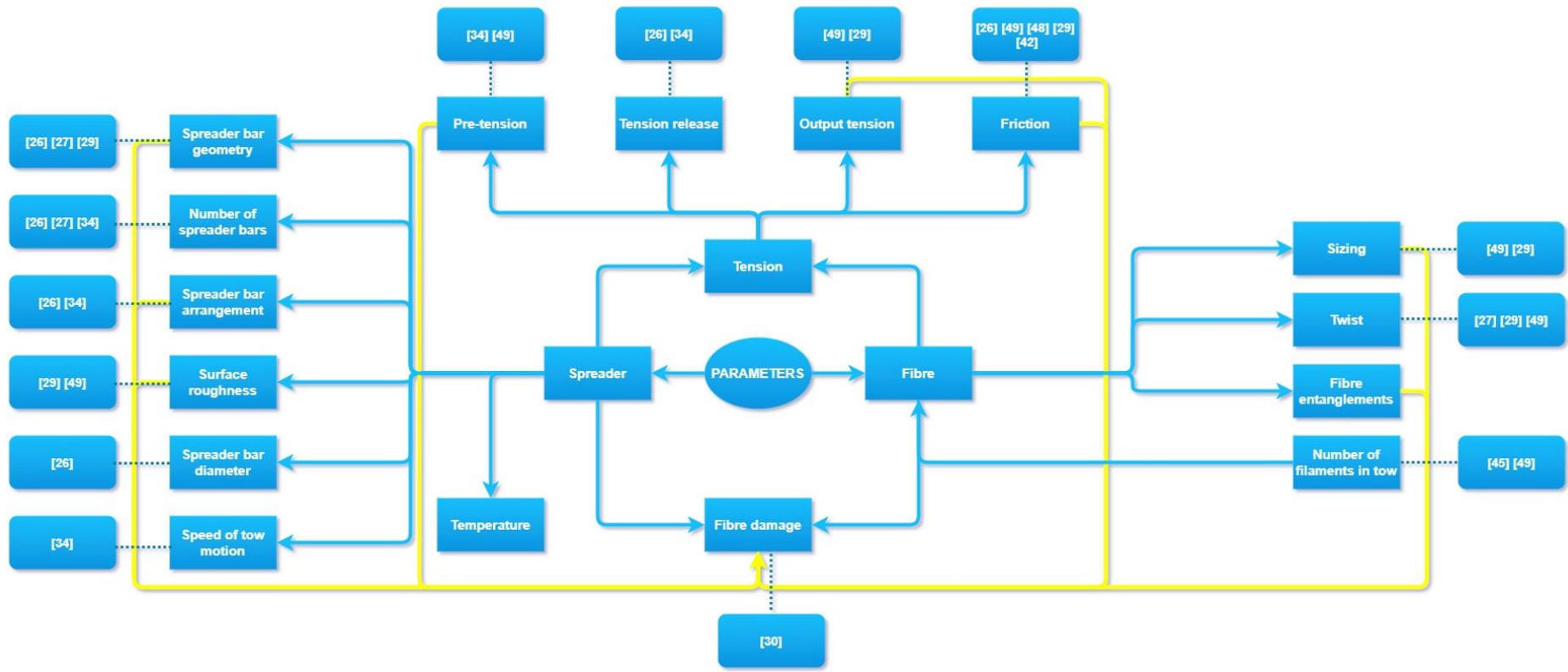


Figure 1.24: Interaction flowchart of parameters in mechanical tow spreading

In figure 1.24, each parameter is arranged on basis of its contribution and interaction in a mechanical spreader. The blue arrows indicate a flow from main elements/parameters to sub-parameters and the yellow arrows are especially sketched to highlight the factors that directly contribute to fibre damage. Mechanical tow spreading has two key elements that constitute several parameters or aspects that influence how they affect the behaviour of tow flattening and the extent to which they do. Those two elements are the mechanical spreader and the tow material properties.

As can be seen in figure 1.24, the spreader has various aspects that control the amount of spread. Spreader bar geometry or its profile can control the very mechanism with which spreading occurs. For instance, as can be recalled in section B, a cylindrical bar will have a different spreading mechanism compared to a convex bar. Spreader bar arrangement as proved in Wilson and Irfan's studies shows that the relative position of one spreader bar to another and the tow wrapped around it has a significant impact on the amount of spread. Surface roughness is a property of the bars that controls the interaction between the bar surface and the fibres in contact with it through changing the friction interaction. Too high a surface roughness can although cause fibre damage. Spreader bar diameter and speed of the tow running through the spreader are additional parameters that were found to influence the spreading behaviour.

Concerning the fibre behaviour, a crucial parameter is a presence of sizing especially because while desized fibres increase the amount of spread, sizing also protects the fibres from damage and improves their resin impregnation properties. Two parameters with respect to fibre tows are the twists and entanglements present in them that cause lateral obstructions during the process of deformation. But they are important nonetheless because these two parameters are often inevitable when the material supplied is directly from the creel.

It may be assumed at the present stage that the biggest role as an influence is played by tension in the system for mechanical tow spreading. Tension as a parameter directly correlates to the friction between the fibres and the fibre-spreader bar. A higher value of tension suggests a higher amount of friction present in the system and they both directly contribute to any damage that fibres go through including breakage, fuzz formation or a peel-off of fibre layers on the spreader bar. Numerous studies in the literature have been performed on fibre-bar and fibre-fibre interaction to understand the friction behaviour between them which may be a crucial influencing parameter on the spreading behaviour.

### 1.3 RESEARCH QUESTIONS AND THESIS OBJECTIVE

The state of the art in the previous section was used as a foundation for generating the research scope and subsequent research questions of this thesis. Given below are some general takeaways from the literature study that were kept in mind while defining the thesis goals:

- The number of researchers in the field investigating fibre spreading is quite limited and as a consequence, there are not enough research papers strictly related to the topic. At the same time, patents don't reveal insightful information which further makes a strong case for why more research is therefore needed.
- Several techniques for spreading (both active and passive) were evaluated to adopt the most suitable spreading technique that can be developed. Apart from the quality of spreading that was investigated for different spreading techniques, the focus was also given to the ease of development for a lab-scale system.
- Typically in older studies, tape/manual measure was used to evaluate the spread extent as a data acquisition means but that has developed into more sophisticated technology with laser sensors, cameras and other such high accuracy sensors. The data from them is currently post-processed through relevant software and suitable algorithms.
- Multiple parameters influence spreading behaviour such as tension, spreader bar arrangement et cetera. Each study done on understanding the spreading behaviour was found to have analysed different influences and aspects of spreading, however, a comprehensive study covering all or most of these parameters is missing.
- The patents contained robust and highly sophisticated machines that unwound fibre tows, spread them and wound them in an automated and controllable manner; whereas a majority of research studies used a simplified setup based on Wilson's experiment. Wilson's setup consisted of the length of tow over a spreader bar with weights attached to it. This stark difference in spreading systems highlighted a gap between industrial technology and research setups.
- Each technique of spreading was unique with different results for the obtained final width. But while final width was the most important deliverable of a spreading system, damage to the fibres was also a very important factor to consider. Active methods claimed to be advantageous over passive methods due to minimal fibre damage without compromising on the potential increment in width. Some techniques (Harmoni with Industrial Technology Centre in Fukui) were able to spread their fibre tow by 400% without damage sustained by the tow.

To make the research scope clear and more coherent, a set of research questions are defined to keep the workflow in check.

### 1.3.1. Research questions

I. How can we develop and build an experimental tow spreading unit with multiple subunits (unwinding, spreading, data acquisition and winding units) that allows investigation of spreading phenomena?

a. What are the most influential parameters (input) that contribute to spreading (output) using a tow spreader?

- *Literature survey, discussion with experts.*

This goal consists of a diligent investigation into the concept of tow spreading, industrial developments and academic research performed in this field. The literature study then is used to identify the knowledge gaps in the field of tow spreading, structure a research plan and realize an objective for the thesis.

- *Realize the arguments that contribute to understanding the behaviour of widening of tape.*

An investigation into the input influences/parameters needs to be done to understand the physics of spreading behaviour such that the spreading system can be designed to control the nature and extent of spreading. This controllable aspect provides the means to make spreading tests repeatable in their results thus making the system reliable.

- *For mechanical spreading as the chosen technique, perform a thorough study of spreading mechanics, industrial practices and develop a preliminary plan for building a tow spreader.*

This goal focuses primarily on mechanical spreading techniques and developing a build plan. As was established earlier in the literature study, mechanical spreading out of all its alternatives is easier to understand and control in its boundary conditions compared to other techniques hence it is the chosen technique of this study. First, all requirements from the tow spreader are realized based on the parameters of mechanical spreading. Then, a list of necessary steps to implement the requirements is established. Finally, a plan is drafted in terms of logistics and feasibility to build the spreading machine.

b. How can an integral spreading system be built and validated such that it can accommodate these parameters? Additionally, what constitutes the scope of controlled width?

- *Determine design scope within which tow spreading can be understood/experimented upon.*

With a design plan in hand, a design scope also must be sketched. Mechanical spreading has several dimensions and techniques that studies have utilized over the years. But implementing them all is highly complex and beyond the scope of this thesis. Thus, decisions must be made on what are the necessary elements that must be inclusive to create a robust spreading system. A design scope helps keep this exploration in check.

- *Draft plans and iterate, build and iterate to minimize error in spreading unit cohesion.*

As the goal states, this step is to build and iterate upon the tow spreading system such that a reliable and smooth operation of spreading is achieved. The focus here is to gain repeatability in results for the same parameters instead of maximizing the spreader performance with minimal errors of operation. An error here implies any obstructions in the flow of movement that a tow may experience through the spreader. This goal will be satisfied once the results are predictable based on input parameters and can be replicated over a series of same experiments.

II. What are the hardware and software to be included in the spreading system so that it can be automated and controllable?

- a. What identifies as relevant information (related to input and output) that should be collected during the operation of this integral system?

- *What information is sufficient to capture the behaviour of spreading?*

While the width of the spread tow is the main output that is desirable to check for spreading behaviour, does it suffice the knowledge requirements of this study? This needs to be investigated and if there is a scope for extracting additional information should be checked.

- *Does the collected data provide reliable information to quantify the spreading? Verify.*

A validation plan is needed to check for the accuracy and reliability of the data that is collected. This can be done once the data acquisition system is tried and tested; some data is collected from it and post-processed to check for any remnant noise or errors that could cause deviations from the actual results.

- b. What are the hardware and software that is needed for an easy to use and reliable system?
- c. How can these data acquisition and control components be used under one single virtual interface?



### III. How can we evaluate the system and its fitness to our goals?

- a. How can the level of control as well as achieving an acceptable level of spreading be quantified?
- *Do the system parameters have limits of application? Can thresholds be defined for these limits irrespective of the material that may be used to spread?*

Maximum and minimum values of each influencing parameter need to be defined for the user of the tow spreading unit such that each operation is well within the bounds of these limits and yields spreading results. These limits help design a sweet spot/range of operation in which user data can be retrieved for understanding the spreading behaviour. Further, repeatability of results for the same process parameters provide confidence in the spreading system and makes the system reliable for any experimentation and following a detailed investigation into spreading influences.

- *How important is the role of fibre damage in developing a robust system?*

Fibre damage is a frequently mentioned downside in literature when using a mechanical technique for spreading fibre bundles. This leads to the question of its cruciality in understanding and developing a tow spreading system. If fibre damage were to be excluded out of the scope of this study, would the spreader still function well in providing the necessary information that fulfils the final objective? Experiments are needed to verify this.

- b. How can a relationship be established between input and output defined in the above questions?
- *Post-processing of the collected data to draw conclusions and observe input/output relationship rules.*
- *Aim for capturing dry fibre in a frozen state for further microstructural investigation.*

As the final step to guide this tow spreading study to a microstructural level, a specimen needs to be designed that has spread tow captured inside of it. This is to be done by taking the tow within the spreading unit and freezing it in resin on the spot without any disturbance caused to the fibre arrangement or final width. This specimen is further prepared for inspection under the microscope to check for its quality and visualization of fibre arrangement. Once the technique is deemed satisfactory, some images of the fibre microstructure can be taken to display the potential of the technique for further microstructural investigation.

### 1.3.2. Thesis objective

Based on the research questions defined, the research objective is,

*“To develop a controlled tow spreading system to generate specimens for microstructural investigation of unidirectional spread tow composites by carrying out experimental studies and performing subsequent iterations on the spreading system.”*

The motivation of this thesis is to gain an understanding of the process of tow spreading and create a direction for its microstructural investigation to further generate information on the spreading behaviour at a fibre level.

To fulfil the research objective, a thorough investigation into the industrial practices for spreading is needed to do a performance evaluation for potential implementable techniques. With the background information in mind, a tow spreader has to be built and iterated upon until it is smoothly operating and satisfying the requirements defined by the research questions. The chosen strategy for developing the tow spreader is to focus on a select few parameters that may influence the spreading behaviour and explore their relationship with the width of the tow instead of aiming for a spreader that can spread the tow to its highest potential.

Following this, the spreader needs to be established as controllable with repeatable output in spreading which by extension indicates its reliability of operation. An experimental analysis is then needed to understand the process of tow spreading where the selected parameters are tested for their influence on the spreading that occurs in the fibre tow.

Lastly, a technique needs to be developed for capturing the spread tow in resin on-site the spreading setup without any loss of width and minimal disturbance to the fibre orientation. This may be possible through trial and error and a subsequent evaluation of the quality of the specimen produced. The microstructural investigation that follows aims to visualize the changes in fibre distribution at different stages of spreading.

This chapter describes the research approach adopted in this thesis. The methodology is mainly divided into three parts:

- *Development of a mechanical tow spreader*
- *Approach for experimental analysis of spreading parameters*
- *Developing a technique to capture the spread of fibre tow in resin for a microstructural specimen generation*

### 2.1 DEVELOPMENT OF A TOW SPREADER

This section describes the design of the developed tow spreader and highlights the different units that constitute the spreading system. This section aims to emphasize the input parameters that will later be used to analyse and test the spreading behaviour of the fibre tow. It also describes the requirements in terms of performance from the spreader and presents an operational flow diagram of the spreading process.

As described in the state of art section B, mechanical spreaders spread the fibre tows by inducing forces in the fibre filaments to displace them with respect to their previous relative positions (see figure 1.20). Mechanical spreaders generally consist of a set of particular spreading elements (cylindrical bars, convex bars, expandable wheels etc) that upon contact with the tow, increase its width and reduce its thickness.

It has been suggested that high forces in the tow induced by mechanical spreading can lead to fibre damage [26] which may make mechanical spreaders relatively unsuitable for spreading. Despite this potential risk, mechanical spreading is adopted as the technique of study in this project due to its simplicity in implementation, relatively large availability of past literature and this project's primary objective of understanding spreading behaviour along with connecting it to a microstructural scope of the study.

#### 2.1.1 The base design of the spreader

The mechanical tow spreader used in this study iterates upon the base design developed by Daniel Wiangyangkung [47] for a graduation project at the TU Delft Aerospace Manufacturing Technologies research group. His deliverable of a tow spreader contained the basic necessary components for spreading. In the study, the spreader was categorized into three main components: the winding unit that contained the material spool for the supply of fibre tow; the spreading unit that contained cylindrical spreader bars with adjustable geometric orientation for the tow to wrap around and spread and lastly; the winding unit that consisted of an empty spool attached to a stepper motor for the motion of the tow running through the spreader. The spreader also consisted of a control unit and a data acquisition unit.

The functioning/features of the base design of the spreader were compared to the desirable features/needs derived from the research questions of this study. Features in this context mean the necessary functions or components the spreader should contain in order to answer the research questions in this thesis. If certain features were missing, changes were made to the spreader design. This led to the development of the upgraded tow spreader through the approach illustrated in figure 2.1 given below.

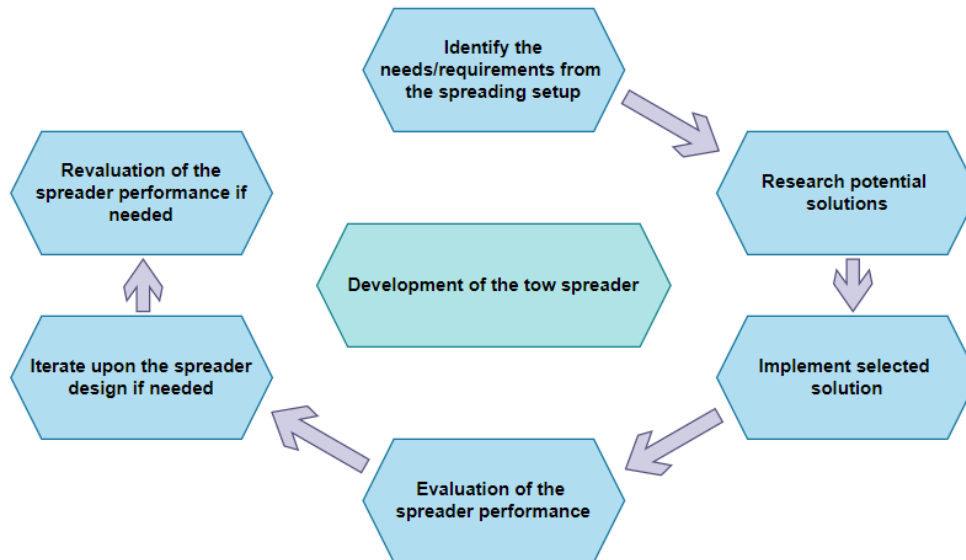


Figure 2.1: Approach for developing the tow spreader

### 2.1.2. Upgraded setup, its validation and flow of operation

The upgraded tow spreader (figure 2.2) adopted the categorisation of the base design setup and divided the components into five units (specifications of components available in Appendix A):

- Unwinding unit
- Spreading unit
- Winding unit
- Control unit
- Data acquisition unit



Figure 2.2: Developed tow spreader design

### Unwinding unit

The unwinding unit is the part of the tow spreader that supplies the unspread fibre tow to the rest of the units. It comprises of a material spool slid over a mechanical brake from which the tow is pulled (figure 2.3). The mechanical brake is responsible for supplying initial tension into the fibres of the tow by changing the resistance it presents against the rotation during unwinding. It has resistance/tension settings from 1 to 5 with one supplying the lowest resistance against rotation of the brake and 5 having the maximum resistance. Since the material spool is slid over the mechanical brake, the resistance against rotation from the brake is observed in the material spool too thus generating tension in the tow.

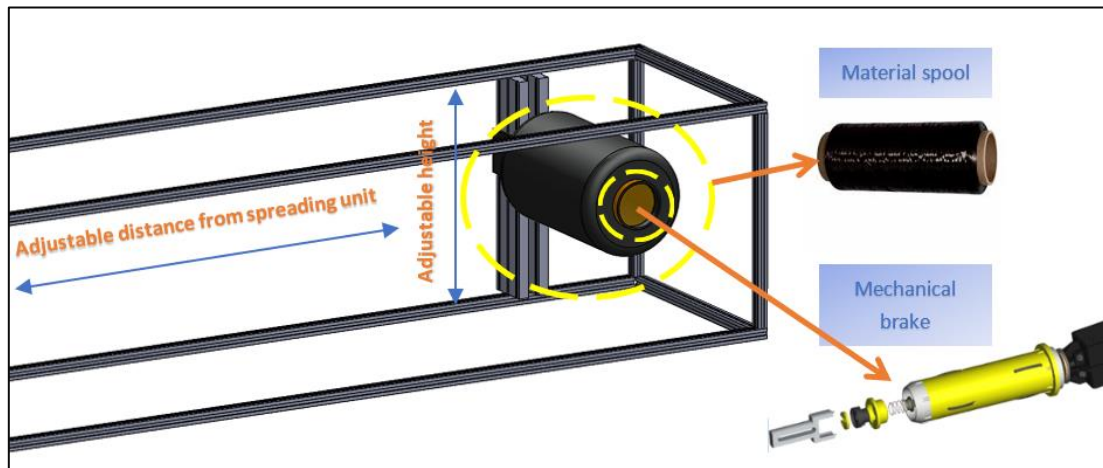


Figure 2.3: Unwinding unit with mechanical brake [48] and fibre spool

### Spreading unit

The role of the spreading unit (**Error! Reference source not found.**) is to induce mechanical forces in the fibres of the tow forcing them to spread and by extension increasing the width of the tow. In this tow spreader, it is done via spreader bars. As the tow wraps over them, the tension in the tow and the friction due to contact with the bars are two factors responsible for spreading [26]. The elements in the spreading unit can be arranged geometrically to produce the desired spread in the tow.

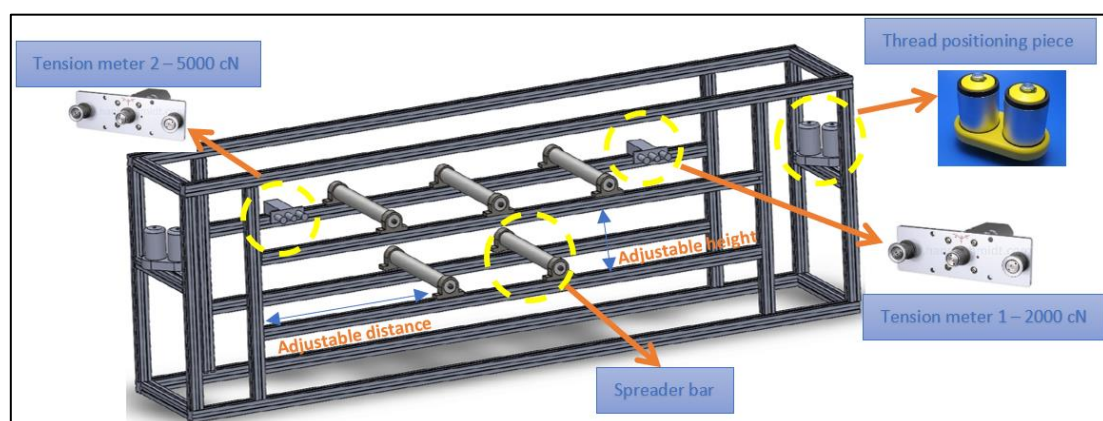


Figure 2.4: Spreading unit with spreader bars, positioning pieces [48] tension meters [49]

The spreader bars are 25 mm cylindrical bars with a topocrom coating (figure 2.5) that reduces the friction between the fibres and the bar surface because a high amount of friction may lead to fibre damage. The diameter of the bars can be selected by studying how the spreading behaviour can change with respect to it however previous studies have found that the diameter of the bar is inversely proportional to the spreading width [29] [26]. Five bars are selected to be a part of the unit after an experiment was done to test the effect of the number of bars on the spreading behaviour (section 3.4.1) but the spreading unit allows for seven bars to be installed. The orientation/arrangement of the spreader bars can be changed by changing the height, distance and length between them.

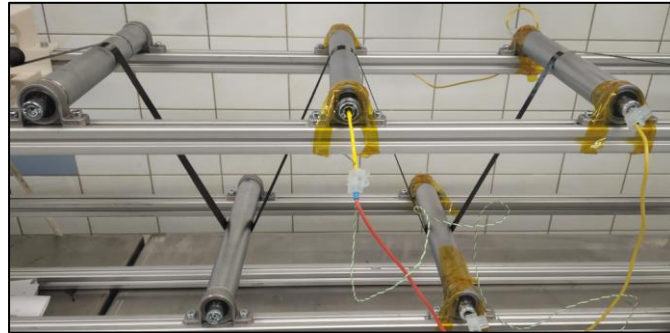


Figure 2.5: Spreader bar arrangement

An additional feature was added to the spreader bars to test the effect of temperature on the spreading tow. It was a heating element inserted into the hollow of the bars that increases the bar surface temperature up to 125°C. High resistance wire was wrapped around a conductive tube in coils and supplied with power to build the heating element (figure 2.6). For a certain power input to the heating element, the resistance in the wire would increase, leading to a high amount of heat being generated which in turn would transfer to the bar surface through convection.

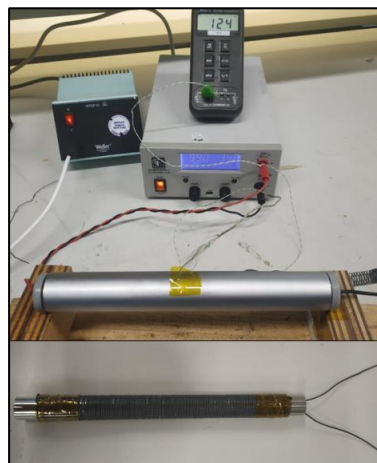


Figure 2.6: Construction of heated spreader bar

The heated elements were built for three spreader bars and each bar had its power supply with input current and voltage. Tests were done to select the input currents for different temperature outputs on the bar surface that were monitored through thermocouples.

### Winding unit

The winding unit (figure 2.7) contains an empty spool attached to a stepper motor that rotates and pulls the tow with it. The rotating shaft of the motor is responsible for collecting the spread tow on the empty spool and controls the speed with which the tow is pulled into the winding unit. The spool has an adjustable width for winding by sliding the rings along the length of the tube to control the amount of tow that gets wrapped during the operation of the tow spreader.

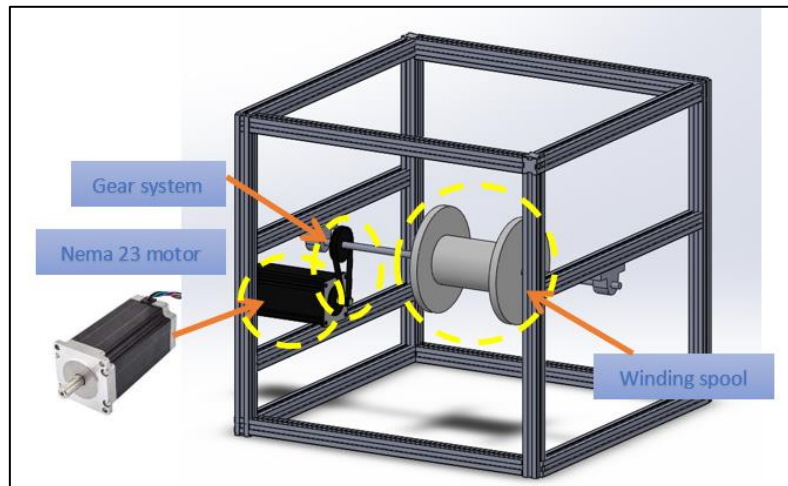


Figure 2.7: Winding unit of the tow spreader

### Data acquisition unit

The data acquisition unit consists of a camera mounted above the 5<sup>th</sup> spreader bar to capture the final spread of the tow. A 3d printed frame is used to ensure that the camera is facing downwards at exactly 90° to prevent any parallax error. Images of the tow are collected every 2 seconds. This frequency is sufficient to display any variations in width that occur during a run of the tow spreader.

Figure 2.8 shows a colour block of grey, red, green, blue and black to distinguish between different elements in an image like the bar, the tow and the background. The code created to calculate the width recognises this contrast in colours and uses object recognition technique to determine the tow width. In this code, each pixel of the image is allotted an RGB (red, blue, green) value, and significant changes in the RGB value tells a shift in an object. A purely black pixel will have an RGB value of (0,0,0) and a purely white pixel will have an RGB value of (255,255,255). The shade of the spreader bar will have an approximate RGB value of (192,192,192) if the three colours are balanced and the colour of the bar is completely flat which is not the case in reality.

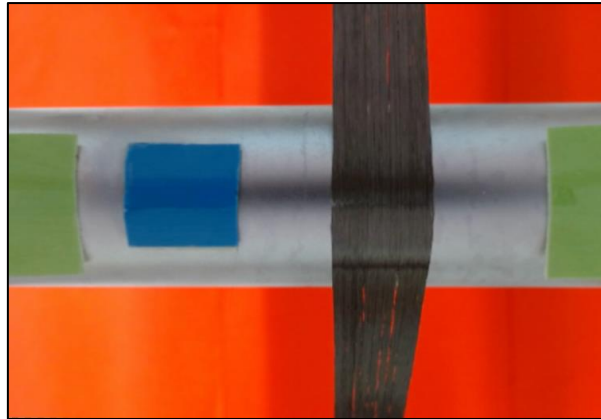


Figure 2.8: Colour blocking 5<sup>th</sup> spreader bar for tow width calculation

The code is instructed to observe a single row of pixels on the horizontal centreline and distinguish the variations in RGB combinations for each pixel. As the code runs for each pixel from left to right, it first notices the blue patch of known size, calculates the number of pixels for it and then does the same for the black pixels which is the spread tape. The formula for width simply becomes:

$$\text{width of tape} = \frac{\text{length of blue patch}}{\text{pixels of blue patch}} \times \text{pixels of tape}$$

To ensure the accuracy of each measurement, the light exposure of each picture should be the same and the distance between the camera and the length of the spreader bar should be vertically the same at each given point on the bar.

### *Control unit*

The control unit is responsible for running the tow spreader and collecting data from it to capture the spreading behaviour. This is done via the LabVIEW state machine. The LabVIEW state machine is a part of the LabVIEW software that allows for visually programming multiple control elements into a single interface. Simply put, it is possible to simultaneously run different programs, develop triggers that interconnect those programs and get combined output if desirable.

The tow spreading program on LabVIEW (figure 2.9) runs the stepper motor via Arduino, triggers the installed camera to take images of desirable quality and records the tension from the tension meters by converting its voltage output to a measurable unit of tension. The program also allows to input the rate of data collection. In return, it produces a text file with *input speed, tension at the two sensors and their corresponding images captured by the camera.*



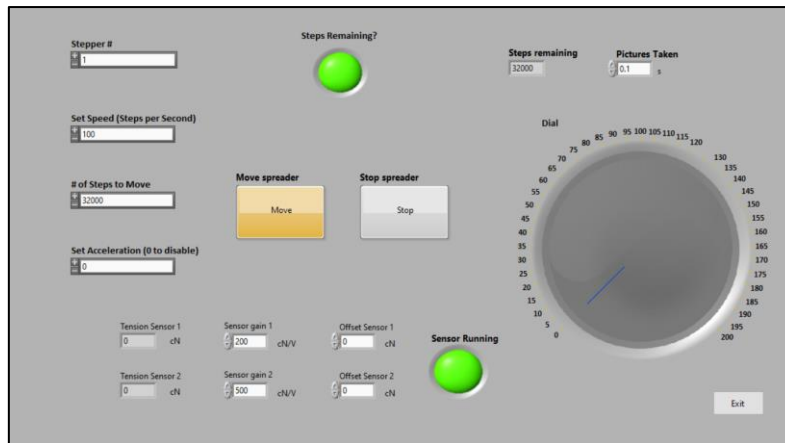


Figure 2.9: LabVIEW program for tow spreader

### 2.1.3. Flow of operation

For the tow spreader to generate accurate results that help understand the spreading behaviour, it may be beneficial to sketch the requirements from the tow spreader that are needed to retrieve the useful data. The term “requirements” implies certain features, characteristics or components necessary in the tow spreader to be at a stage where it functions sufficiently and produces reliable output widths based on the input parameters.

Qualities/requirements from a reliable tow spreader:

- The tow at no given point should get stuck in the tow spreader. The tow getting stuck at any particular instance or even periodically will compromise the data that is being collected (tension, spreading with) by inducing unexpected forces in the filaments that may affect the final spreading quality.
- The motion of the tow in the spreader should be longitudinal i.e., in the direction of pulling only. Lateral shifts or straying of fibre tow will not only disturb the spreading width due to its force components, but it will also degrade the image quality of the final spreading width captured through the camera on the 5<sup>th</sup> spreader bar which may produce unreliable results during an experimental investigation.
- The noise in the spreader should be dampened as much as possible. Noise in this context is the large vibrations caused by the stepper motor that can also affect the quality of data and orientation of fibres during spreading itself. While spreading due to vibrations is a spreading technique, it is irrelevant to the technique adopted in this project and hence should be isolated and eliminated as much as possible.
- Any element apart from the spreader bars itself should not physically change the width of the tow whether they reduce or increase it. For example, when the tow passes through the thread positioning piece, the width of the tow should not get crumpled or crushed due to contact with them.

- Finally, and most importantly, the results from the tow spreader should be repeatable for a given set of input parameters. This indicates two very important aspects of spreader design: a) The tow spreader is controllable i.e., by knowing that there are no external influences apart from the input parameters, the spreading width of the tow can be controlled by entering the right input parameters and b) the reliability of the data itself; a reliable and controllable tow spreader would produce repeatable results in terms of spreading width which is a very desirable and crucial characteristic for the spreader to have especially for a study of understanding spreading behaviour.

Based on the troubleshooting of the upgraded tow spreading setup (see Appendix B) and the list of requirements, an operational flow diagram of tow spreading is given in figure 2.10 below:

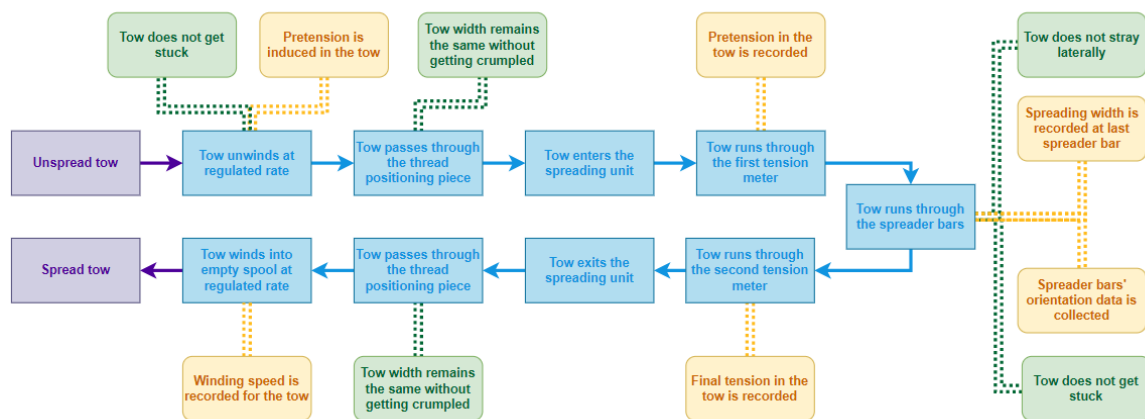


Figure 2.10: Operational flow of the tow spreader

The figure above shows each physical stage/process of the tow spreading as the unspread fibre tow unwinds from the material spool, passes the several units of the tow spreader and after spreading, winds onto the empty spool. In an industrial setup, after spreading this tow would most likely be immersed in a resin bath for impregnation or in a textile producing setup to generate weaves/fabrics instead of winding back as dry fibre. In the figure, the purple boxes represent the pre and post spreading state of fibre tow that passes through the spreader. The blue boxes represent each stage/element of the spreader that comes in contact with the running tow. They show the “journey” of the tow from an unspread state to a spread state. The yellow boxes highlight the points at which data is collected (e.g., spreading width) to evaluate the spreading behaviour of the tow and green boxes represent certain unfavourable behaviours (e.g., stuck tow) the tow may have at a certain stage (e.g., during unwinding) that should be avoided every time. In conclusion, the goal of this figure was to help visualise and break down the steps in tow spreading from a mechanical perspective and to provide a simplified summary of building a tow spreader.

## 2.2 EXPERIMENT METHODOLOGY

This section describes the methodology with which experiments to investigate the spreading behaviour are conducted along with the underlying assumptions made during this study. After the tow spreader was built and troubleshot, an approach to conduct the experiments was designed. A list of parameters that can be input into the tow spreader was realised. Each of these parameters was isolated as the only varying parameter against a set of fixed/baseline parameters to obtain the required results.

The experiments and their results could be split into two categories: a) Tests that check an element of the tow spreader to establish their proper functioning b) Tests that relate directly to the spreading behaviour of the tow. Results from category (a) were kept in mind while observing the results in category (b).

The fixed parameters were a set of baseline parameters input for every experiment (Table 3). They were selected on basis of ease of implementation between each experiment run. These parameters were also used to do a repeatability test (section 3.2) to determine whether the spreader was reliable and reproduced the same results for the same set of input parameters.

Baseline parameters	Input Value
Speed	50 RPM
Tension input	1T on the mechanical brake
Number of spreader bars	5
Temperature of bars	Room temperature
Length between spreader bars	150 mm
Distance between spreader bars	150 mm
Running time (stabilise the system)	2 minutes
Running time for tests	1 – 1.5 minutes
Images collected	every 2 seconds
Fibre tow material	T700SC 24K 50C

Table 3: Baseline input parameters of tow spreader

Given below in table 4 is the implementation strategy of the experimentation approach developed in this section. It shows how an experiment was conducted for each parameter. For an arbitrary parameter A of the spreader with an operating range from A1 to A5, a sample size of 5 tests were conducted to capture the distribution of results for the same input values. Between each test run, the tow spreader was subjected to a “stability run”. Tow spreader stability implies that the tow spreader has reached its stability/equilibrium stage and has recovered from the test run it was previously subjected to. This stability run uses baseline parameters as input and ensures that the next test run (e.g. A4) of the spreader will be unaffected by the changes induced by the previous run (e.g. A3) and the spreader is returned to its equilibrium state. Each stability run is done for 2 minutes.

A1		A2		A3		A4		A5	
1st test	Stability run	1st test	Stability run	1st test	Stability run	1st test	Stability run	1st test	Stability run
2nd test	Stability run	2nd test	Stability run	2nd test	Stability run	2nd test	Stability run	2nd test	Stability run
3rd test	Stability run	3rd test	Stability run	3rd test	Stability run	3rd test	Stability run	3rd test	Stability run
4th test	Stability run	4th test	Stability run	4th test	Stability run	4th test	Stability run	4th test	Stability run
5th test	Stability run	5th test	Stability run	5th test	Stability run	5th test	Stability run	5th test	Stability run

Table 4: Experiment approach for evaluation of input parameters

Certain assumptions were made in the experimental study to simplify the test approach and to fit the tests performed within the research scope of producing a preliminary study of spreading behaviour. While these assumptions may lead to certain unexplained behaviour in the results, an exhaustive study of tow spreading was beyond the time frame of this project. Given below are the assumptions made:

- a) There are no additional forces generated in the tow by the passive elements (e.g. tension meters, thread positioning pieces) of the spreader. These elements are used to capture data and position the tow in a particular trajectory and counting their contribution to the spreading behaviour makes the study complex.
- b) Noise generated in the spreader does not play a significant role in spreading behaviour. The vibrations in the tow spreader caused due to the stepper motor may be attributed as noise and trying to quantify them and subsequently eliminate them is a highly difficult and time-consuming activity. It may be tackled during the optimization or further extensive iterations of the current spreader design.
- c) The tow from the material spool does not have any variations in width. Ideally, the supplied tow should have a uniform width throughout its wrapped length in the spool but such is not the case and small variations can be noticed.
- d) During the heating process of spreader bars, the temperature of the bar surface is allowed to stabilise before a test is conducted. Despite this, a few degrees of temperature change is noticeable. This change is assumed to have no impact on the tow and on the larger scale, the effect of temperature on the tow remains the same.
- e) No geometrical changes occur in the elements of the spreader or the frame components (aluminium profiles) during a run due to loads acting on them. This means that for instance if the frames on which the spreader bars are mounted are subjected to high loads, they remain fixed in their position, do not experience any bending forces. Before each run, a check is performed to ensure all the positions of the elements in the tow spreader are accurate but high loads may cause very small changes in these positions but due to the frequency of these checks, this factor is ignored.

## 2.3 MICROSTRUCTURE SPECIMEN GENERATION

This section describes the approach adopted to generate a specimen for investigating the microstructure of the spread tow under a microscope. The fibres in the tow were embedded in resin, polished and observed under a Keyence confocal microscope. Capturing dry fibres without disturbing the microstructure was a complex task so some requirements/factors for embedding the fibres in resin were realised. Factors affecting the impregnation of dry fibre in resin are:

- Applied pressure/tension on tow to be captured – The tow must be kept in high tension such that when resin passes through the fibres, their relative position does not change.
- Wettability and fibre interaction with resin – The resin should be able to wet the fibres properly which in turn would lead to good impregnation.
- Viscosity of resin – The viscosity of the resin should be low such that it easily runs in between the fibres and through the tow impregnating them in the process.



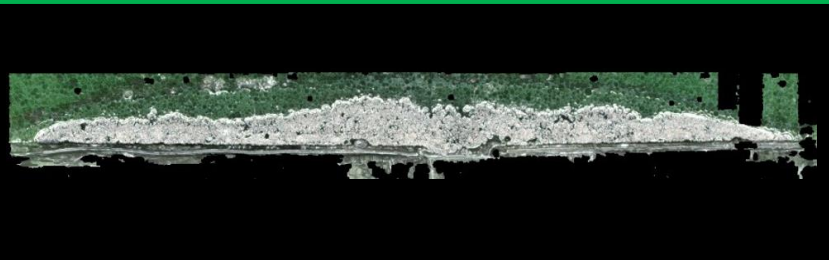

### 2.3.1 Sample quality assessment

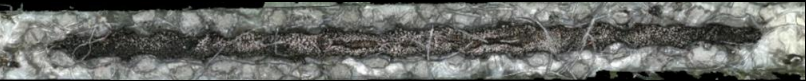


Selection of the best technique for embedding spread tow in resin for microstructural investigation was done by designing an assessment criterion and rating different aspects of the sample quality according to it. Three ratings of *poor*, *moderate* and *good* were allotted to each assessment criteria and a final evaluation was done based on these scores accumulated for each technique. Given below are the judgement parameters:

- Ease of manufacturing - This parameter evaluates the ease with which the fibre tow can be manufactured from the point of embedding till the final sample is prepared for being observed under the microscope. The intermediate stages are cutting, further embedding the sample in a resin vessel, grinding and polishing. A poor rating implies the manufacturing is complicated and good implies that the technique is easy to use.
- Physical interaction - This parameter evaluates the amount of physical contact (human interaction) with the spread tow during the process of embedding. An important consideration during capturing fibres in resin is minimal touching/shifting to make sure no fibres are disturbed during the process. This preserves the fibre orientation during spreading of the tow thus makes for very crucial assessment criteria. A poor rating implies the possibility of physical interaction disturbing the fibres is high and a good rating means the fibres are minimally disturbed.
- Impregnation quality - The most important parameter to consider is the impregnation quality of the sample generated. The presence of defects like voids, trapped grime, cracks act as noise and may cause issues in the microstructural investigation in terms of changing fibre distribution, assessing spreading quality et cetera. A poor rating means that there are a high number of defects present in the sample and the fibres are not impregnated well. A good quality sample has minimal defects and the fibres are completely impregnated in the resin.

### 2.3.2. Embedding techniques for sample generation

Given below are the different techniques tried and, their images under a confocal microscope and their evaluation based on the assessment criteria:

	Embedding technique	Sample image	Image quality assessment
1.	Double-sided tape is stuck on a microscope slide and the tow is stuck to it. Cyanoacrylate is then poured and dried over the tow, followed by the top slide with double-sided tape.		<ul style="list-style-type: none"> <li>○ Ease of manufacturing – Moderate</li> <li>○ Physical interaction – Poor</li> <li>○ Impregnation quality – Poor</li> </ul>
2.	Double-sided tape is placed on the slide and the tow is stuck to it. Cyanoacrylate is then poured and dried over the tow, followed by a fast-curing Technovit 4071 resin.		<ul style="list-style-type: none"> <li>○ Ease of manufacturing – Moderate</li> <li>○ Physical interaction – Poor</li> <li>○ Impregnation quality – Poor</li> </ul>
3.	Double-sided tape is placed on the slide and the tow is stuck to it. Cyanoacrylate is then poured over the tow and while wet, a fast-curing Technovit 4071 resin is poured over the sample.		<ul style="list-style-type: none"> <li>○ Ease of manufacturing – Moderate</li> <li>○ Physical interaction – Poor</li> <li>○ Impregnation quality – Moderate</li> </ul>
4.	The tow is sandwiched between two slides aligned with an offset such that the superglue poured in has a flow surface/path before contacting the fibres for improved impregnation.		<ul style="list-style-type: none"> <li>○ Ease of manufacturing – Poor</li> <li>○ Physical interaction – Moderate</li> <li>○ Impregnation quality – Good</li> </ul>

5.	<p>The tow is sandwiched between two slides covered with a thick double-sided tape. The stickiness of the tape keeps the tow together but no impregnation is done.</p>		<ul style="list-style-type: none"> <li>○ Ease of manufacturing – Good</li> <li>○ Physical interaction – Moderate</li> <li>○ Impregnation quality – Poor</li> </ul>
6.	<p>Resin poured on tow. The portion of the tow to be embedded is supported on its base by the slide following which a fast-curing resin is poured on top. The resin's viscosity can be reduced for improved impregnation but the curing time increases in the process.</p>		<ul style="list-style-type: none"> <li>○ Ease of manufacturing – Good</li> <li>○ Physical interaction – Poor</li> <li>○ Impregnation quality – Moderate</li> </ul>
7.	<p>Fibre tow is sandwiched between 3d printed moulds<sup>1</sup> with a slim cavity in high tension and fast curing resin is injected through a tiny hole. A release agent is applied for easy removal from the mould.</p>		<ul style="list-style-type: none"> <li>○ Ease of manufacturing – Moderate</li> <li>○ Physical interaction – Good</li> <li>○ Impregnation quality – Good</li> </ul>

<sup>1</sup> The design for the 3d printed mould can be found upon further reading of this section.

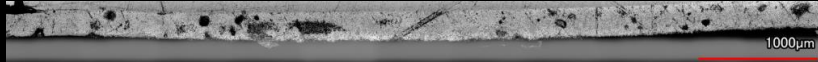
<p>8. Slides are clamped together over the tow with a pre-applied layer of cyanoacrylate and later injected with cyanoacrylate again. The tow is sandwiched between two slides aligned with an offset such that the liquid poured in has a flow surface/path before contacting the fibres for improved impregnation.</p>		<ul style="list-style-type: none"> <li>○ Ease of manufacturing – Poor</li> <li>○ Physical interaction – Good</li> <li>○ Impregnation quality – Poor</li> </ul>
--	--	--

Table 5: List of embedding techniques evaluated for microstructural sample generation



### 2.3.3. Selected embedding technique

In section 2.3.2 several techniques for embedding spread tow in resin were discussed and evaluated on basis of assessment criteria that best suited what was needed for a satisfactory investigation into spread tow microstructure. Of all the techniques, number 7 which used a 3d printed mould was found to be the most suitable option. Figure 2.11 shows a preliminary drawing of the mould used for capturing the spread tow.

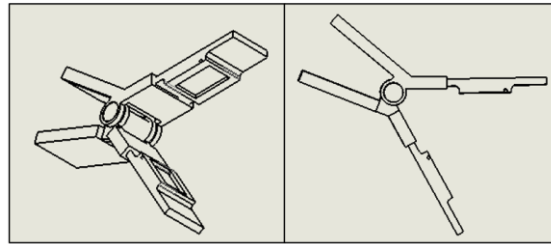


Figure 2.11: Drawing of mould for capturing tow in resin

The mould latched onto the tow by a clamping mechanism (figure 2.12). Rubber bands or a torsion spring were attached to the clip of the mould with very high torque that forced the mould slides to snap shut over the spread tow. Two holes were built into the slides for injecting the resin and letting the air escape as the resin fills the embedding space. The mould slides were coated with four layers of Marbocote 227 CEE release agent to aid an easy release of the sample. The resin used for impregnation was Technovit 4071 which is a fast-curing resin and could cure the sample on the spreader in 3-5 minutes.

Once the mould was clamped over the spread tow, the resin was injected into the empty embedding space with a syringe and the sample was left to cure. Following that, the cured sample was further placed in a small plastic cylindrical vessel and the same resin was poured over it to make the specimen ready for grinding and polishing. The sample from the mould alone would be too fragile during harsh processes like polishing and thus needed a bulk volume surrounding and protecting it. During the grinding stage, care was taken to monitor the sample quality through every step of the process and continuous checks were done to analyse the surface quality by image observation under a microscope.

Finally, when the samples were ready, they were observed under a Keyence confocal microscope at 20x optical zoom where fibres were distinctly visible (figure 2.13) and images were taken from one end of the tape to the other.

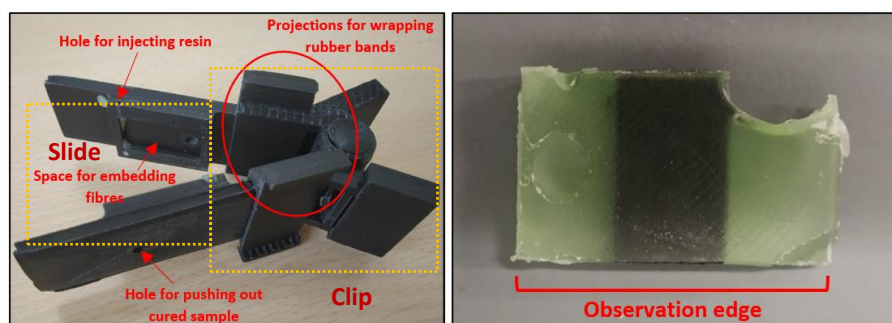


Figure 2.12: 3d printed mould and sample generated

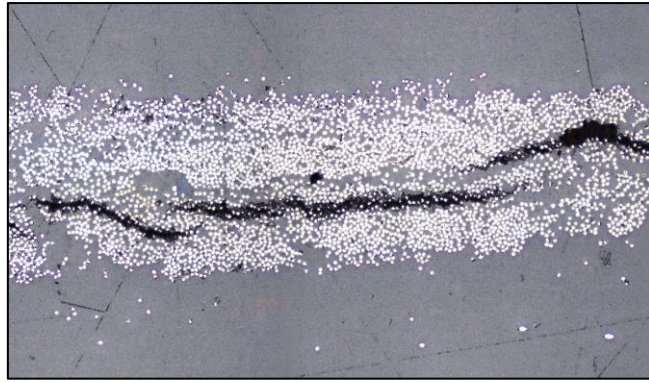


Figure 2.13: Clarity of microstructural image

The locations at which the spread tow was captured was between two spreader bars (figure 2.14). These locations were selected to observe the different stages of tow spreading and how the microstructure evolves from passing over one spreader bar to another.

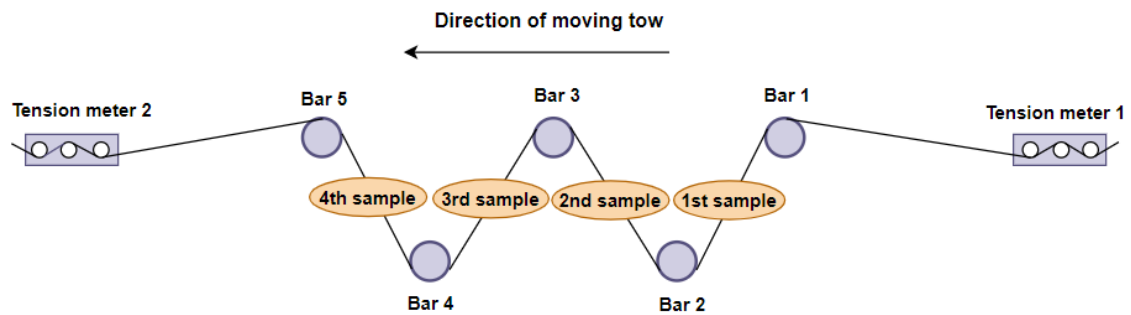


Figure 2.14: Locations for microstructure samples captured

With a technique developed to manufacture spread tow specimens, a detailed evaluation of the microscopic image quality was done which is described in section 4.1 of the microstructural investigation.

# 3 Experimental analysis of spreading parameters

This chapter details the results of the experiments done to evaluate the tow spreader performance and gain an understanding of the spreading behaviour of fibre bundles. The approach consists of an analysis of a single input parameter against spreading width obtained. This means that each parameter investigated is isolated and varied over a test range and the results are plotted to determine its influence on the spreading behaviour. At the end of the chapter, a summation of these results is provided in the form of a linear regression model to visualize the influence of each parameter on the overall spreading behaviour.

## 3.1 PARAMETERS EVALUATED

As mentioned in the previous chapter, the study of the tow spreader is split into three parts: the unwinding unit, the spreading unit and the winding unit. Each of the units further consists of several components that individually may contribute to the spreading of the fibre bundles in the tow. Based on the literature survey done as a prerequisite to this thesis (section 1.2), a flowchart (Figure 3.1) for the testing was designed with different parameters that could be analysed and their data quantified during the spreading operation. Some additional parameters were added to this study for further insight into the spreading behaviour during the progression of the project. The current spreader design is capable of spreading the fibre tow up to 150 % (20 mm wide).

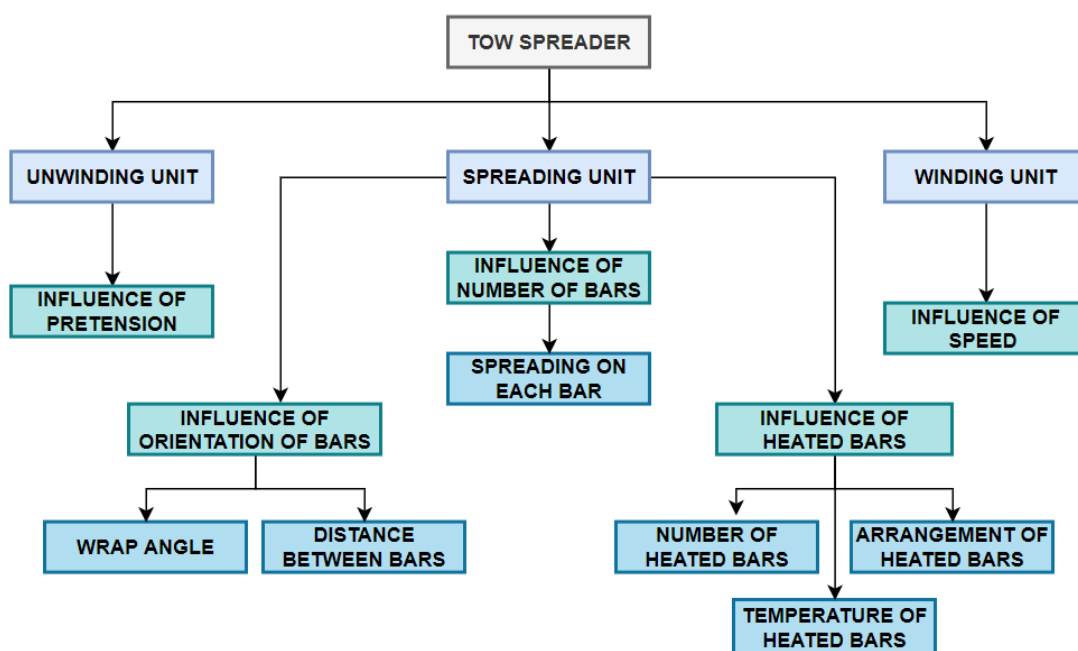


Figure 3.1: A general categorisation of spreader parameters tested

### 3.2 REPEATABILITY

Repeatability in the context of this study implies the ability of the tow spreader to produce the same results at different periods and usage and over several runs. It is a crucial factor to consider because repeatability in results is a quality of the tow spreader that can:

1. Determine the reliability of data collected for variation of parameters, changes in time and wear in the parts caused due to long term usage.
2. Indicate the level of control that has been achieved. If the tow spreader is controllable by achieving the same results for the same set of input parameters, it is safe to say that for instance, the spreader is dependable for any experiments that may need repetition in case of loss of data.

To quantify the repeatability behaviour of the spreading system, a sample size of 25 runs was carried out at random times and in between the various experiments described below (sections 3.3-3.5). The baseline parameters were input into the spreader to establish a fixed set of input data to avoid errors in order to make sure that the initial conditions for the spreader operation were the same every time. This was the chosen strategy to subject the spreader to different forces by varying parameters followed by bringing it to the equilibrium state of the reference parameters. Simply stated, the spreading process started with the same input values for all its runs and the final spreading width obtained is shown in figure 3.2 below:

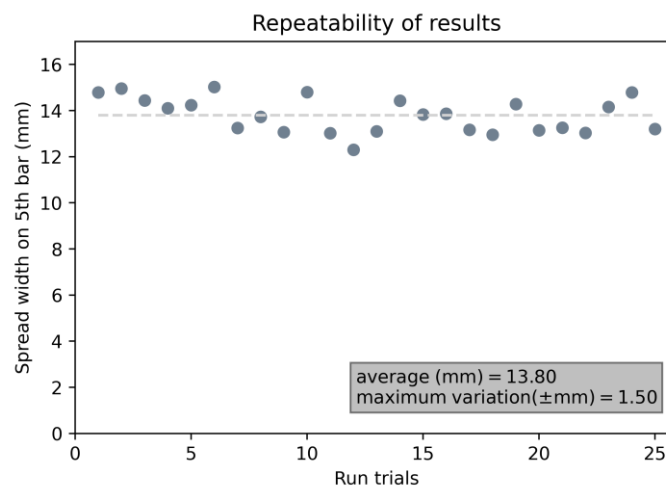


Figure 3.2: Repeatability of results

As can be noticed in Figure 3.2 given above, for each of the runs (x-axis), the final spreading width was observed on the 5<sup>th</sup> spreading bar (y-axis) before exiting the spreading unit. Each scatter point in the plot was found to be in the vicinity of 14mm and collectively, the spreading width for the reference parameters averaged at 13.80 mm with a maximum variation of  $\pm 1.5$  mm.

This plot can be beneficial to gain an insight into the tow spreader performance and its repeatability in output. Firstly, the scatter in the plot shows the distribution of final widths and variations that can be expected for the same set of input parameters. Secondly, it raises the question about whether the variation in the obtained widths may be a consequence of the noise that is generated during the

spreading operation through motor vibrations or a variation within the input parameters themselves despite their fixed values. It suggests a need for further and more extensive sensitivity analysis to reduce this variation observed in the spread width distribution.

### 3.3 UNWINDING UNIT

The unwinding unit as mentioned earlier in the report consists of the fibre tow spool attached to a mechanical brake that allows for changes in tension that is initially induced in the tow as it unwinds. This means that it is possible to change the force with which the tow is pulled into the spreading unit thus overall changing the tension in the tow. This initial tension provided to the tow is referred to as 'pretension' in the tow. The final aim of testing the pretension was to check for its influence on the spreading behaviour but to do that, certain additional experiments were necessary in order to establish a clear relationship between the spreading of the tow and the pretension in it. A description of these experiments and the reason to conduct them are given below:

#### 3.3.1 Translation of pretension from the mechanical brake settings

The mechanical brake over which the fibre spool is placed has tension settings from 1 to 5 but no clear specification is available for what these values may be in actuality. This experiment aims to convert these settings into tension values. Thus, the tension is recorded for each of these settings at the first tension sensor (pretension) to get a clear picture of the distribution of tension for a single value and its increments as the setting in the brake is increased.

To find out the pretension values for their respective mechanical brake settings, each setting was tested with five experiment trials and their respective observed values of tension in centi-Newton (cN) were noted down. Note here that pretension was the only parameter varied and every other input parameter was kept the same to isolate its behaviour.

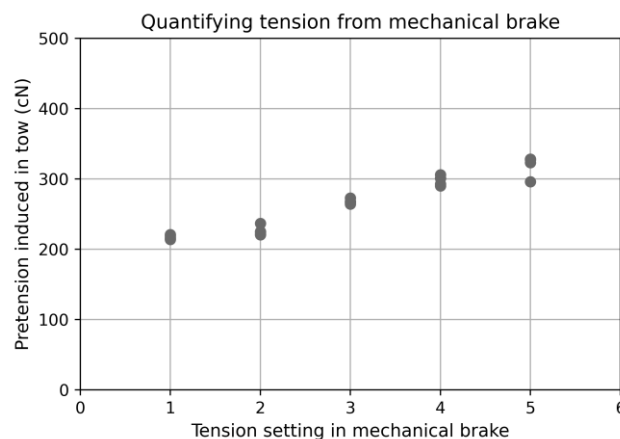


Figure 3.3: Induced pretension in tow via a mechanical brake

Figure 3.3 above shows that for each mechanical brake setting (x-axis), there is an observable increment in its corresponding pretension value in centi-Newton (y-axis). The tension at the first brake setting is 218 cN and it increases up to 318 cN at the fifth setting of the brake. The difference in increments from one setting to the next is not equal in the plot. For instance, the difference in the average value of settings 1 and 2 on the x-axis is 18 cN but the difference in settings 3 and 4 is 32 cN.

Two notable behaviours can be derived from the results of this test. Firstly, the tension with an increment in brake settings increases approximately linearly in observable values. Secondly, however, the increment between these settings is not equal which could be attributed to the presence of noise in the system. Another reason for the unequal increments may be the suboptimal performance of the brake itself. The functioning of the brake may not provide consistent tension output due to its mechanical operation but since there is no internal monitoring/sensor in the brake to provide a signal for the changes in induced forces, this part remains mere speculation until tested. These factors may influence the spreading behaviour by providing a variation in the spreading width.

### 3.3.2. Tension variation along the length of the material spool

As the tow unwinds from the spool and passes through the thread positioning piece; at each step along the length of the spool, the angle it makes from the centreline of the spool and the thread positioning piece is different (see figure 3.4), that means  $\angle l^\circ < \angle m^\circ < \angle 90^\circ$  and so on. This may cause changes in the force with which the tow is being unwound and thus to check for this behaviour, an experiment is conducted. The reason for this experiment is to identify any changes in the pretension that may be noticeable from the tow at any given point along the length of the spool which may, in turn, provide information about the consistency in tension values during the process of unwinding.

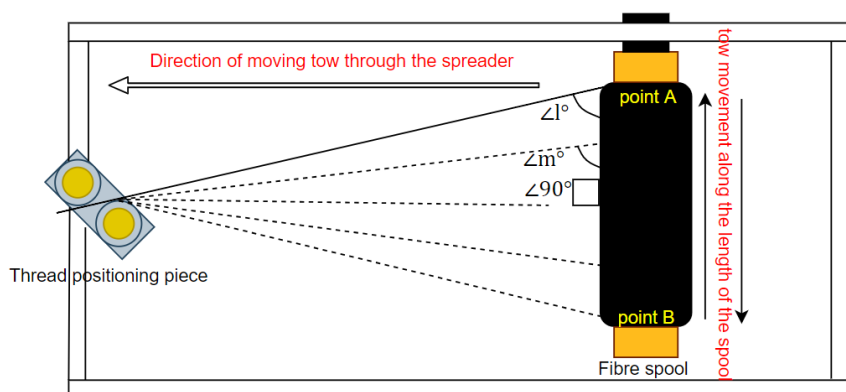


Figure 3.4: Fibre unwinding from the spool is passed through a thread positioning piece

To visualize any changes in the pretension that may occur during unwinding at any given position along the length of the spool, the tow is unwound for three cycles and the respective pretension values are noted. A cycle in this context means the unwinding of tow from one end of the spool till it reaches the opposite end and then back to the same point where it started (point A to B to A in figure 3.4).

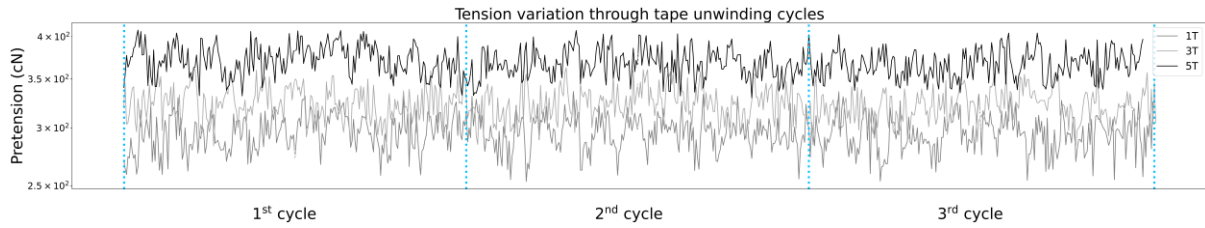


Figure 3.5: Pretension variation along the length of the spool

In the given figure 3.5 above, the x-axis represents the three continuous cycles for which tow unwinding was done and the y axis represents the pretension in the tow recorded at the first tension sensor. The three data lines in the plot labelled '1T', '3T' and '5T' are the tension sensor outputs recorded for three different settings of the mechanical brake (setting 1, 3 and 5). Upon visual inspection, no such dips or elevations are noticeable as cycles change that surpass the variations of the signal plotted from the tension meter itself. On observing the pretension variations in the plot, it may be appropriate to assume that the pretension in the tow at any given point on the length of the spool is regular and no drops or increase in the tension is contributed by the position of the tow during unwinding itself.

### 3.3.3. Influence of pretension on spreading behaviour

This experiment is performed to check for the effect pretension on the spreading behaviour. To investigate the pretension influence; the spreading width of the tow and the overall tension at the second tension meter (final tension), after the tow passes through the five spreader bars, are compared to the pretension values.

The LabVIEW program that controls the tow spreader and produces data as described in section 2.1.2 generates a text file with tension in the tow at the first and second tension meter thus providing valuable information about the tension changes in the tow at the start and the end of the spreading unit. Those values are noted for each mechanical brake setting along with the spreading width of the tow at the 5<sup>th</sup> spreader bar to quantify the pretension's influence on spreading behaviour.

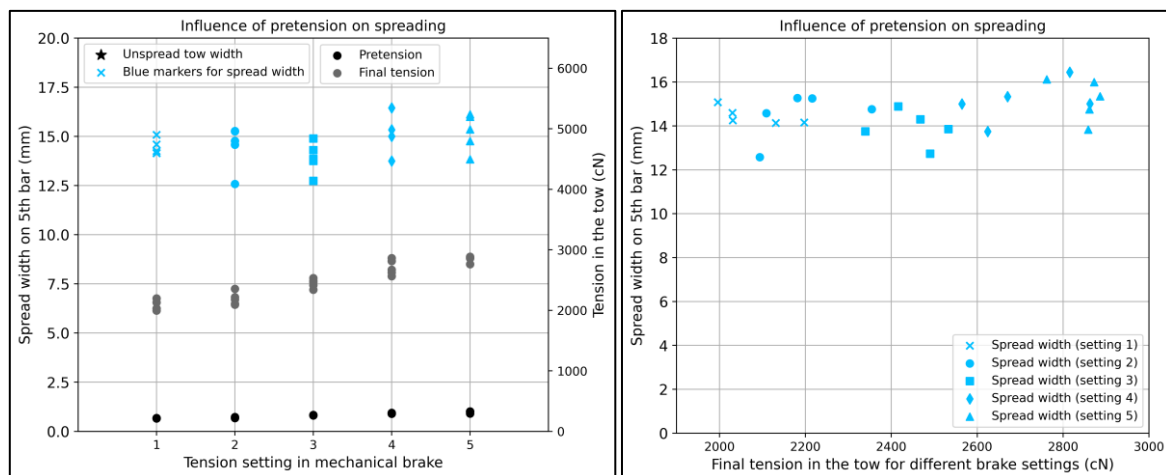


Figure 3.6: a): Influence of pretension on spreading b): Spread width-tension distribution for pretension

Figure 3.6 a) shows the spreading width on the primary y-axis (y1) along with the relationship between tension at the first and second tension meter on the secondary y-axis (y2) against different tension settings in the mechanical brake (x-axis). The pretension (at first tension meter) increases from approximately 218 cN to 318 cN and the final tension (at second tension meter) increases from approximately 2000 cN to 2900 cN. The spreading width (y1 axis), however, shows no observable trend.

In figure 3.6 b), a relationship between the spreading width distribution and final tension distribution is quantified. The spreading width distribution (y-axis) is plotted against the final tension distribution (x-axis) for the different mechanical brake settings. The spreading width distribution is between 12.5 mm to 16.5 mm with tension variation of approximately 2000 cN to 2900 cN.

The tensions in the two tension meters in figure 3.6 a) show an increase in values as the setting on the mechanical brake changes from 1 to 5. There is also a build-up of tension that can be noticed by observing the initial and final tension for each mechanical brake setting. The spreading has no visible trend as can be seen in the plotted data in both figure 3.6 a and b. This information suggests two notable influences of pretension: One, as the tow passes through the spreading unit, the tension in the tow increases. Two, this increase in final tension does not appear to affect the spreading width. The presence of tension, although, could spread the tow from 8mm unspread width to around 14mm on average.

The increase in tension may be attributed to the presence of friction in the spreader bar-tow contact. Since the spreader bars are fixed and the tow comes in contact with all of them, there will be a certain amount of friction present between the tow and the bar surface [50]. It may be the reason for the increase in tension between the two tension meters. This idea is explored later in the report as a part of the friction study (see section 3.4.4).

This test shows that spreading width does not appear to be affected by the induced pretension. This agrees with the result of pretension from the studies conducted by Irfan et al. [34] and Amir [29] where it was concluded that spreading of fibres was independent of pretension acting on the tow. Although, in this study, the test may be limited by the testing range (~100 cN) of pretension induced by the brake, which could be too small to cause any visible changes in the width. Perhaps, to reach a confident conclusion, a mechanical brake with a higher tension range may be used as a suitable solution for confirmation of this result.

In sum, while there is an increment in tension observed through the mechanical brake, its influence does not display a trend in the distribution of spreading width. It can be assumed that the effect of pretension on width is still unknown due to the small testing range that was available. The test, nevertheless, raises questions about the relationship between pretension and final tension in the tow and creates a necessity to explore the phenomenon behind the changing tension values.



### 3.4. SPREADING UNIT

The spreading unit comprises of five spreader bars arranged in a specific orientation to facilitate the spreading process through the induction of mechanical forces acting on the fibre bundles (section 1.2.3). Several parameters can be tested in the spreading unit to make decisions about what the ideal spreading unit orientation should comprise (figure 3.7). Parameters in the spreading system that can be changed are distance, height and length between the spreader bars. Through these parameters, the contact angle between the tow and the spreader bar or the 'wrap angle' can also be adjusted. Additionally, the spreading unit volume allows for up to seven spreader bars to be added to the frame. Lastly, the spreader bars can be fixed or allowed to rotate. Therefore, the following subsections test different aspects of the unit that may affect the spreading of tow.

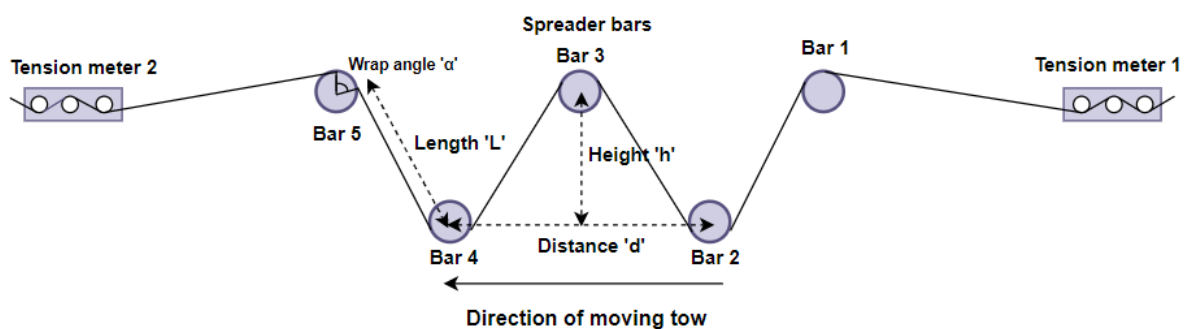


Figure 3.7: Representation of spreading unit

#### 3.4.1. Influence of number of bars on spreading behaviour

For selecting the ideal number of spreader bars needed to spread the tow to its maximum potential for a given set of input parameters, an experiment is done to check for how each spreading bar contributes to the changes in the width of the tow as it passes through them.

A sample size of 5 runs is used to measure the spreading width on each bar for the same set of input parameters (see Table 3 for baseline parameters). As the tow runs over the spreader bars, the width on the top of each spreader bar is noted down (see figure 3.8). Since the camera is only present above the 5<sup>th</sup> spreader bar, the width of the tow is measured on the other spreader bars with a measuring tape.

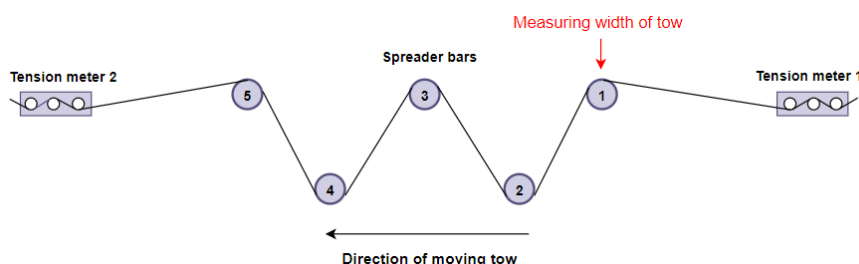


Figure 3.8: Setup for testing the influence of the number of bars

In figure 3.9 given below, the spreading width (y-axis) is plotted against each bar (x-axis). The star in the plot represents the width of the unspread tow (8mm). As is shown in the plot, the average width of the tow on the first bar is 8.5 mm, the second bar is 12.9 mm, the third bar is 15.1 mm, the fourth bar is 15.4 and the fifth bar is 15.9 mm.

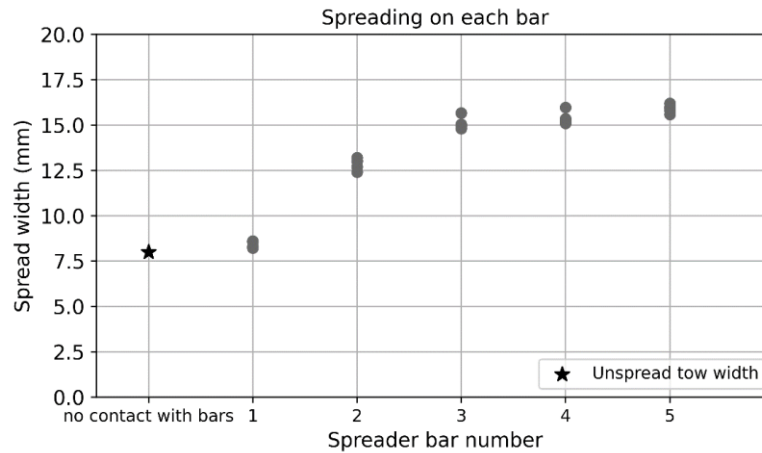


Figure 3.9: Spreading relationship with the number of bars

From the tow's unspread width of 8mm, an increase of 0.5 mm in width is observed on the first spreader bar. This changes at the second spreader bar where an increment of 4.4 mm is seen and a 2.2 mm increment is seen on the third bar. Beyond the third bar, the increments in width are much smaller of 0.3 and 0.5 mm on the fourth and fifth bar respectively. Therefore, a trend is visible where the increase in width is high till the third bar beyond which the trend plateaus and this implies that the spreading of the tow stabilises. Thus, this behaviour of bars can be categorised into two zones of spreading; the first zone which has a larger amount of spreading occurring in the first three spreader bars and the second zone which suggests that adding additional bars after three have a smaller contribution to spreading.

The result above differs from the results in Irfan's study [26] where it was found that the first spreader bar caused the maximum spread and while any additional bars did increase the width slightly, the increase was not significant. This was also the idea proposed by Wilson [27] in the theoretical model of spreading width prediction. However, the experimental setup in Irfan's study involved a tow being attached to a dead weight and subjected to tension cycles. . A tension cycle here refers to a back-and-forth motion of the tow over a spreader bar. Therefore, it may be assumed that the spreading behaviour of the tow as it is subjected to tension cycles and as it runs over the spreader bars is not equivalent hence the results for the point of spreading stability do not align.

### 3.4.2. Rotating and fixed bars

In the design of the tow spreader, the spreader bars can be fixed or allowed to rotate. The experiment aims to decide on a suitable option of bar motion, where the tension recorded in the second tension meter (final tension of the tow) is used as a judgement parameter. Figure 3.10 below shows a tension relationship between the fixed and rotatable bars (y-axis) against a sample size of 5 runs (x-axis).

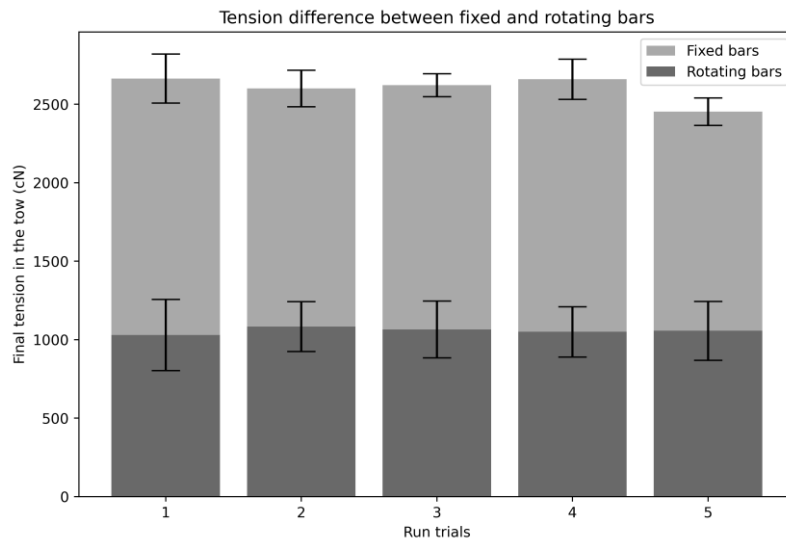


Figure 3.10: Tension output with fixed and rotating bars

In the figure, it can be observed that the average tension in the tow moving through fixed bars is approximately 2.5 times the tension of the moving tow through rotatable bars. From the previous experiment, it was found that the pretension induced from the mechanical brake was small, which suggests that to generate more tension in the tow, fixed spreader bars need to be used. Rotating bars do not generate sufficient tension, hence, fixed spreader bars appear to be a more suitable option. This, however, can be changed if the high tension in the fibre creates fibre damage.

### 3.4.3. Influence of wrap angle on spreading behaviour

Wrap angle is the angle of contact the tow makes with the spreader bar (figure 3.11). Changing the height, distance and length between the spreader bars change the wrap angle thus the wrap angles as an input parameter can collectively check the influence of geometric changes in the spreading orientation on the spreading behaviour. However, in this study the wrap angle is adjusted using by changing the height and distance between the bars and the influence of length is checked separately.

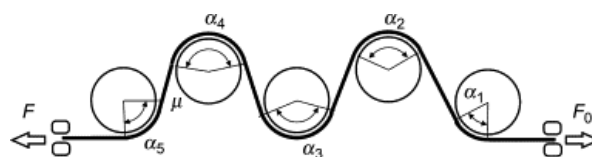


Figure 3.11: Representation of wrap angles in spreader bars [50]

The changes in the spreader bar orientation are illustrated in figures 3.12 a, b and c given below with setup (a) having the smallest wrap angles and setup (c) having the largest wrap angles. For the same input parameters, these three bar orientations are tested for their effect on the spreading width observed on the 5<sup>th</sup> spreader bar.

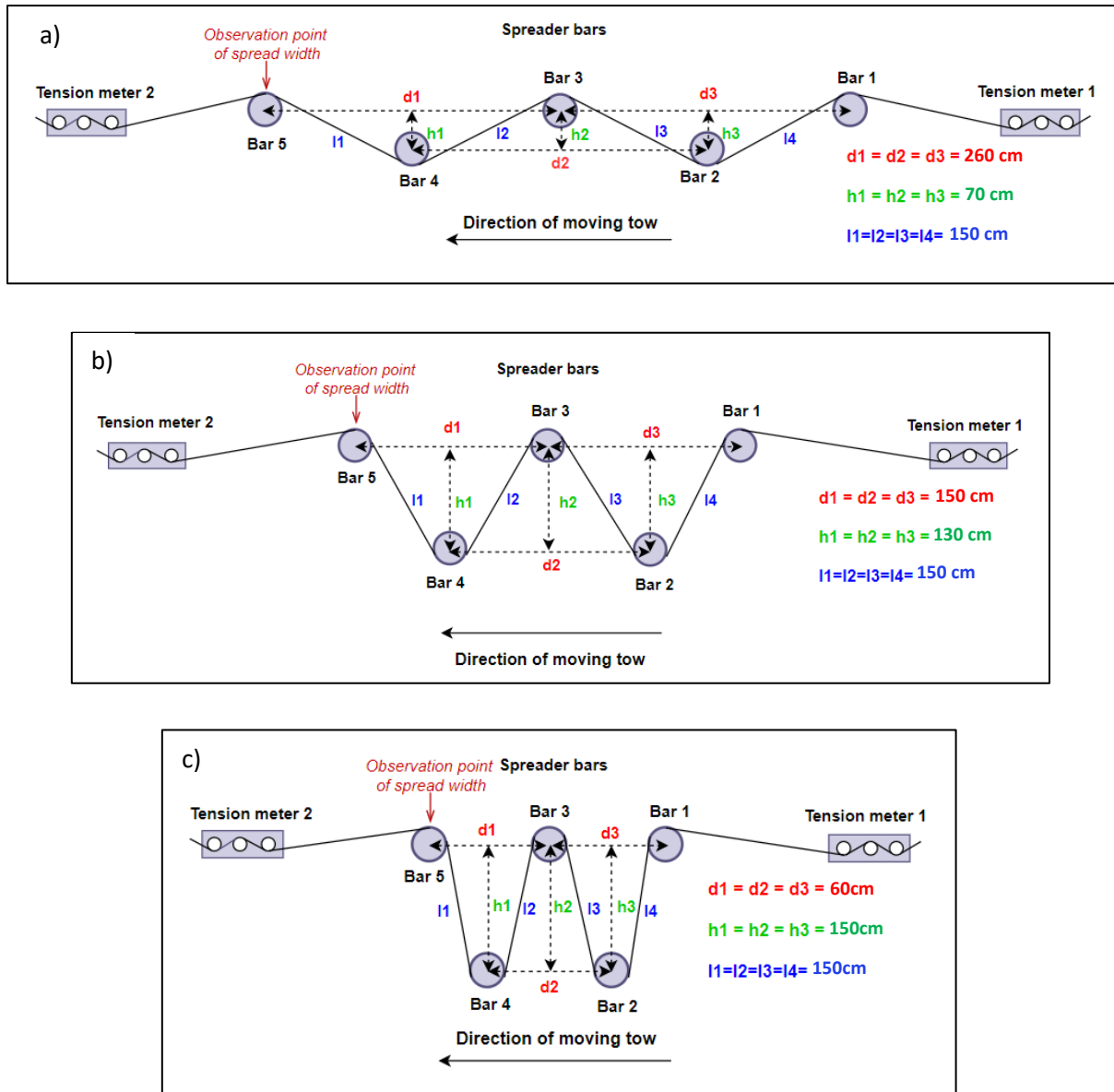


Figure 3.12: a) Bars orientation 1 b) Bars orientation 2 c) Bars orientation 3

Figure 3.13 a) below shows the spreading width on the primary y-axis ( $y_1$ ) along with the pretension and final tension on the secondary y-axis ( $y_2$ ) plotted against the different sum of wrap angles (x-axis). Y2 axis displays that the final tension increases for constant pretension. The final tension (at the second tension meter) increases from approximately 1000 cN to 4000 cN. The spreading width ( $y_1$  axis) is observed to increase from approximately 9 mm to 14.2 mm on average.

In figure 3.13 b), the relationship between the spreading width and final tension is quantified. The spreading width distribution (y-axis) is plotted against the final tension distribution (x-axis) for varying

wrap angles. The spreading width distribution is between 9 mm to 16mm with a tension variation of approximately 1000 cN to 4000 cN.

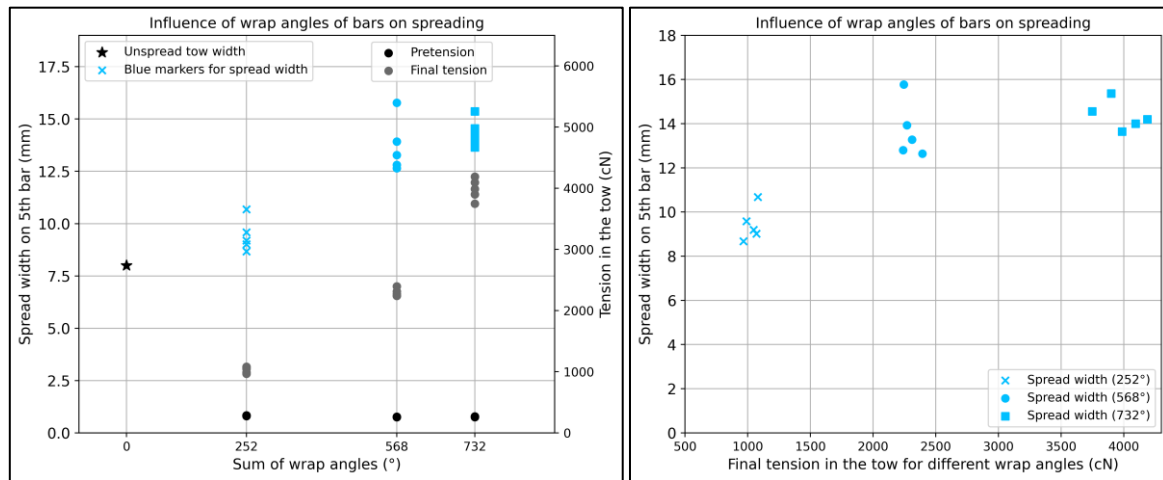


Figure 3.13: a) Influence of wrap angles on spreading b) Spread width-Tension distribution for wrap angles

Figure 3.13 a) shows an increase in tension and the spreading width as the sum of the wrap angles increase. This happens so while pretension shows no variation. Figure 3.13 b) displays spreading width increase as final tension in the tow increases for increasing wrap angles. This suggests that wrap angles and/or tension affect the spreading behaviour and are directly proportional to it.

Certain studies on tow spreading in literature have had differing results for the role of tension in spreading behaviour. Wilson’s mathematical model stated that tension had no impact on the spreading width and the primary parameters influencing the spreading were the length and angle between the bars [27]. A possibility in the model, however, may be that changing the length and the angle between the spreader bars itself could change the wrap angle and by extension, the tension in the fibre tow.

Wilson’s model was further extended by Irfan [26] where the tension was included as a parameter for spreading and the results in this test agree with his findings. There were two notable observations in his study; first, that spreading increases up to a certain increase in tension and then stabilises and second, a higher amount of tension can lead to fibre damage. For the tow spreader in this project, the tension in tow never reached a level high enough to cause fibre damage and the stability of the spreading width of the tow was ensured by using five spreader bars (as was established in section 3.4.1).

As was noted earlier, the results in this experiment may suggest that an increase in tension causes the fibres to spread. This speculation, however, contradicts the results of the test for pretension’s influence on spreading (section 3.3). In the said test, with increasing pretension, the final tension in the tow increases by  $\Delta 1000$  cN approximately but does not affect the spreading behaviour. Whereas with increasing wrap angles, the final tension increases by  $\Delta 3000$  cN and causes the spreading width to increase by 5 mm roughly. Two known parameters changing with changing wrap angles are tension and contact area of the tow with the spreader bars. Therefore, it may be reasonable to assume that

tension alone may not be sufficient to spread the fibres and the contact area is an additional parameter that can be further investigated for its effect on the spreading behaviour.

If the assumption of tension affecting the spreading width holds weight, this test presents an opportunity to study the mechanics of fibre spreading over bars. The forces acting on the fibres in the tow can be analysed to develop a theory for the spreading interactions on a microstructural level. To initialise this, friction interaction between the tow and spreader bars is analysed and its relationship with tension is speculated upon.

### 3.4.4. Determining the coefficient of friction between tow and spreader bars

The role of friction in tow spreading can be divided into two interactions; one is of the **tow and the spreader bar** and the second is **fibre-fibre contact** (see figure 3.14) [51]. The tow and spreader bar friction on a larger scale can be analysed through a simple Coulomb friction model and a suitable way to do that is with the Capstan equation or the Eytelwein's equation explained below. Through the presence of tension meters, it was feasible to determine the friction behaviour between the fibre tow and spreader bar but determining fibre-fibre friction is more complex and thus this analysis is not included within the scope of this project.

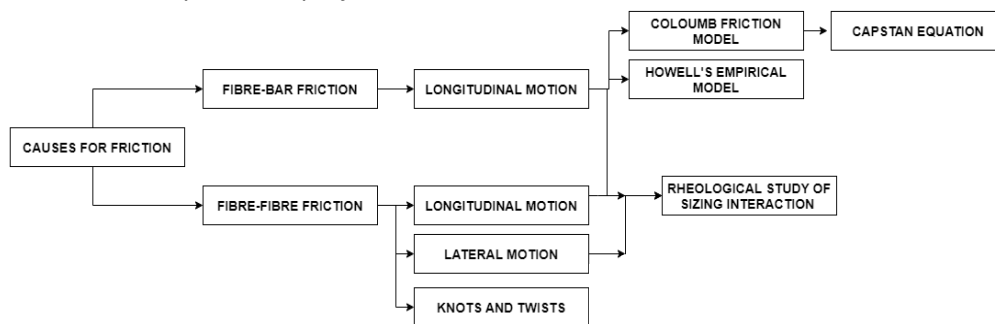


Figure 3.14: Analysis of friction in the tow during spreading

The Capstan equation provides a relationship between the entry and exit tension/force of a belt over a cylindrical bar with the coefficient of friction and the wrap angle ' $\alpha$ ' of the belt with the bar (see figure 3.15). The equation determines a multiplicative response of the frictional force acting on the belt area in contact with the bar thus explaining the tension increase that is experienced when the belt winds over the cylinder. In the Capstan equation given below:

$$T_2 = T_1 e^{\mu_s \alpha}$$

or

$$\frac{T_2}{T_1} = e^{\mu_s \alpha} \quad \dots \text{equation 3.4.1}$$

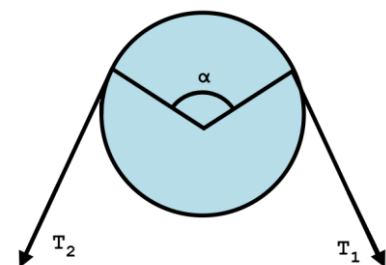


Figure 3.15: Schematic of a belt wrapped over a cylinder

Where  $T_1$  is the tension in the belt upon entry and  $T_2$  is the increased tension upon exit.  $\mu_s$  is the coefficient of static friction and  $\alpha$  is the angle of contact/wrap angle of the belt around the bar in radians.

From the equation above, it is clear that the role of friction is what causes resistance for the belt from sliding over the cylinder with the wrap angle being the control factor for the amount of tension increment.  $T_2$  is the maximum tension value that needs to be overcome to make the belt slide completely. If the cylinder were to be frictionless, the two values of tension  $T_1$  and  $T_2$  would be equal. In the figure to the right (see figure 3.16), an infinitesimal portion of the belt is analysed through its free body diagram to explain the theory behind the capstan equation. For a belt with tension  $T$  over the rod,  $d\theta$  is the angle of wrap which is very small creating an additional tension  $dT$  on the exiting belt. The frictional force  $F_f$  acts in the opposite direction of the belt motion and a normal force  $dN$  acts upon the belt in the positive y-direction. Since the system is in equilibrium, the net force acting on it will amount up to zero. On solving the vector equations in the x and y direction, the result obtained is capstan's equation for maximum tension without slip.

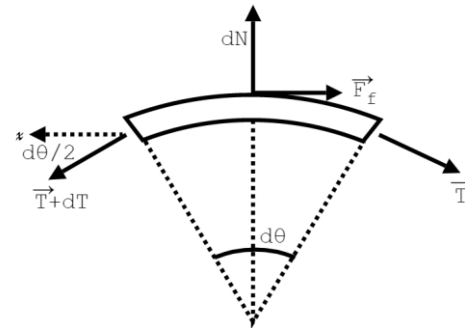


Figure 3.16: Schematic of a very small slice of belt over the rod

For a system where a belt goes over multiple cylinders (see figure 3.17), the effect of wrap angles is cumulative i.e. each of the angles of contact is added to enter into the capstan equation for getting the net tension output in the belt due to the winding system. It is important to note that the orientation of the wrap angles makes no difference in the tension generated. Thus, the equation becomes:

$$T_5 = T_0 e^{\mu_s(\alpha_1 + \alpha_2 + \alpha_3 + \alpha_4 + \alpha_5)} \quad \dots \text{equation 3.4.2}$$

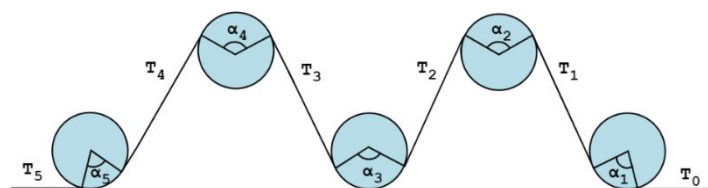


Figure 3.17: Schematic of a spreading unit to calculate tension ratios

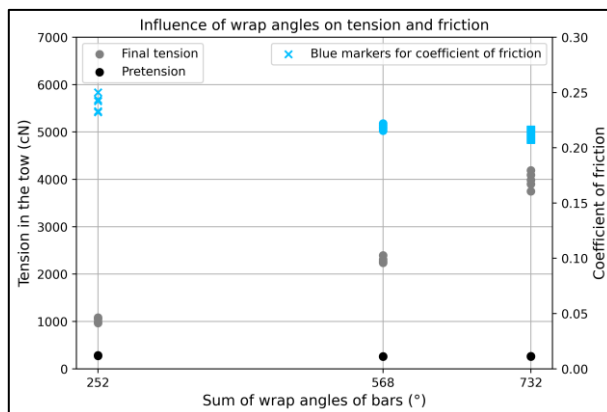
Application of capstan's equation to understand tension generation in tow spreading can be done by assuming that the fibre tow is a continuum. The tow then can be assumed to mimic the role of a rope or a belt to simplify the analysis for tension generation. Thus, the above equations provide the tension ratios through the system due to the tow-bar contact. During the process of spreading, it is important to keep caution of the wrap angle of the tow around the spreader bars. Since the increase in tension is exponential and a regulated tension through the system is desirable for even spreading, smaller

wrap angles may be better suited, as was observed in yarn winding mechanisms [50] and a balance between the number of bars and their configuration can be used to control the amount of tension.

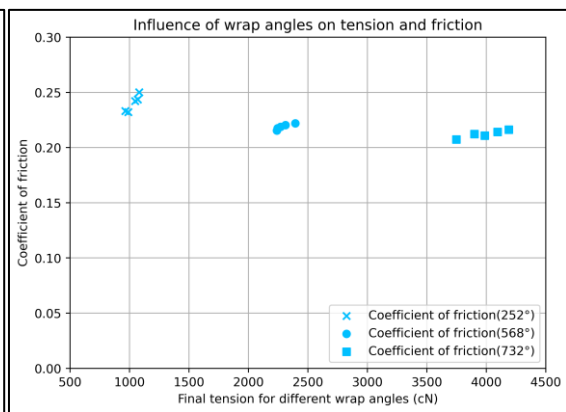
To calculate the coefficient of friction; the input values that can be changed are the sum of wrap angles and  $\frac{T_5}{T_0}$  ratio. Therefore, three approaches were taken to determine the coefficient of friction from equation 3.4.2:

- By varying wrap angles, the value of  $\sum \alpha$  is substituted for different configurations in the capstan equation.
- By varying pretension, the  $\frac{T_5}{T_0}$  ratio is varied to check for their corresponding coefficients of friction.
- Over the course of experimental runs, it was noticed that an increase in speed caused an increase in tension (see section 3.5) therefore the winding speed is varied and its  $\frac{T_5}{T_0}$  ratio is substituted in the capstan equation.

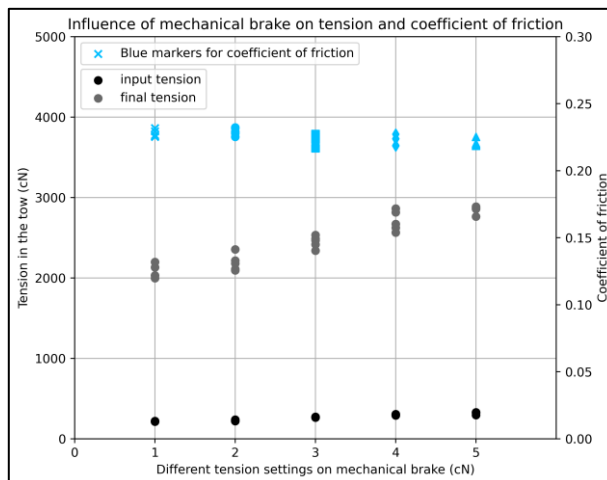
Subplot (a)



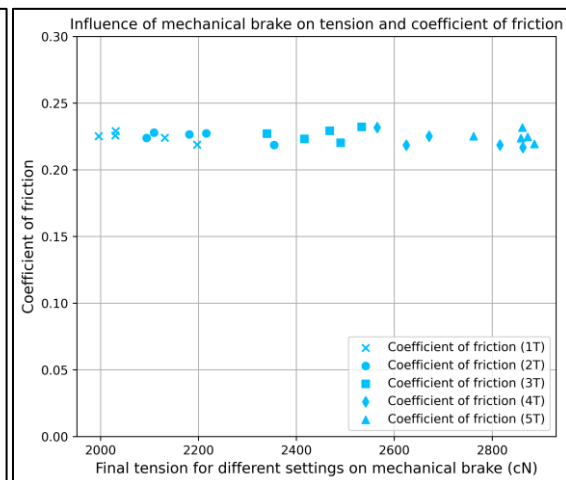
Subplot (b)



Subplot (c)



Subplot (d)





Subplot (e)

Subplot (f)

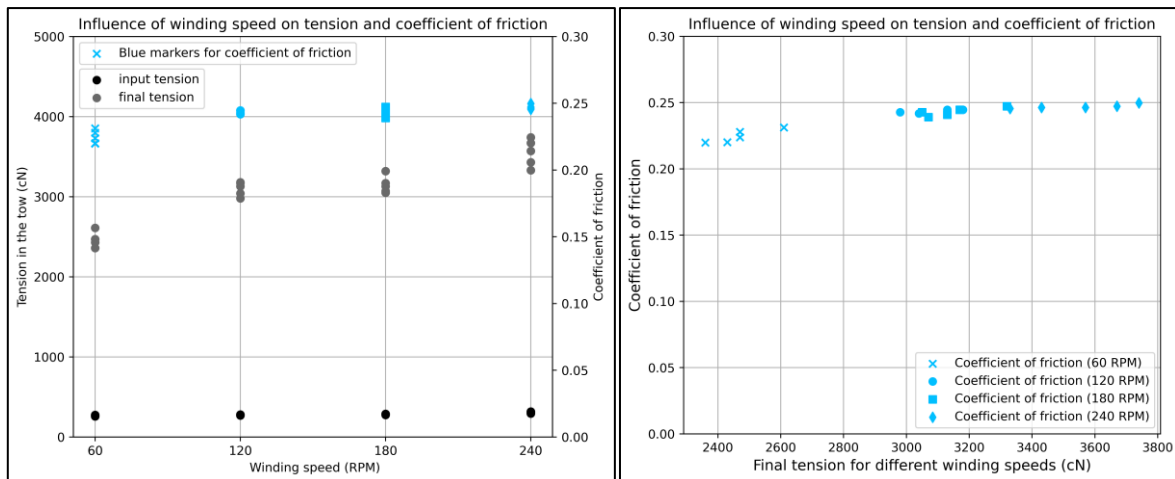


Figure 3.18: Influence of input parameters on coefficient of friction

In figure 3.18 above, the individual plots represent the following:

- Subplot a: The plot shows the pretension and final tension on the primary y-axis (y1) along with the coefficient of friction on the secondary y-axis (y2) and the sum of wrap angles on the x-axis. While the pretension for increasing wrap angles remains the same, the final tension increases from 1000 cN to 4000 cN and the coefficient of friction values lie between 0.2 and 0.25.
- Subplot b: The plot shows the distribution of coefficient of friction as a function of final tension distribution for varying wrap angles. With increasing tension values, a slight decrease in friction coefficient values can be noticed as an overall trend.
- Subplot c: The plot shows pretension and final tension on the primary y-axis (y1) along with the coefficient of friction on the secondary y-axis (y2) and the mechanical brake settings on the x-axis. The pretension increases from 218 cN to 318 cN, the final tension increases from 2000 cN to 2900 cN and the coefficient of friction values lie between 0.2 and 0.25.
- Subplot d: The plot shows the distribution of coefficient of friction as a function of final tension distribution for varying brake settings. The friction coefficient circles around 0.23 as tension increases and no positive or negative slope is observed.
- Subplot e: The plot shows pretension and final tension on the primary y-axis (y1) along with the coefficient of friction on the secondary y-axis (y2) and the winding speeds on the x-axis. The pretension increases from 266 cN to 307 cN, the final tension increases from 2400 cN to 3700 cN and the coefficient of friction values lie between 0.2 and 0.25.
- Subplot f: The plot shows the distribution of coefficient of friction as a function of final tension distribution for varying winding speeds. The friction coefficient approaches a value of 0.25 and stabilises.

The common observation found in subplots 3.18 a,c,e is an increase in final tension as wrap angles, tension setting in mechanical brake and winding speed increase respectively. Another common observation between 3.18 subplots b,d,f shows that the coefficient of friction distribution lies between 0.2 to 0.25. However, the coefficient of friction with increasing wrap angles seems to have a small negative slope while the coefficient of friction with increasing tension setting and winding speed have a roughly horizontal distribution.

The negative slope of the coefficient of friction distribution as wrap angles increase suggests that there is an additional phenomenon that affects the friction behaviour as the tow contact area and the tension in the tow increase. The relationship between friction and tension or 'pressure' was observed by Cornelissen [51] while investigating the tow interaction with a metal drum in a Capstan experimental setup. He observed that with increasing tension, the apparent coefficient of friction based on the Coulomb friction model decreased. It was suggested that the coefficient of friction was dependent on the load it was subjected to. This observation agrees with the results in subplots 3.18 a and b. With a tension increase of approximately 3000 cN, the coefficient of friction values gradually decrease. Change in wrap angles changes the tension and the contact area of the tow with the spreader bar which may imply that either one or collective of the two parameters change the friction behaviour of the tow with the bars. Whereas the increase in tension with increasing pretension and winding speed does not appear to affect the coefficient of friction.

A study done by Chakladar et al. [52] while investigating the effect of carbon fibre tow size on the coefficient of friction found that for increasing size of the tow (3k to 12k), the coefficient of friction values increased but ultimately stabilised at 0.21 as it approached the 12k tow. This suggests that if the stability of the coefficient friction value remains the same for an increasing tow size beyond 12k, then the coefficient of friction values observed in the results above (0.2-0.25) for a 24k carbon fibre tow fall close to this value of 0.21.

Nevertheless, a further investigation into these observed trends through extensive experiments may be beneficial. If these phenomena/behaviours are identified, it may provide an insight into some 'passive' parameters affecting the spreading behaviour that haven't been identified yet.

### 3.4.5. Influence of length between spreader bars on spreading behaviour

The previous experiment to check for the influence of wrap angles on spreading behaviour was done by adjusting the wrap angles with a constant length between bars and only the height and distance were changed. The goal of this experiment is to specifically check for the influence of length between the spreader bars while keeping the wrap angles constant. The results from this investigation may provide an insight into how far apart the spreader bars must be to provide maximum spreading and how this length changes the width of the spread tow.

The test consists of three different spreader bar configurations with varying lengths between the spreader bars while keeping the wrap angles constant. A sample size of 5 runs was analysed and the spread width was observed through camera images on the 5<sup>th</sup> spreader bar.

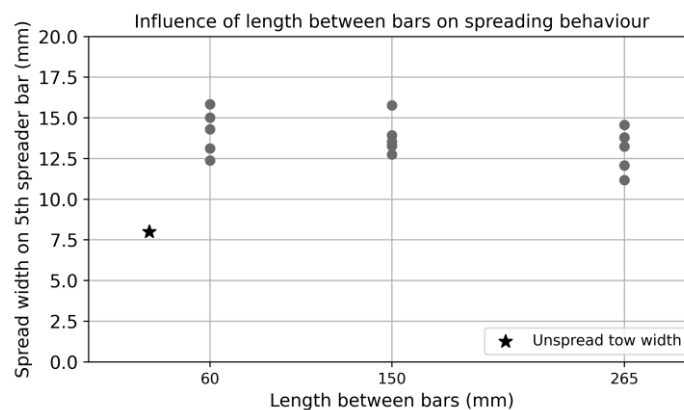


Figure 3.19: Influence of length between bars on spread width

Figure 3.19 above shows the relationship between the spreading width obtained (y-axis) and the length between bars for different spreader bar orientations (x-axis). The average spreading width observed for 60 mm length is 14.3 mm, for 150 mm is 13.85 mm and for 265 mm is 12.97 mm.

The spreading width as length increases from 60 to 150mm decreases by 0.45 mm and as the length increases from 150 to 265 mm, the spreading width decreases by 0.88 mm. This implies that length between bars contributes to the final spreading width by acting inversely proportional to it. It further suggests that at some point during the spreading process, there may be a loss of spread width for the same wrap angle but increased length. This may occur if the fibres in the tow between two spreader bars try to reach their initial unspread state due to a possible local loss of tension i.e. try to reverse to their original shape. This causes the following spreader bars to compensate for the loss in spreading width instead of spreading the tow more.

It is possible to understand this behaviour further by performing a series of experiments. Firstly, for the same setup described above, spreading on each bar can be observed to check for any loss of width and subsequent evolution of spreading. This may indicate how much loss in width occurs at each spreading stage and whether the positions of all spreader bars contribute to this behaviour. Two, for the same setup stated above, the width of the tow at the centre between the spreader bars can be compared to that on the edges near the bars for quantifying any loss in spread width locally.

### 3.4.6. Influence of heat on spreading behaviour

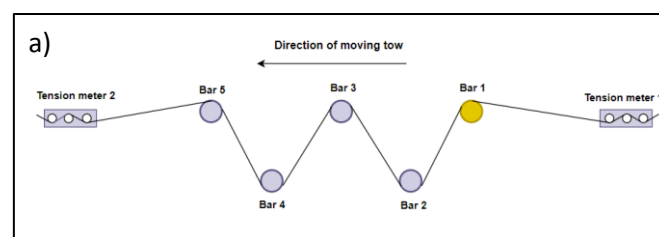
Fibres in the supplied material are most often coated in 'sizing' and the sizing is composed of silane coupling agents that are responsible for the impregnation quality, various additives to control static behaviour, lubrication, binding etc and 'film formers' that are primarily responsible for protecting the fibres in the tow, holding them together before composite manufacturing and to promote the wetting of fibres [53]. These film formers are chemically similar to the target resins for the fibres [54]. During experiment runs, it was speculated that the presence of sizing in the fibres was the cause of reduced spreading because the film formers and other components in the sizing were preventing the fibres from being separated. Thus, there were two methods proposed to overcome the forces of adhesion of fibres due to sizing:

- 1) Using force/high tension to break the adhesion in fibres: High tension in fibres can be used to overpower the lateral forces of sizing that are holding the fibres together. This, however, makes fibres more susceptible to damage and defeats the end goal to produce better performing composites.
- 2) Softening the sizing by using heat: Increasing the temperature of the tow may soften/melt the sizing reducing its viscosity thus allowing for fibres to spread more easily. Although the permanent effects of heating the sizing on the impregnation of fibres and mechanical properties of composites are unknown, it may be a better option to understand the spreading behaviour because the fibres wouldn't get damaged in the process.

To subject the fibre tow to high temperatures, heated bars were used with a test range of 50-125° C on the surface of the bars. Tests were done to determine the ideal temperature for spreading, the number of heated bars that should be used and the arrangement of hot and cold bars.

#### *Influence of number of heated bars*

The goal of this experiment is to determine how many heated spreader bars are needed to spread the tow until it has reached its stability point (see figure 3.20). From a spreader construction point of view, the results for this experiment can provide an insight into selecting the number of heated bars for maximum spreading. Ideally, more heated bars would facilitate higher spreading because the tow is being subjected to more consistent heat for the sizing to melt.



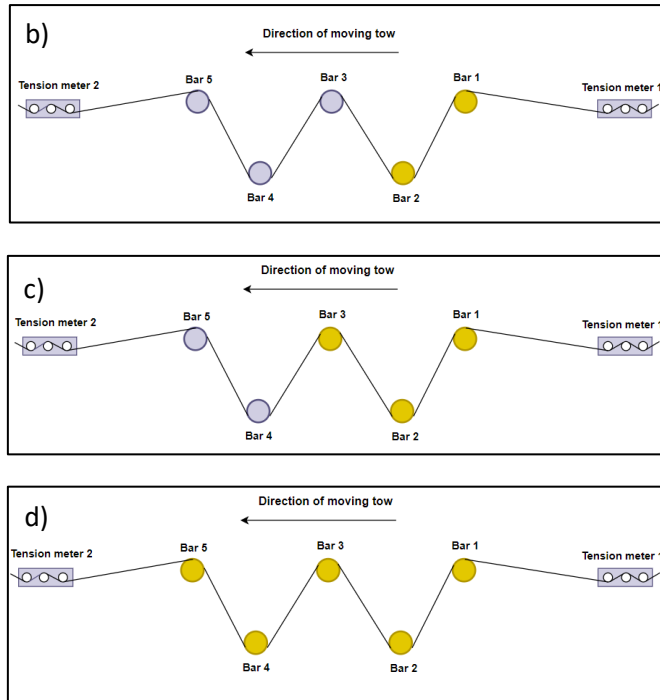


Figure 3.20: Schematics of number of heated bars placement in spreading unit (heated bar = yellow)

This test consisted of using 1-5 heated bars at 100° C with the tow spreader running on the same input parameters. Care was taken to ensure that each spreader bar had enough time to reach a stable temperature of 100° C and to do so, thermocouples were attached to each bar for monitoring the stability. The spreading width was observed on the 5<sup>th</sup> spreader bar. For the particular case of all heated rods, the measurement for the final width was taken by sliding callipers to avoid damage to the camera.

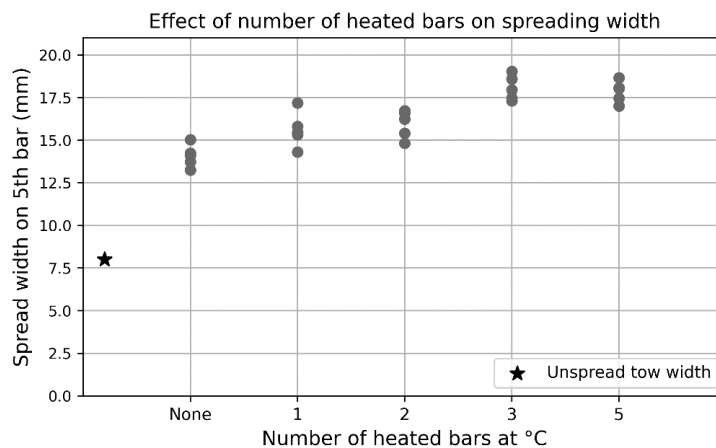


Figure 3.21: Influence of number of heated bars on spreading

In the given figure 3.21 above, a relationship between the number of heated bars (x-axis) and the spreading width (y-axis) is described. When all the bars are cold, a spreading width of around 14 mm is obtained which increases to 18 mm approximately for three heated bars and remains in a similar vicinity on using five heated bars with a spreading width of 17.5 mm.

The trend observed in this experiment is positive which means that while one heated spreader bar does increase the width of the tow when compared to no heated bars; adding additional heated bars increases the width even further. This, however, stabilises at three heated bars beyond which more heat does not seem to affect spreading. This could mean that at this point, the sizing has softened sufficiently and the maximum spreading due to heat is taking place. It is thus concluded that a sufficient number of heated bars in the tow spreader is three.

### Influence of temperature

In the previous experiment, an ideal number of heated bars were selected based on spreading width as the judging criteria. It is also important to know what temperature would work well for heating the tows. Whether the tow sizing is sufficiently softened at 50° C or it softens even more as temperature increases, this information is unknown still. Thus, the goal of this experiment is to find the optimal temperature of heated rods based on the degree of spreading of fibres. Since any data about sizing is intellectual property and thus inaccessible, predicting its temperature behaviour is complex. Which makes this experiment insightful for the operation of the spreading system using heated bars.

Three heated bars based on the previous result are placed in the tow spreader to evaluate the effect of bar surface temperature on the spreading width. The test range for the temperature is 50°C to 125°C with each increment of 25°C. Care was taken to let the temperature of the bar surface stabilise before running the tow spreader with the same input parameters. The final spreading width was observed on the 5<sup>th</sup> spreader bar.

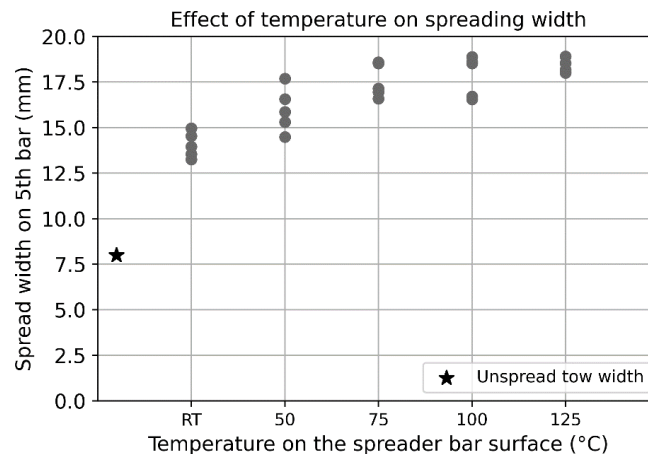


Figure 3.22: Influence of temperature on spreading width

The variation of spreading width (y-axis) with increasing temperature of the spreader bar surface (x-axis) can be observed in figure 3.22. The bars at room temperature have an average spreading width of 14 mm but the spreading width increases to approximately 18 mm at 125°C.

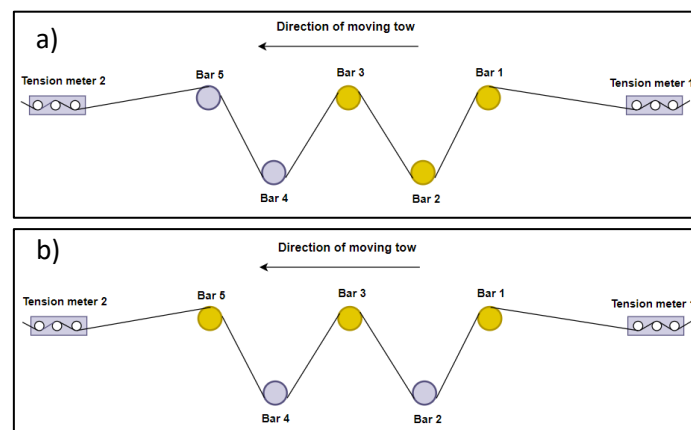
The figure shows an increase in spreading width as bar temperature increases from room temperature to 125°C. It can be seen that there is an increase in spreading width at 50°C itself which indicates that the sizing begins to lower its viscosity. It lowers further at 75°C and 100°C with an increase in spreading width but beyond this temperature, the spreading stabilises and therefore it may be reasonable to assume that the viscosity has lowered to its minimal point. Two notable things can be observed in the

figure above. One, 100°C is the point of lowest sizing viscosity and maximum spreading width so any temperature beyond this value may yield a width in the same size vicinity. Two, while 100° may appear to be sufficient, the distribution for the spreading widths at 125°C is much lower than that of 100°C. It may indicate higher stability in spreading width at 125°C which creates the need to investigate the effect of high temperature on spreading width variations for the same set of input parameters.

### *Influence of heated bars arrangement*

In this experiment, the arrangement of heated bars in the spreading unit is tested. With sufficient data collected on the ideal temperature and number of heated bars for their influence on spreading width, the last question unanswered is about the placement of the heated bars in the spreading orientation. To check for that, different arrangements of heated spreader bars were tried and tested:

- 1) 1,2,3 spreader bars (figure 3.23 a)- First three bars were heated to provide a continuous supply of heat to the fibres without any cold bars in the middle that could reduce the temperature in the sizing before they have an ample opportunity to spread. Recalling the experiment of spreading on each bar (section 3.4.1), maximum spreading occurred on the first three bars, thus, heating those bars could be a suitable option.
- 2) 1,3,5 spreader bars (figure 3.23 b)- Alternate arrangement of bars may allow for a uniform and periodic supply of heat to the fibres. If the cooling effect on fibres due to cold bars is minimal, the tows are continuously subjected to high temperature. Additionally, if the cooling effect does occur, it may be suitable to avoid placing the cold bars in the 4<sup>th</sup> and 5<sup>th</sup> position to prevent cooling of sizing and by extension the possibility of the fibres adhering together.
- 3) 1,2,4 spreader bars (figure 3.23 c)- This arrangement was selected on basis of a combination of heating and spreading opportunities. As the tow passes over the 1<sup>st</sup> and 2<sup>nd</sup> spreader bar, it gets heated up while still being in the maximum spreading zone. The 3<sup>rd</sup> cold spreader bar may reduce or not affect the temperature of the tow but due to the high temperature of the tow from the first two bars, still effectively spread the fibres. The fourth spreader bar on the other hand heats the tow again allowing for increased spreading on the 4<sup>th</sup> and 5<sup>th</sup> bars. Another advantage of this arrangement may be the same as that of 1,3,5; avoiding cooling of sizing and thus preventing the fibres from getting close together.



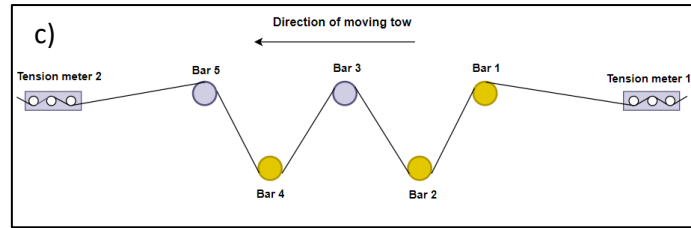


Figure 3.23: Schematics of different arrangements of heated bars in the spreading unit

Different arrangements were tested at 100°C with the same input parameters for a sample size of 5 runs each. The temperature on the bar surface was allowed to stabilise before testing and constantly monitored through attached thermocouples. Since the camera for capturing spreading width was placed directly above and close to the spreader bar, the measurements for 1,3,5 arrangement were done with sliding callipers.

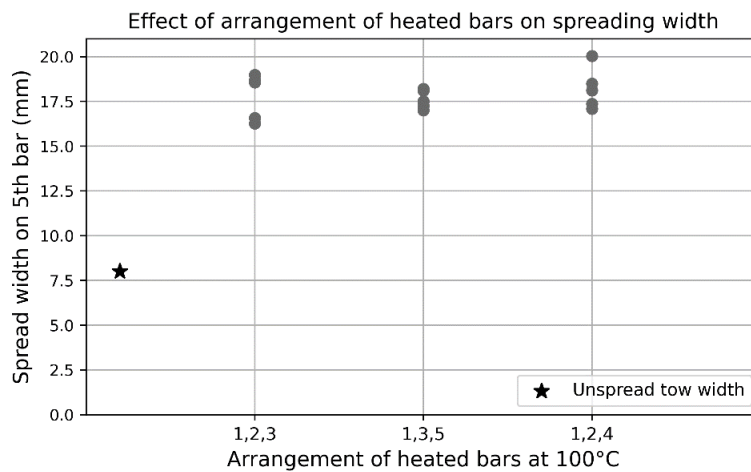


Figure 3.24: Influence of arrangement of heated bars on spreading

Figure 3.24 shows a relationship between the spreading width (y-axis) and different arrangements of spreader bars (x-axis). In the plotted data, the average spreading width of 1,2,3 bars, for 1,3,5 bars and 1,2,4 bars is around 17.5 mm.

With such a low difference in width, it is uncertain which arrangement provides an improved spreading behaviour. It may be concluded that an arrangement of heated spreader bars makes no substantial difference to the spreading width as long as the number of spreader bars and temperature of the heated bar surface is sufficient.



### 3.5. WINDING UNIT

This experiment investigates the effect of winding speed of tow on spreading behaviour. As can be recalled from the winding unit description, the stepper motor is attached to the shaft of the winding spool by a gear system that decreases the speed of winding but increases the torque which allows for tows with a higher amount of tension to be pulled. This experiment aims to determine whether the speed at which the tow is being moved through the spreader affects the spreading behaviour of the fibre tow.

Different speed inputs of 60, 120, 180 and 240 RPM are input into the spreader. The remaining input parameters are kept constant and a sample size of 5 tests is performed for each input value. The final spreading width is observed on the 5<sup>th</sup> spreader bar.

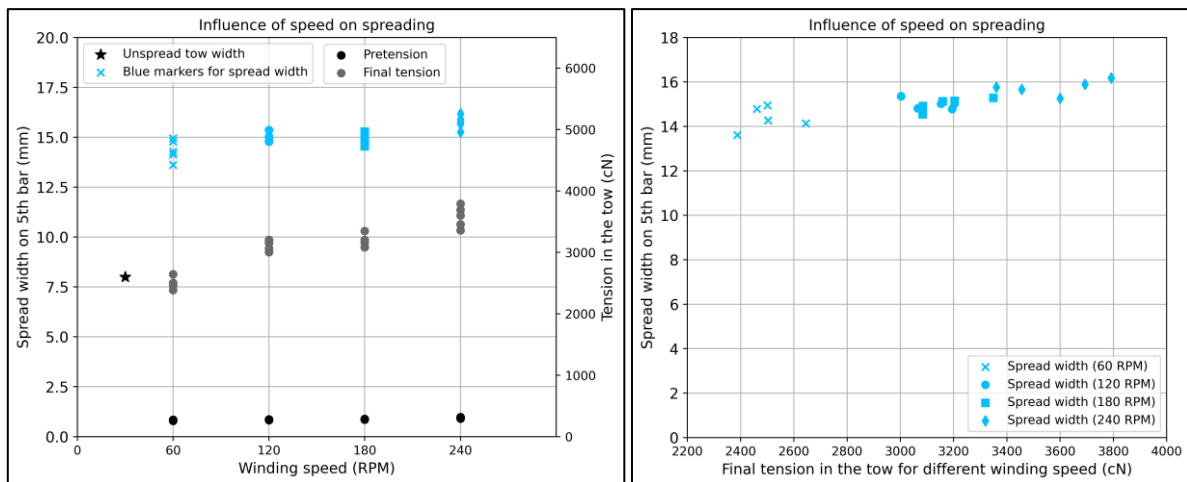


Figure 3.25: a) Influence of winding speed on spreading b) Spread width- tension distribution for winding speed

Figure 3.25 (a) describes relationships between tension in the tow and spreading width with the input winding speed. The primary y-axis (y1) represents the final spreading width of the tow and the secondary y-axis (y2) represents the pretension and final tension in the tow against the range of the winding speed in the tow (x-axis). The spreading width is observed to increase from approximately 14 mm to 16mm as the speed increases from 60 RPM to 240 RPM. The pretension with a fixed input value in the spreader changes from 266 cN to 307 cN as the speed increases. Lastly, the final tension in the tow increases from 2400 cN to 3700 cN approximately with the increase in speed.

Figure 3.25 (b) further shows the distribution of spread width obtained (y-axis) for the distribution of final tension (x-axis) as the speed increases. The distribution of the spreading width increases from roughly 14 mm at around 2350 cN and reaches up to 16mm at 3750 cN.

The width increases as the winding speed increases and a similar observation can be made for the final tension. This result does not agree with the finding of Irfan et al. [34] in his spreading study where it was concluded that a lower ‘haul-off’ speed was more favourable to the amount of spread.

The increase in width may be a consequence of an increase in final tension as has been suggested in the earlier experiments of this study as well. The increase in final tension in the tow may be due to the 40 cN increase in pretension, however, the increment in pretension is small which raises the

question of whether this increase in pretension is sufficient enough to increase the final tension by 1300 cN. This phenomenon can be further investigated and the focus of the study can be on the tension relationship with speed which by consequence may explain the increasing amount of spread with increasing speed.

### 3.6. STATISTICAL ANALYSIS

With multiple parameters influencing the spreading width collectively during a run, each input parameter may be assumed to have its specific contribution to the width through a particular empirical factor of influence. It can be visualised in equation 3.6.1 where the spreading width 'w' is a function of all the input parameters in the tow spreader. It can be further expanded upon into an empirical equation where  $a_1, a_2, a_3, a_4, a_5, a_6$  are unknown weightage factors by which each parameter influences the final width.

$$w = f(\text{pretension, wrap angle, length between bars, winding speed, number of heated bars, temperature of heated bars}) \quad \dots\text{equation 3.6.1}$$

$$w = a_1(\text{pretension}) + a_2(\text{wrap angle}) + a_3(\text{length}) + a_4(\text{speed}) + a_5(\text{number of heated bars}) + a_6(\text{temperature of heated bars}) \quad \dots\text{equation 3.6.2}$$

**Regression model:** To get an idea about these coefficients, a linear regression analysis is done through IBM SPSS tool with a data set of 25 averaged values of sample size runs and a data set of 125 values inclusive of the sample size distribution. The aim to use the two sizes of data sets is to check the contribution of the number of datasets in a regression fit. Table 6 shows the results with an R square fit of the data sets with a potential estimate error. The R square value was found to be 0.915 with an error of 0.053 for 25 data sets and 0.785 with an error of 0.0814 for 125 data sets suggesting how well the parameters perform to predict the spreading width.

Model Summary				
Model	R	R Square	Adjusted R Square	Std. Error of the Estimate
1	.957 <sup>a</sup>	.915	.887	.05310
a. Predictors: (Constant), Speed, Length between spreader bars, wrap angle, Pretension, Number of heated bars, Temperature				

Model Summary				
Model	R	R Square	Adjusted R Square	Std. Error of the Estimate
1	.886 <sup>a</sup>	.785	.775	.08145
a. Predictors: (Constant), Speed, Length between spreader bars, wrap angle, Pretension, Number of heated bars, Temperature				

Table 6: R square for input spreading parameters for 25 data sets (left) and 125 data sets (right)

Table 6 shows that as the number of data sets increased, the R square fit decreased and the standard error of estimate increased. This suggests that 25 data sets are not sufficient to predict the spreading width as an increase in data sets increased the error and lowered the R square value. However, 125 data sets do not appear to be sufficient either due to their lower R square value and higher estimated error.

*Equation for spreading width prediction:* Table 7 shows the coefficients of influence that build the predictive equations for the spreading width (equation 3.6.3, 3.6.4):

Model		Unstandardized	Coefficients Std. Error	Standardized	t	Sig.
		B		Beta		
1	(Constant)	.232	.058		3.960	.001
	Pretension	.108	.044	.179	2.458	.024
	Number of heated bars	.256	.071	.485	3.620	.002
	Temperature	.183	.060	.407	3.018	.007
	wrap angle	.468	.072	.447	6.479	.000
	Length between spreader bars	-.113	.075	-.104	-1.516	.147
	Speed	.160	.047	.247	3.412	.003

a. Dependent Variable: width

Model		Unstandardized	Coefficients Std. Error	Standardized	t	Sig.
		B		Beta		
1	(Constant)	.218	.040		5.439	.000
	Pretension	.123	.030	.184	4.071	.000
	Number of heated bars	.263	.048	.451	5.422	.000
	Temperature	.192	.041	.388	4.633	.000
	wrap angle	.462	.050	.399	9.326	.000
	Length between spreader bars	-.099	.051	-.083	-1.934	.056
	Speed	.174	.032	.244	5.438	.000

a. Dependent Variable: width

Table 7: Coefficients of input parameters for 25 data sets (left) and 125 data sets (right)

On comparing the coefficients of the two data sets, it can be observed that despite the inclusion of more runs, the coefficients of influence for each parameter are similar in values. Given below are the predictive equations for spreading width derived from the coefficients of influence calculated through the regression analysis with an R square fit of 0.915 and 0.785 for 25 and 125 data sets respectively:

$$w = 0.108(\text{Pretension}) + 0.256(\text{Number of heated bars}) + 0.183(\text{Temperature of heated bars}) + 0.468(\text{Wrap angle}) - 0.113(\text{Length between bars}) + 0.16(\text{Winding speed}) + 0.232$$

...equation 3.6.3

$$w = 0.123(\text{Pretension}) + 0.263(\text{Number of heated bars}) + 0.192(\text{Temperature of heated bars}) + 0.462(\text{Wrap angle}) - 0.099(\text{Length between bars}) + 0.174(\text{Winding speed}) + 0.218$$

...equation 3.6.4

*Individual contribution of parameters:* Table 8 below shows an individual R square value for each of the input parameters for spreading width (appendix C) for 25 and 125 data sets; these values indicate if a certain input parameter is a good variable for predicting the output width based on the input datasets. A low R square value indicates a poor performance in terms of width prediction. According to the table, wrap angle, number of heated bars and temperature of heated bars are more reliable prediction variables whereas pretension, speed and length between the spreader bars are the poor predictors of spreading width.

Independent/ Influencing parameters	Coefficient of determination (r square)
Pretension	0.003
Number of heated bars	0.582
Temperature of heated bars	0.562
Wrap angle	0.258
Length between bars	0.016
Winding speed	0.001

Independent/ Influencing parameters	Coefficient of determination (r square)
Pretension	0.001
Number of heated bars	0.503
Temperature of heated bars	0.486
Wrap angle	0.21
Length between bars	0.011
Winding speed	0.002

Table 8: R square data for each input spreading parameter

*Evaluation of regression analysis:* The linear regression model aims to analyse whether the experimental data collected can be used to predict the relationship between the spreader input parameters and the spreading width. The R squared value represents the scatter of the spreading data around a fitted regression line. Using the prediction model coefficients for each input parameter, a predictive linear equation is generated and tested. However, some caveats must be kept in mind while evaluating the data:

- The R square value of 125 data sets was lower than that of 25 data sets. This suggests that more data sets are needed to train the model better such that the predictive equation can be improved and made more accurate. A larger amount of data may improve the fit of the regression model.
- Another approach to reducing the error in width prediction is adopting a non-linear regression model instead of a linear regression model. The advantage of using a non-linear model over a linear model is that it can be more efficient for small datasets and produce a more suitable curve fitting. It is also equipped to quantify the non-linear relationships of input parameters that may exist in the tow spreader. However, the decision to select a suitable statistical model depends on the scatter of the data.
- When analysing R squared values of individual parameters; pretension, the length between bars and winding speed had a value closer to zero which suggests that these parameters did not contribute sufficiently to predict the spreading width. A conclusion may be derived that an increased density in sample size may be needed from these parameters to re-evaluate their contribution. A larger testing range for these parameters may also improve the regression model for spreading.

### 3.7. SUMMARY

This chapter described an analysis done on the parameters influencing the spreading behaviour through experiments performed. The repeatability test established the distribution of spreading width for a given set of parameters. Pretension investigation did not show any trend of how it affects the spreading width. But it was also concluded that the testing range of pretension values may be too small to have any discernible conclusions for its influence on spreading.

Increase in wrap angles on the other hand increased the width of the tape. The increase in wrap angle also caused an increase in the final tension of the tow which led to the speculation of whether spreading width may be directly proportional to the tension in the tow. This investigation further extended to an investigation into the tow-spreader bar interaction of friction which was quantified through the capstan equation and the coefficient of friction was found to be in the range of 0.2-0.25.

Results for the experiments on spreading behaviour with heated bars were quantified and it was found that the heated spreader bars increase the spreading width possibly by softening the sizing present in the fibre tow. It was also found that three spreader bars at a temperature of 125°C were an ideal configuration to facilitate maximum spreading and their arrangement was insignificant.

Finally, an investigation into the winding speed revealed that as the speed increases, the final tension in the tow along with the spreading width increase too. Based on these results, a linear regression analysis was performed to generate a predictive equation for the spreading width.

In sum, certain results in this chapter posed more detailed questions about the spreading behaviour than allowing for specific conclusions to be made but this may be beneficial nonetheless because these questions carve a trajectory for a more detailed dive into the tow spreading investigation in future studies.

## 4 Microstructural analysis of spread tow specimens

This chapter presents an investigation done on the microstructural specimens developed of spread tow. Recalling from section 2.3, a microstructural specimen of spread tow is spread fibre embedded in resin, processed for image analysis and observed under the microscope at 20x optical zoom to visualise the fibre distribution as the tow spreads at different locations of the spreading unit. Fibres during theoretical analysis, ideally, are assumed to be homogeneous (square/hexagonal) in arrangement and straight along their length but in reality, the fibres are inhomogeneous in content with a presence of tortuosity along their length [39] (figure 4.1). Therefore, a fibre investigation into the tow microstructure may provide some information about the interaction between fibres, their orientation post-spreading, fibre waviness et cetera and may also help understand spreading through a microstructural lens. This investigation aims to visualize the change in the distribution of fibres in a tow as they spread within the spreader.

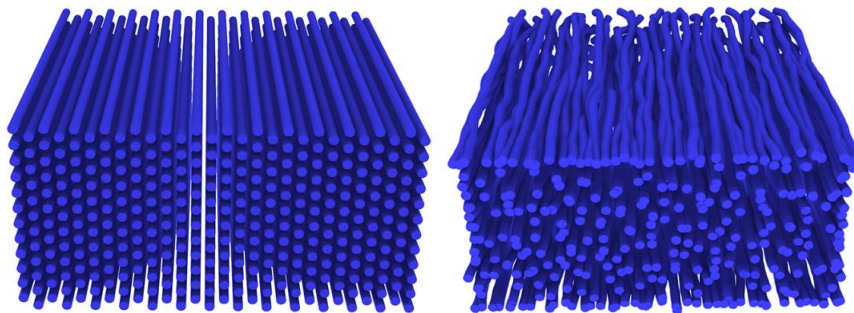


Figure 4.1: Fibres in ideal state (homogeneous and straight) (left) and real state (inhomogeneous and tortuous) (right) [55]

### 4.1. EVALUATION OF SPECIMEN'S IMAGE QUALITY

Figure 4.2 shows a zoomed in image of the specimen's microstructure. The white speckles represent the fibres embedded in a resin represented by the colour grey. While the specimen intended to display the resin and fibres only, certain manufacturing defects were noticeable. The black dashed lines in the image are scratches from the suboptimal grinding and polishing process despite an automatic polishing machine being used. There are also microcracks present as black grooves in between the fibre concentrations. This may be due to a combination of high forces through the grinding and polishing process and vulnerability of the fibre matrix interphase that made the sample more prone to cracks in that specific area. Another reason for the formation of these microcracks maybe that fibres in that particular region did not get impregnated sufficiently and a lack of resin in those local areas made the sample vulnerable to high shear forces supplied by the grinding and polishing process.

Loss of fibres from damage during the spreading process and those also damaged by the formation of microcracks is a caveat to be considered during the microstructural investigation. While the fibre damage during the spreading process was not noticeable to the naked eye, it can be expected that due to the high forces in the tow, some fibres would get broken. In the case of microcracks, during their formation, some fibres may break and get lost while being exposed to the fluids during grinding.

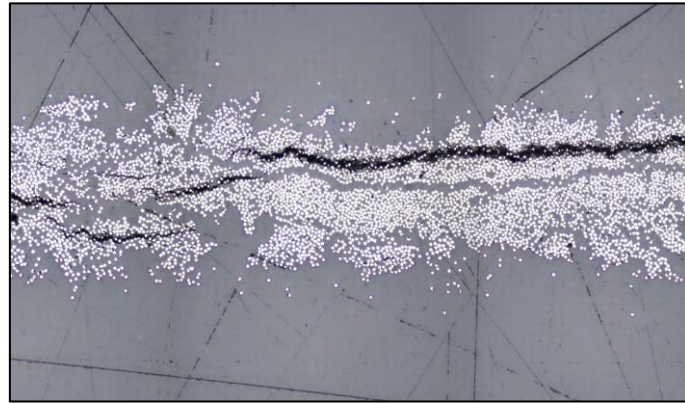


Figure 4.2: Close up of a microscopic image of tow sample

While plotting the fibre distribution across the width of the tape (explained later in the chapter), it was noticed that the fibre distribution line had some local crests and troughs significantly larger than its surrounding area (see figure 4.3a). This can be understood by observing the plot corresponding microstructure image of the specimen (figure 4.3 b) and the image of the tape (figure 4.3 c). The local crests could be attributed to the locally present high concentration of fibres (fibre rich area) in the microstructure image which in turn could be a consequence of clumped fibres present in the tow or due to the capillary action of the resin that forces the fibres to adhere to each other closely and form a high concentration area. The troughs on the other hand could be attributed to the low number of fibres in the local area which may be due to the presence of gaps in the spread tow or separation of fibres locally due to resin concentration (resin-rich area).

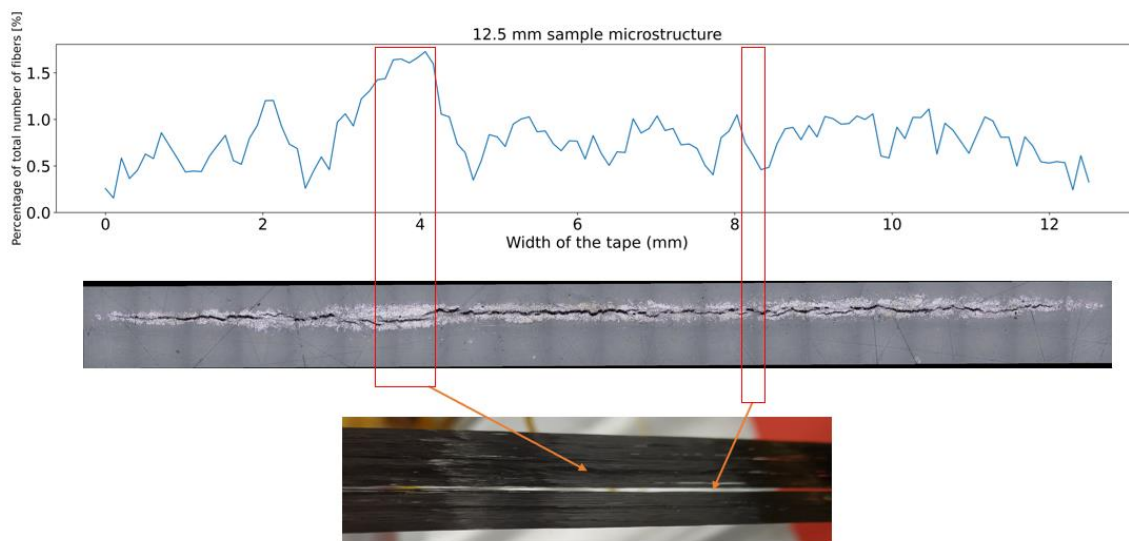


Figure 4.3: a) Fibre distribution plot (top) b) Image displaying tow microstructure (middle)  
c) Image of the spread tow (bottom)

## 4.2. SETUP FOR SPREADING VISUALISATION

The visualisation of fibre distribution is done through thresholding and pixel recognition of fibres in the microstructure image. The presence of fibres is calculated along the width of the tow by identifying shifts in colours as the processing code runs through the pixels in the image. Thresholding implies that the image to be processed is converted into a binary image of two distinct colours. This is done so because these images of the microstructure appear to be grayscale but in actuality contain different colours on the RGB (red, green, blue) spectrum. This makes object recognition through shifts in colours more complex. A binary colour image through thresholding makes it simpler for the code to understand and recognise the tiny fibres present (figure 4.4).

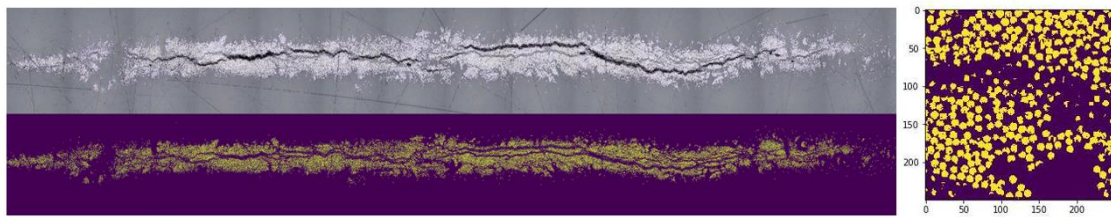


Figure 4.4: a) Original image displaying tow microstructure b) Threshold binary image c) Close up of the binary image

There were two strategies adopted to represent the presence of fibres in the specimens-

- *Percentage of the total number of fibres against spread width:* The approach to make this representation is done by calculating the number of pixels representing fibres locally and comparing it to the total number of pixels representing the fibres. For instance, if the total number of white pixels is 100 (total fibre area), the plot shows how these 100 pixels vary across the horizontal axis (width of the tow). The image is divided into multiple equal-sized pixel columns (step size) and the number of white pixels is counted for each of those blocks. This number is then used to calculate their percentage against the total number of white pixels. This approach has two control variables, thresholding limit and step size which decides the size of a column the image is split into. Their values are decided by trial-and-error quality inspection of the image and of the output plot it produces. Too small of a step size produces a plot with high noise and makes shape recognition of the tow at different spreading stages complex. These plots intend to provide a general look of the contour/shape of tow as it spreads.
- *Fibre density (fibre volume fraction) heatmaps:* This representation shows 'hot' and 'cold' areas of the presence of fibres. Hot areas represent a high concentration of fibres and cold areas represent a low presence of fibres. This is done so by dividing the threshold binary image into small square blocks and calculating the volume content of fibres present in that block through pixel recognition. This approach, too, contains two control variables, thresholding limit and step size which are decided by trial-and-error quality inspection of the image and the heatmap it produces. These heatmaps intend to show the fibre concentrations in the tow cross-section as it spreads. Histograms are also plotted for further representation of fibre volume content across the width of the tow along with the frequency of occurrence of that fibre volume content.



### 4.3. SPREAD TOW MICROSTRUCTURE

It was mentioned earlier in section 2.3 that five specimens were manufactured for microstructural investigation; one sample consisted of unspread tow embedded in resin and the other samples were taken from in between the spreader bars. The goal of this investigation is to see how the distribution of the fibres in the tow evolves as it goes from an unspread state to a spread state. The input parameters of the spreader used to generate the specimens were the baseline parameters established earlier in the study (section 2.2) hence these specimens do not represent the maximum spreading capacity of the spreader. The reason for selecting these parameters was that the distribution of spreading width with them as the input was previously investigated through the repeatability test hence the spreading width range in this test can be checked for whether it falls within the distribution. Additionally, the spreading observed on the spreader bars may be higher than that in between them due to the fanning effect the tow is subjected to while it is supported by the surface of the bar. This difference may be avoided if the length between the bars is minimised.

Figure 4.5 below is a representation of the contours of all the specimens in a single plot. The x-axis represents the width of the tow (in mm) and the z-axis represents the percentage distribution of the total number of fibres present in the tow. Values on the z-axis are a function of the step size input into the processing code. The effect of fibre-rich and resin-rich areas is ignored here and focus is shone upon the evolution of the overall shape of the tow as it spreads. The tow spreads from 8mm unspread state to 14.2 mm spread state. The final spreading width is found to be within the range of the expected distribution for the given set of input parameters. The individual images and their corresponding plots can be found in Appendix D for further reference.

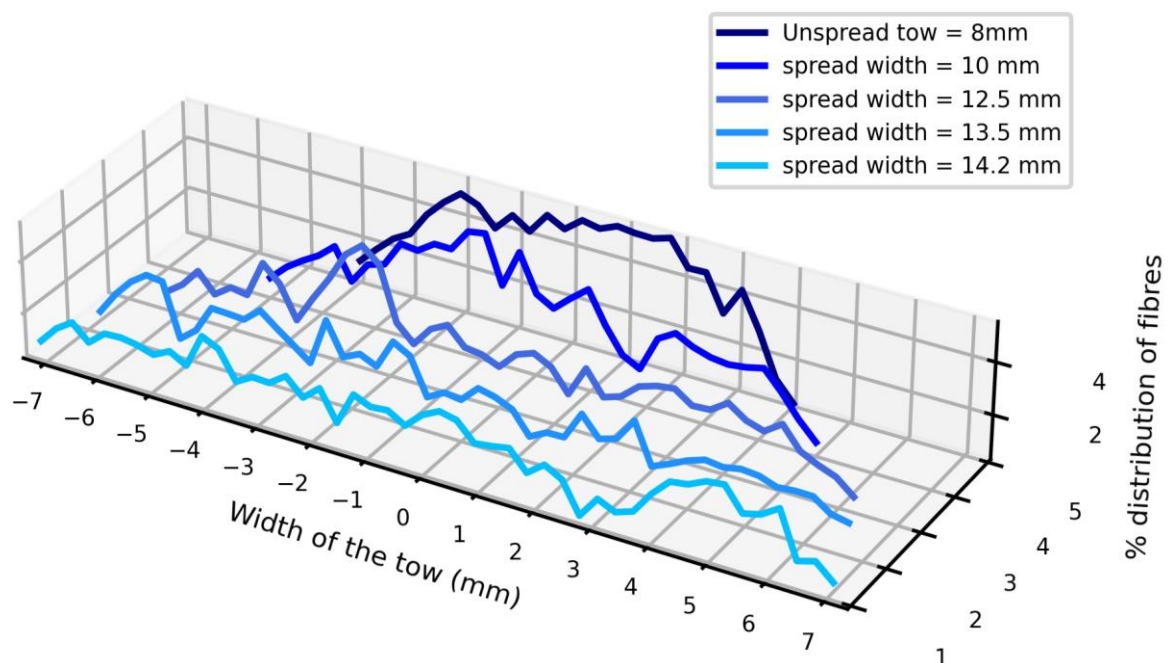


Figure 4.5: Evolution of spreading visualised through fibre distribution

As can be seen in figure 4.5 above, the fibre distribution in the unspread tow in the centre area is around 6% of the total number of fibres and this value gradually decreases as the width of the tow increases with the 14.2 mm spread tow showing an average distribution at 2% of the total number of fibres. A similar trend can be noticed with respect to the shape of the tow (refer to microstructural images in Appendix D for image observation). For an unspread tow, the contour appears to be roughly elliptical and as the tow spreads, it begins to flatten until it reaches an almost rectangular shape in the spread tow of 14.2mm.

From the observations given above, it may be suggested that as the tow is subjected to the spreading process, the fibres present in the tow redistribute themselves due to the forces acting on them and the unspread tow transforms from an elliptical shape to a flat and rectangular shape. It may also be inferred that as the width increases, the thickness of the tow decreases thus leading to a formation of thinner and wider tapes with a low aerial weight.

A caution to mention here, however, is the presence of fibre-rich and resin-rich areas that were earlier ignored to analyse the general shape of the tow during spreading. During the manufacturing of composites, the presence of these areas could cause unexpected effects on the overall performance of the structure [56]. The specimens may have these areas present specifically due to the nature of the resin and its suboptimal impregnation capacity but it may be beneficial to investigate this phenomenon nevertheless with resins specifically compatible with the fibre material properties.

Given in figure 4.6 below is the fibre volume content representation of tow cross-sections through heatmaps and histograms. In figure 4.6 (a), the microstructural image of unspread tow is shown. It is followed by the heatmap of the image, where the x-axis represents the width of the tow and the colour bar represents the fibre volume fraction. The last plot is the histogram of the fibre volume content of unspread tow; where the x-axis represents the width of the tow, the y-axis represents the fibre volume content and the colour bar represents the frequency of occurrence of different fibre concentrations. Figure 4.6 (b) follows the same structure of plots for 14.2 mm width of spread tow. The step size of each block for computation in the original image is 0.027 mm. The heatmaps and histograms for the total of 5 samples can be found in Appendix D.

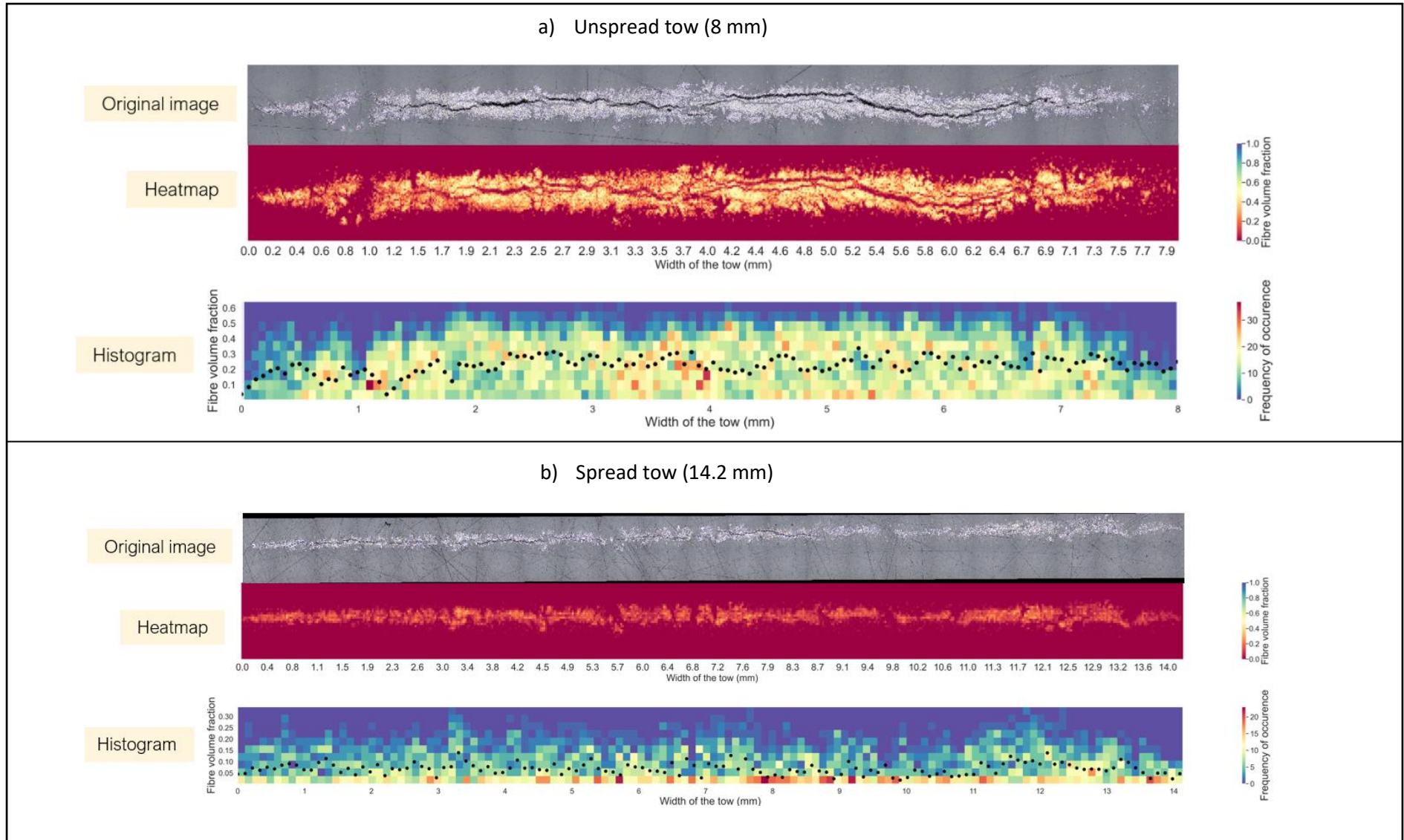


Figure 4.6: Heatmap and histogram of a) Unspread tow – 8 mm b) Spread tow – 14.2 mm

The heatmap in figure 4.6 a) shows a fibre volume distribution spectrum from 0 (red) to 1 (blue) for the unspread tow. The heatmap shows the colours of high fibre concentrations (hot areas) more predominant in the centre and sparser at the edges. A similar result can be observed in the histogram where the frequency of occurrence for fibre volume content is higher in the centre and lower on the edges. The histogram also shows a maximum fibre volume content of 0.6. It suggests that for an unspread state, the shape of the tow is elliptical with more fibres present in the middle area and lesser in the edges. This observation aligns with the fibre distribution plot for the unspread state which too displays an elliptical shape of the tow (Figure 4.5).

The heatmap for 14.2 mm spread tow in figure 4.6 b) shows a fibre volume distribution from 0 (red) to 1 (blue). The plot displays a dimmer presence of fibres along the spread width. Additionally, the fibre volume content appears to be uniform across the width which can also be seen in its corresponding histogram. The histogram shows a maximum fibre volume fraction of 0.3 which is approximately half of the maximum fibre volume fraction of unspread tow. This suggests that as the tow spreads, the fibres get uniformly distributed across the width and the concentration of fibres locally reduces. Another observation that can be made is the rectangular shape of the spread tow as opposed to the elliptical shape of the unspread tow. This too can be observed in the fibre distribution plot of the 14.2 mm spread tow (Figure 4.5). Therefore, it may be safe to assume that as the width increases, the shape of the tow changes from elliptical to rectangular and the fibre distribution becomes more uniform across the width with increasing spread.

## 5 Conclusions

---

The objective of this study was to develop a controlled tow spreading system in order to generate specimens for microstructural investigation of unidirectional spread tow by carrying out experimental studies and performing subsequent iterations on the spreading system. Simply stated, the objective was split into three parts: building a tow spreader, understanding the spreading behaviour through an experimental study and generating a technique for developing specimens for microstructural investigation.

A mechanical tow spreader was developed that utilized cylindrical spreader bars for spreading the fibre bundles. The spreader comprises of three main units: the unwinding unit, the spreading unit and the winding unit. The unwinding unit consists of the material pool (Toray T700SC-24K-50C) that is attached to a mechanical brake which generates pretension in the fibre tow. The spreading unit consists of topocrom coated spreader bars that are the main components responsible for the spreading of fibres. The bars also consist of internal heating elements that heat the bar surface for increased spreading. There are two tension meters placed on either side of the spreader bars to monitor the tension in the tow before and after the tow runs through the spreader bars. The winding unit consists of an empty spool for winding the fibre tow after it is spread and the spool is attached to a stepper motor that is also responsible for the motion of the tow through the spreader. A camera is placed over the 5<sup>th</sup> spreader bar to monitor the change in width as it is the last bar for spreading the tow. The data from the camera, tension meters and the stepper motor is collected in a text file through a LabVIEW program that collectively runs the spreader too. The tow spreader's performance was evaluated by checking if the spreading output was controllable and repeatable. This was checked through a series of repeatability experiments where the spreader was run with a set of baseline input parameters at random occasions in between experiments. Through this test, the obtained repeatability and control over the spreading width indicated the level of reliability of the spreader.

Development of the tow spreader is followed by an experimental analysis where several input parameters are isolated and varied for a sample size of five runs each to check for their influence on spreading behaviour. Pretension in the tow does not appear to influence the spreading behaviour of the fibre tow. However, this observation is based on limited data, therefore it is recommended to test this parameter again with a larger range of values by using a different mechanical brake. When testing the effect of each spreader bar on the amount of spread, it is concluded that the first three bars contributed the most to spreading width but any additional number of bars lead to a small increment hence five spreader bars are sufficient to achieve spreading stability. Wrap angles also seem to affect spreading behaviour and the relationship between them and the spreading width is found to be directly proportional. A friction study on the interaction between spreader bars and tow is done by adopting the Coulomb friction model's Capstan equation. Three parameters are varied: pretension, wrap angles and winding speed and the coefficient of friction distribution is found to be between 0.2-0.25. Lastly, the winding speed is tested for its influence on spreading width and it is found that with an increase in winding speed, the final tension in the tow increases due to which the spreading width may have increased a small amount.

After the experimental analysis, a microstructural investigation of spread tow follows. The samples are generated by using a 3d printed mould that clips onto the tow on-site the spreader. The mould is then injected with a fast-curing resin and the sample is grinded and polished to get a clear image of fibres under a confocal microscope. The microstructural investigation of spread tow allows for visualisation of fibre distribution evolution as the tow becomes wider and thinner. It is observed that the unspread tow is approximately elliptical but as it is spread and flattened, it transforms into a rectangular shape of increasingly sparse fibre distribution. Heatmaps are also plotted along with their corresponding histograms that display the concentration of fibre density over the cross-section of the spread tow. It is noted that the unspread tow has a higher fibre density concentration over its area compared to spread tow where the fibres appear to be more distributed and less clustered together. This is further confirmed by the histograms that display the frequency of occurrence of different fibre densities across the width of the tow.

In summation, the research in this thesis explores the functioning of the developed tow spreader and its input parameters. The results from this study while answering primary spreading behaviour questions also create newer trajectories and opportunities to further optimize and understand the nature of tow spreading. The microstructural study of generated specimens mainly focuses on the visualisation of tow cross-sections and their evolution of fibre distribution as the spreading increases but that is merely a starting point. This shift to microstructure investigation can be used to observe the changes in spreading behaviour on fibre level which implies that the spreading behaviour that was observed on a mesostructural level in the current research can be tested on a microstructural level too. In the following chapter, some recommendations are provided to further carry on the investigative work based on the work experience in this study.

## 6 Recommendations for future work

---

The recommendations to further the task of understanding the process of tow spreading are provided in this chapter. These recommendations include improvements that can be made to the tow spreader for optimisation, extending the experimental analysis for a more extensive understanding of spreading behaviour and improving the quality of specimens produced for microstructural investigation. They are mainly divided into three categories based on the structure of this study and report:

### *Development of tow spreader*

This section comprises suggestions specifically intended for improving the tow spreader design and functioning.

- The primary concern with the spreader to be tackled is the presence of noise. Vibrations in the spreader are transferred from the stepper motor to each component through joints and connections. Each joint/connection in the spreader is metal which means there is a direct undamped transfer of vibrations as they travel through the system. In this study, thick silicon sheets were used in between joints in the winding unit to reduce this transfer as much as possible. Additionally, a thick fabric film was placed in between the spreader and the metal table to further dampen the vibrations. However, the solution to vibration damping can be made more sophisticated and efficient. Therefore, the recommendation is to find a way to measure the amount of noise present in the system and develop techniques to reduce it to a minimum. The issue of transfer of vibrations may be tackled through separating and fixing the unwinding, spreading and winding units such that they are not in contact with each other and also by placing them on a surface that absorbs vibrations like silicon or rubber.
- As was mentioned in section 3.3.3, the mechanical brake is suggested to be replaced in order to incorporate a larger range of inducible pretension in the tow. The current mechanical brake only supplies a pretension range of 100 cN approximately. This aspect may have made the results of testing the influence of pretension on spreading behaviour uncertain. An electric brake may be a more suitable alternative to a mechanically functioning brake as it is easier to monitor the performance of the former and would be expected to have more control over the pretension.
- There are several types of mechanical spreading elements (for eg convex bars, expandable wheel, combs etc – see section 1.2) that can be tested in the spreading unit and compared to the cylindrical bars in this study for their spreading performance and the associated fibre damage if any.
- An interesting aspect to study may be using different fibre materials (e.g., glass fibre) and checking their response to the spreading behaviour. This creates an opportunity to establish the tow spreader as a universal spreading machine. Different filament counts (6k, 12k, 24k) of the same material may also be subjected to experimental analysis and their behaviour can be compared for different input parameters.

### *Experimental analysis of input parameters*

This section has suggestions for further continuing the experimental analysis of the parameters in the tow spreader.

- Chapter 3 in this report details the findings of the experimental analysis done on input parameters of the spreader. The results while highlighting some trends also create further trajectories and questions for a more detailed investigation. It may be beneficial to examine those questions and create further experiments to answer them.
- Each parameter was tested by isolating it and maintaining the remaining parameters at baseline values which do provide an insight into their contributions to spreading behaviour but they do not suggest anything about the dependency of one parameter on another. Therefore, in order to check for those dependencies, experiments can be designed testing two or more parameters at once. This may provide information about how one parameter reacts with another and in the end, may help coalesce all the interactions within the spreader responsible for the spreading of fibre tows.
- Lastly, the linear regression model can be improved by increasing the amount of test data sets and possibly shifting to a non-linear regression model. So far, spreading width was the only dependent variable in the model but it was found that several input parameters have an influence on the final tension of the tow so this tension can be used as a dependent as well and then later related to the spreading width.

### *Microstructural analysis*

This section has suggestions for further continuing the experimental analysis of the parameters in the tow spreader.

- During the image quality assessment of the specimens generated for microstructural investigation, certain defects on the samples were noticed. Cracks formed during grinding and polishing operation, resin and fibre rich areas and difficulty in manufacturing the samples can be avoided. The resin used currently is a fast-curing resin that is very convenient for on-site sample manufacturing but the material may not impregnate the fibres well or may be too soft to undergo harsh processes like polishing and grinding without causing damages. A suitable resin alternative with a better embedding quality may be needed to avoid the formation of cracks on the sample surface. Additionally, the reason for the formation of fibre and resin-rich areas needs to be investigated.
- Currently, the 3d printed mould is only capable of capturing the spread tow between the spreader bars but if this technique can be translated to the surface of the spreader bar, it would be possible to observe the fibre behaviour as it comes in contact with a spreading surface. This may be valuable to understand the difference in spread tow fibre orientation when it is fanned over the bar and when it is in between two spreader bars.



## A. TOW SPREADER COMPONENTS/EXTERNAL TOOLS AND THEIR SPECIFICATIONS

This appendix presents the specifications of different components within the spreader along with the additional tools used during the course of this study as reference for any future studies that may be conducted on the current spreader design.

<i>Component</i>	<i>Specifications</i>	<i>Supplier</i>
Fibre material	T700SC-24K-50C	Toray Industries
Mechanical brake	Input values unknown	Texmer GmbH
Thread positioning pieces	Topocrom coated vertical rollers	Texmer GmbH
Tension meter 1	Range: 0 - 2000 cN	Hans-Schmidt & Co GmbH
Tension meter 2	Range: 0 - 5000 cN	Hans-Schmidt & Co GmbH
Spreader bar tube	Topocrom coated tube 25mm	Texmer GmbH
Camera	C920Pro	Logitech
3D printer	Ultimaker 2+	Ultimaker
Print material	PLA	Colorfabb
Stepper motor	Nema 23	-
Frame profiles	20X20 mm aluminium profile	Item 24
Stepper motor controller	Arduino Uno	-
Power supply for heated elements	0-30V input current/input voltage	RS components
Resin	Technovit 4071	Technovit
Polishing and grinding machine	Tegramatic (Automatic)	Struers
Confocal microscope	Laser scanning confocal microscope	Keyence
High resistance wire	Nickel-chrome alloy	RS components
Stepper motor driver	TB 6600	-
Control program	LabVIEW statemachine	National Instruments
DAQ	USB-6525	National instruments

Table 9: Specifications of spreader components

## B. SPREADER TROUBLESHOOTING KEY POINTS

This appendix describes the troubleshooting of issues over the course of this study and during the development phase of the tow spreader. After the implantation of these troubleshoots, the tow spreader was considered to be smoothly operating. Given below is a list of the issues and their corresponding troubleshoots:

- **Distance of unwinding spool from the thread positioning unit:** A hypothesis was developed during observation of the unwinding unit that as the tow unwinds from the spool, it experiences higher forces at the edges due to the high angle the tow makes with the centreline. Therefore, the tow should enter the spreading unit aligned with the centreline. Hence, the distance between the spool and the entry point of the spreading unit i.e., the thread positioning piece is made as large as possible. The position of the spool is adjustable in **height and distance** from the spreading unit and these two factors are responsible for the trajectory of the tow's entry into the spreading unit. Looking at the illustration in figure B.1 of the unwinding unit, it can be observed that at the extreme ends of the spool, the tow being pulled forms a certain angle with the centreline of the spreader. This angle ( $\angle A^\circ$ ) decreases as the distance between the material spool and the spreading unit (first element: thread positioning piece) increases. A bigger value of  $\angle A^\circ$  would cause the tow to enter the thread positioning piece at very sharp angles which could potentially cause additional forces/tension in the tow that are undesirable and difficult to monitor. Hence, the goal was to place the material spool as far away from the thread positioning piece as possible so the angle  $\angle A^\circ$  approaches  $0^\circ$  with the centreline. This assures that the tow travels through the unwinding unit undisturbed. The height of the material spool is adjusted to be at the same level as the rest of the components in the tow spreader and care was taken to ensure that the tow does not get crumpled by the thread positioning piece by pushing down on it.

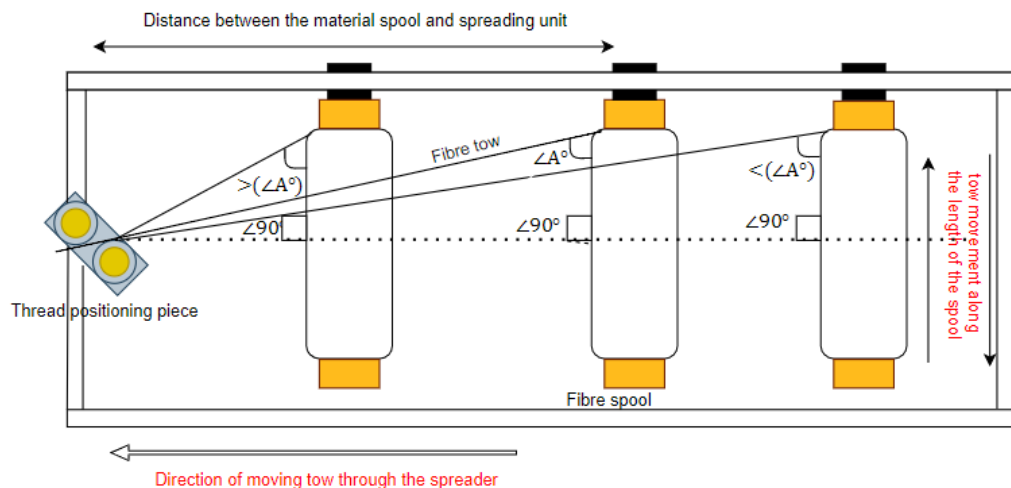


Figure B.1: Cyclic unwinding of tow from the material spool

- **Entry and exit thread positioning pieces:** The thread positioning pieces in the spreading unit are a set of vertical topocrom rotatable rollers placed along the centreline of the tow spreader to position the tow and prevent it from straying laterally. However, the rollers of the thread positioning piece have a small gap between them which does allow for fibre tow to stray in the spreading unit laterally by a small amount which is undesirable for image capturing and may inhibit the tow from spreading to its full potential. To resolve this, the piece is fixed in the centre at an angle such that the tow irrespective of its position of unwinding along the length of the spool comes in contact with both the rollers and no gap is present for any lateral motion (**Error! Reference source not found.**). This makes sure that the tow always exits from the same point from the thread positioning pieces.

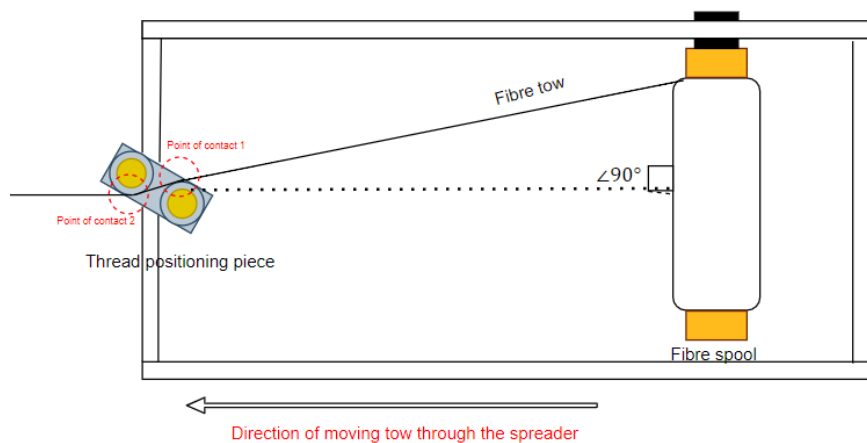
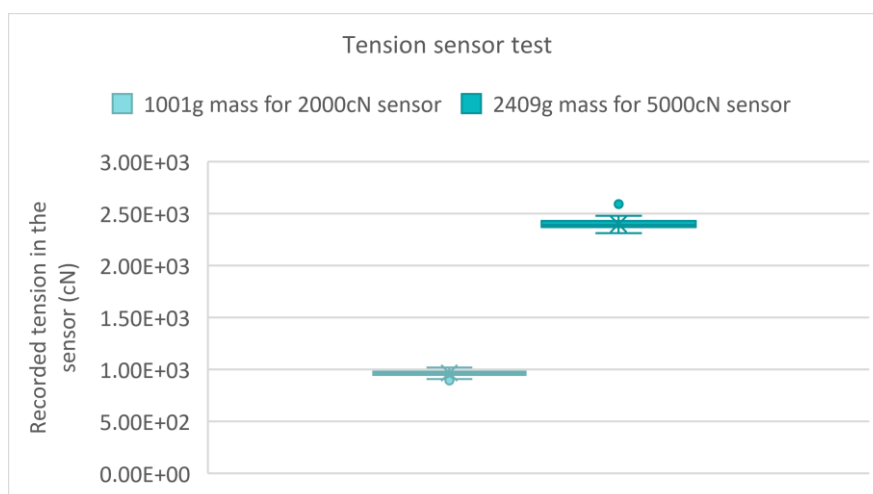


Figure B.2: Schematic of tow interaction with thread positioning piece

- **Tension sensor calibration test:** In order to check for the accuracy of the tension meters, dead weights of 1001g and 2409 g were used for 2000 cN sensor and 5000 cN sensor respectively. These values were roughly half of the maximum limit of each sensor. The figures below show the values of tension observed in the sensors for each of their test dead weights and the corresponding errors in observed values. According to the specifications of the product handbook, the errors were found to lie within the expected error limit.



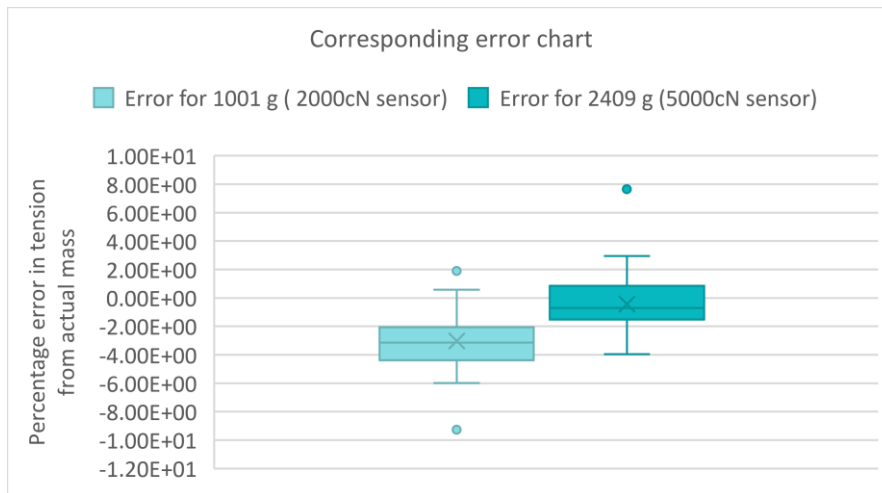


Figure B.3: Tension meter(s) accuracy check

- **Cleaning fibre residue from spreader bars:** During initial test runs of the spreader, it was noticed that the tow during spreading left slight fibre residue over the spreader bars due to damage. The bars are thus cleaned with the bar cleaning solution before every run to avoid any undesirable influence of small damaged fibres on spreading behaviour.
- **Adding additional thread positioning piece:** Despite fixing the tow trajectory at the entry of the spreading unit by turning the thread positioning piece at 45°, further fibre straying was observed at the exit of the spreading unit due to random wrapping position over the winding spool. Therefore, another thread positioning piece is placed at the exit of the spreading unit before it winds onto the empty spool.
- **Camera vs laser sensor:** The initial goal for the data acquisition unit was to use a high-resolution laser line scanner (Microepsilon 2950) to capture the spreading width. However, since the dry fibre tow is not a smooth surface and porous due to very small spacing between fibres, a large amount of noise was observed from the signal received by the scanner. The sensor was placed over the tow on the spreader bar and the tow in the air but the results did not seem to be any different and noise existed in both signals. The noisy signal was manipulated through autoexposure, interpolation and averaging which muted the noise but in the process, it also made the edges of the tow harder to determine (highlighted yellow box area in the figure below). This made the processed signal less reliable and as a consequence, the laser line scanner was replaced by a camera.

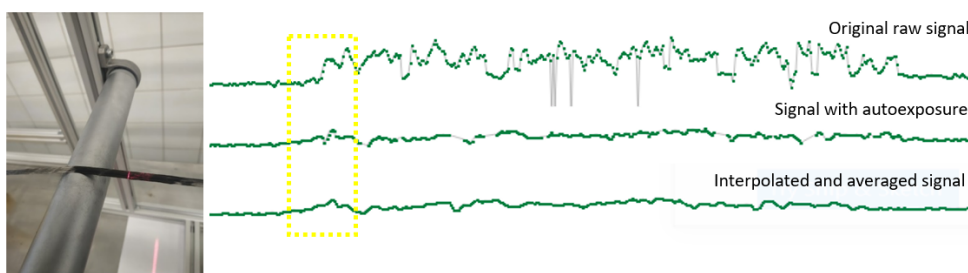


Figure B.4: Signal output from the laser sensor

- **Increasing winding torque:** Nema 23 is the stepper motor used for winding and moving the tow through the spreader. However, at high tension in the tow, the motor would get stuck as the tension in the tow would exceed the maximum torque of the motor. Therefore, a gear system was installed between the shafts of the winding spool and stepper motor to increase the torque of the winding spool by reducing the speed of rotation. The gear with 20 teeth was attached to the motor and 60 teeth gear was attached to the winding spool shaft. The equation for gear ratio is given below:

$$Gear\ ratio = \frac{number\ of\ teeth_B}{number\ of\ teeth_A} = \frac{speed_A}{speed_B} = \frac{Torque_B}{Torque_A} = 3$$

The stepper motor has a maximum torque of 3Nm and by reducing the speed by a factor of three, the torque increases up to 9Nm. This prevents the motor from getting stuck when the tension in the system is very high and ensures that the tow is running in the spreader smoothly

- **Checking dimensions before each experiment:** The dimensions of the spreading unit frame and the position of the spreader bars are checked before each run, in order to ensure that the relative position of each bar remains as desired and does not change due to slip that may occur because of high forces and vibrations in the running system.

## C. R SQUARED VALUES OF INDIVIDUAL PARAMETERS

This appendix presents the R square values of each input parameter with spreading width as the dependent in the linear regression model presented in section 3.6. On comparing the individual r square values of the parameters, the contribution of each of those parameters to the amount of spread can be visualized. It is followed by the raw input data of 25 and 125 data sets used to build the regression model.

Independent variable	Dependent variable	R square coefficient (25 and 125 data sets)															
Pretension	Spread width	<table border="1"> <thead> <tr> <th colspan="5">Model Summary</th> </tr> <tr> <th>Model</th> <th>R</th> <th>R Square</th> <th>Adjusted R Square</th> <th>Std. Error of the Estimate</th> </tr> </thead> <tbody> <tr> <td>1</td> <td>.055<sup>a</sup></td> <td>.003</td> <td>-.040</td> <td>.16093</td> </tr> </tbody> </table> <p>a. Predictors: (Constant), Pretension</p>	Model Summary					Model	R	R Square	Adjusted R Square	Std. Error of the Estimate	1	.055 <sup>a</sup>	.003	-.040	.16093
		Model Summary															
Model	R	R Square	Adjusted R Square	Std. Error of the Estimate													
1	.055 <sup>a</sup>	.003	-.040	.16093													
<table border="1"> <thead> <tr> <th colspan="5">Model Summary</th> </tr> <tr> <th>Model</th> <th>R</th> <th>R Square</th> <th>Adjusted R Square</th> <th>Std. Error of the Estimate</th> </tr> </thead> <tbody> <tr> <td>1</td> <td>.039<sup>a</sup></td> <td>.001</td> <td>-.007</td> <td>.17210</td> </tr> </tbody> </table> <p>a. Predictors: (Constant), Pretension</p>	Model Summary					Model	R	R Square	Adjusted R Square	Std. Error of the Estimate	1	.039 <sup>a</sup>	.001	-.007	.17210		
Model Summary																	
Model	R	R Square	Adjusted R Square	Std. Error of the Estimate													
1	.039 <sup>a</sup>	.001	-.007	.17210													
Number of heated bars	Spread width	<table border="1"> <thead> <tr> <th colspan="5">Model Summary</th> </tr> <tr> <th>Model</th> <th>R</th> <th>R Square</th> <th>Adjusted R Square</th> <th>Std. Error of the Estimate</th> </tr> </thead> <tbody> <tr> <td>1</td> <td>.763<sup>a</sup></td> <td>.582</td> <td>.564</td> <td>.10417</td> </tr> </tbody> </table> <p>a. Predictors: (Constant), Number of heated bars</p>	Model Summary					Model	R	R Square	Adjusted R Square	Std. Error of the Estimate	1	.763 <sup>a</sup>	.582	.564	.10417
		Model Summary															
Model	R	R Square	Adjusted R Square	Std. Error of the Estimate													
1	.763 <sup>a</sup>	.582	.564	.10417													
<table border="1"> <thead> <tr> <th colspan="5">Model Summary</th> </tr> <tr> <th>Model</th> <th>R</th> <th>R Square</th> <th>Adjusted R Square</th> <th>Std. Error of the Estimate</th> </tr> </thead> <tbody> <tr> <td>1</td> <td>.709<sup>a</sup></td> <td>.503</td> <td>.499</td> <td>.12147</td> </tr> </tbody> </table> <p>a. Predictors: (Constant), Number of heated bars</p>	Model Summary					Model	R	R Square	Adjusted R Square	Std. Error of the Estimate	1	.709 <sup>a</sup>	.503	.499	.12147		
Model Summary																	
Model	R	R Square	Adjusted R Square	Std. Error of the Estimate													
1	.709 <sup>a</sup>	.503	.499	.12147													

Temperature of heated bars	Spread width	<table border="1" style="width: 100%; border-collapse: collapse;"> <thead> <tr> <th colspan="5" style="text-align: center;">Model Summary</th> </tr> <tr> <th style="text-align: left;">Model</th> <th style="text-align: center;">R</th> <th style="text-align: center;">R Square</th> <th style="text-align: center;">Adjusted R Square</th> <th style="text-align: center;">Std. Error of the Estimate</th> </tr> </thead> <tbody> <tr> <td style="text-align: center;">1</td> <td style="text-align: center;">.750<sup>a</sup></td> <td style="text-align: center;">.562</td> <td style="text-align: center;">.543</td> <td style="text-align: center;">.10670</td> </tr> <tr> <td colspan="5" style="text-align: center;">a. Predictors: (Constant), Temperature</td> </tr> </tbody> </table> <table border="1" style="width: 100%; border-collapse: collapse;"> <thead> <tr> <th colspan="5" style="text-align: center;">Model Summary</th> </tr> <tr> <th style="text-align: left;">Model</th> <th style="text-align: center;">R</th> <th style="text-align: center;">R Square</th> <th style="text-align: center;">Adjusted R Square</th> <th style="text-align: center;">Std. Error of the Estimate</th> </tr> </thead> <tbody> <tr> <td style="text-align: center;">1</td> <td style="text-align: center;">.697<sup>a</sup></td> <td style="text-align: center;">.486</td> <td style="text-align: center;">.482</td> <td style="text-align: center;">.12343</td> </tr> <tr> <td colspan="5" style="text-align: center;">a. Predictors: (Constant), Temperature</td> </tr> </tbody> </table>	Model Summary					Model	R	R Square	Adjusted R Square	Std. Error of the Estimate	1	.750 <sup>a</sup>	.562	.543	.10670	a. Predictors: (Constant), Temperature					Model Summary					Model	R	R Square	Adjusted R Square	Std. Error of the Estimate	1	.697 <sup>a</sup>	.486	.482	.12343	a. Predictors: (Constant), Temperature				
Model Summary																																										
Model	R	R Square	Adjusted R Square	Std. Error of the Estimate																																						
1	.750 <sup>a</sup>	.562	.543	.10670																																						
a. Predictors: (Constant), Temperature																																										
Model Summary																																										
Model	R	R Square	Adjusted R Square	Std. Error of the Estimate																																						
1	.697 <sup>a</sup>	.486	.482	.12343																																						
a. Predictors: (Constant), Temperature																																										
Wrap angle	Spread width	<table border="1" style="width: 100%; border-collapse: collapse;"> <thead> <tr> <th colspan="5" style="text-align: center;">Model Summary</th> </tr> <tr> <th style="text-align: left;">Model</th> <th style="text-align: center;">R</th> <th style="text-align: center;">R Square</th> <th style="text-align: center;">Adjusted R Square</th> <th style="text-align: center;">Std. Error of the Estimate</th> </tr> </thead> <tbody> <tr> <td style="text-align: center;">1</td> <td style="text-align: center;">.508<sup>a</sup></td> <td style="text-align: center;">.258</td> <td style="text-align: center;">.226</td> <td style="text-align: center;">.13881</td> </tr> <tr> <td colspan="5" style="text-align: center;">a. Predictors: (Constant), wrap angle</td> </tr> </tbody> </table> <table border="1" style="width: 100%; border-collapse: collapse;"> <thead> <tr> <th colspan="5" style="text-align: center;">Model Summary</th> </tr> <tr> <th style="text-align: left;">Model</th> <th style="text-align: center;">R</th> <th style="text-align: center;">R Square</th> <th style="text-align: center;">Adjusted R Square</th> <th style="text-align: center;">Std. Error of the Estimate</th> </tr> </thead> <tbody> <tr> <td style="text-align: center;">1</td> <td style="text-align: center;">.458<sup>a</sup></td> <td style="text-align: center;">.210</td> <td style="text-align: center;">.203</td> <td style="text-align: center;">.15312</td> </tr> <tr> <td colspan="5" style="text-align: center;">a. Predictors: (Constant), wrap angle</td> </tr> </tbody> </table>	Model Summary					Model	R	R Square	Adjusted R Square	Std. Error of the Estimate	1	.508 <sup>a</sup>	.258	.226	.13881	a. Predictors: (Constant), wrap angle					Model Summary					Model	R	R Square	Adjusted R Square	Std. Error of the Estimate	1	.458 <sup>a</sup>	.210	.203	.15312	a. Predictors: (Constant), wrap angle				
Model Summary																																										
Model	R	R Square	Adjusted R Square	Std. Error of the Estimate																																						
1	.508 <sup>a</sup>	.258	.226	.13881																																						
a. Predictors: (Constant), wrap angle																																										
Model Summary																																										
Model	R	R Square	Adjusted R Square	Std. Error of the Estimate																																						
1	.458 <sup>a</sup>	.210	.203	.15312																																						
a. Predictors: (Constant), wrap angle																																										
Length between bars	Spread width	<table border="1" style="width: 100%; border-collapse: collapse;"> <thead> <tr> <th colspan="5" style="text-align: center;">Model Summary</th> </tr> <tr> <th style="text-align: left;">Model</th> <th style="text-align: center;">R</th> <th style="text-align: center;">R Square</th> <th style="text-align: center;">Adjusted R Square</th> <th style="text-align: center;">Std. Error of the Estimate</th> </tr> </thead> <tbody> <tr> <td style="text-align: center;">1</td> <td style="text-align: center;">.128<sup>a</sup></td> <td style="text-align: center;">.016</td> <td style="text-align: center;">-.026</td> <td style="text-align: center;">.15985</td> </tr> <tr> <td colspan="5" style="text-align: center;">a. Predictors: (Constant), Length between spreader bars</td> </tr> </tbody> </table> <table border="1" style="width: 100%; border-collapse: collapse;"> <thead> <tr> <th colspan="5" style="text-align: center;">Model Summary</th> </tr> <tr> <th style="text-align: left;">Model</th> <th style="text-align: center;">R</th> <th style="text-align: center;">R Square</th> <th style="text-align: center;">Adjusted R Square</th> <th style="text-align: center;">Std. Error of the Estimate</th> </tr> </thead> <tbody> <tr> <td style="text-align: center;">1</td> <td style="text-align: center;">.105<sup>a</sup></td> <td style="text-align: center;">.011</td> <td style="text-align: center;">.003</td> <td style="text-align: center;">.17128</td> </tr> <tr> <td colspan="5" style="text-align: center;">a. Predictors: (Constant), Length between spreader bars</td> </tr> </tbody> </table>	Model Summary					Model	R	R Square	Adjusted R Square	Std. Error of the Estimate	1	.128 <sup>a</sup>	.016	-.026	.15985	a. Predictors: (Constant), Length between spreader bars					Model Summary					Model	R	R Square	Adjusted R Square	Std. Error of the Estimate	1	.105 <sup>a</sup>	.011	.003	.17128	a. Predictors: (Constant), Length between spreader bars				
Model Summary																																										
Model	R	R Square	Adjusted R Square	Std. Error of the Estimate																																						
1	.128 <sup>a</sup>	.016	-.026	.15985																																						
a. Predictors: (Constant), Length between spreader bars																																										
Model Summary																																										
Model	R	R Square	Adjusted R Square	Std. Error of the Estimate																																						
1	.105 <sup>a</sup>	.011	.003	.17128																																						
a. Predictors: (Constant), Length between spreader bars																																										
Winding speed	Spread width	<table border="1" style="width: 100%; border-collapse: collapse;"> <thead> <tr> <th colspan="5" style="text-align: center;">Model Summary</th> </tr> <tr> <th style="text-align: left;">Model</th> <th style="text-align: center;">R</th> <th style="text-align: center;">R Square</th> <th style="text-align: center;">Adjusted R Square</th> <th style="text-align: center;">Std. Error of the Estimate</th> </tr> </thead> <tbody> <tr> <td style="text-align: center;">1</td> <td style="text-align: center;">.038<sup>a</sup></td> <td style="text-align: center;">.001</td> <td style="text-align: center;">-.042</td> <td style="text-align: center;">.16106</td> </tr> <tr> <td colspan="5" style="text-align: center;">a. Predictors: (Constant), Speed</td> </tr> </tbody> </table>	Model Summary					Model	R	R Square	Adjusted R Square	Std. Error of the Estimate	1	.038 <sup>a</sup>	.001	-.042	.16106	a. Predictors: (Constant), Speed																								
Model Summary																																										
Model	R	R Square	Adjusted R Square	Std. Error of the Estimate																																						
1	.038 <sup>a</sup>	.001	-.042	.16106																																						
a. Predictors: (Constant), Speed																																										

<b>Model Summary</b>				
Model	R	R Square	Adjusted R Square	Std. Error of the Estimate
1	.044 <sup>a</sup>	.002	-.006	.17206

a. Predictors: (Constant), Speed

Table 10: R square values of individual parameters



**REGRESSION ANALYSIS RAW DATA**

<b>Spread width</b>	<b>Pretension</b>	<b>Number of heated bars</b>	<b>Temperature</b>	<b>Wrap angle</b>	<b>Length between spreader bars</b>	<b>Speed</b>
14.44	218	0	22	9.9148	150	50
14.48	236	0	22	9.9148	150	50
13.9	265	0	22	9.9148	150	50
15.1	297	0	22	9.9148	150	50
15.21	318	0	22	9.9148	150	50
14.07	218	0	22	9.9148	150	50
15.61	218	1	100	9.9148	150	50
15.95	218	2	100	9.9148	150	50
18.07	218	3	100	9.9148	150	50
17.84	218	5	100	9.9148	150	50
14.05	218	0	22	9.9148	150	50
15.98	218	3	50	9.9148	150	50
17.55	218	3	75	9.9148	150	50
17.85	218	3	100	9.9148	150	50
18.33	218	3	125	9.9148	150	50
9.428	218	0	22	4.40128	150	50
13.68	218	0	22	9.9148	150	50
14.35	218	0	22	12.791	150	50
14.8	218	0	22	9.9148	60	50
14.26	218	0	22	9.9148	150	50
13.37	218	0	22	9.9148	200	50
14.34	218	0	22	9.9148	150	60
14.99	218	0	22	9.9148	150	120
15	218	0	22	9.9148	150	180
15.74	218	0	22	9.9148	150	240

Table 11: Input data for regression analysis with 25 data sets

Width	Pretension	Number of heated bars	Temperature	Wrap angle	Length between spreader bars	Speed
14.59	218	0	22	9.9148	150	50
14.25	218	0	22	9.9148	150	50
14.14	218	0	22	9.9148	150	50
14.16	218	0	22	9.9148	150	50
15.07	218	0	22	9.9148	150	50
15.27	236	0	22	9.9148	150	50
14.57	236	0	22	9.9148	150	50
15.25	236	0	22	9.9148	150	50
12.57	236	0	22	9.9148	150	50
14.76	236	0	22	9.9148	150	50
14.29	265	0	22	9.9148	150	50
13.85	265	0	22	9.9148	150	50
14.89	265	0	22	9.9148	150	50
13.75	265	0	22	9.9148	150	50
12.73	265	0	22	9.9148	150	50
15.04	297	0	22	9.9148	150	50
15.33	297	0	22	9.9148	150	50
15	297	0	22	9.9148	150	50
13.74	297	0	22	9.9148	150	50
16.45	297	0	22	9.9148	150	50
16.12	318	0	22	9.9148	150	50
14.75	318	0	22	9.9148	150	50
15.99	318	0	22	9.9148	150	50
13.83	318	0	22	9.9148	150	50
15.34	318	0	22	9.9148	150	50
14.11	218	0	22	9.9148	150	50
14.23	218	0	22	9.9148	150	50
15.03	218	0	22	9.9148	150	50
13.25	218	0	22	9.9148	150	50
13.73	218	0	22	9.9148	150	50
17.19	218	1	100	9.9148	150	50
15.81	218	1	100	9.9148	150	50
14.3	218	1	100	9.9148	150	50
15.32	218	1	100	9.9148	150	50
15.45	218	1	100	9.9148	150	50
14.82	218	2	100	9.9148	150	50
16.24	218	2	100	9.9148	150	50
15.41	218	2	100	9.9148	150	50
16.73	218	2	100	9.9148	150	50
16.58	218	2	100	9.9148	150	50
17.31	218	3	100	9.9148	150	50
19.04	218	3	100	9.9148	150	50

17.95	218	3	100	9.9148	150	50
17.47	218	3	100	9.9148	150	50
18.59	218	3	100	9.9148	150	50
18.66	218	5	100	9.9148	150	50
17	218	5	100	9.9148	150	50
18.07	218	5	100	9.9148	150	50
17.46	218	5	100	9.9148	150	50
18.03	218	5	100	9.9148	150	50
14.96	218	0	22	9.9148	150	50
13.24	218	0	22	9.9148	150	50
13.95	218	0	22	9.9148	150	50
13.54	218	0	22	9.9148	150	50
14.54	218	0	22	9.9148	150	50
15.31	218	3	50	9.9148	150	50
14.48	218	3	50	9.9148	150	50
15.86	218	3	50	9.9148	150	50
17.69	218	3	50	9.9148	150	50
16.56	218	3	50	9.9148	150	50
16.95	218	3	75	9.9148	150	50
18.58	218	3	75	9.9148	150	50
18.52	218	3	75	9.9148	150	50
17.14	218	3	75	9.9148	150	50
16.58	218	3	75	9.9148	150	50
18.52	218	3	100	9.9148	150	50
18.59	218	3	100	9.9148	150	50
18.88	218	3	100	9.9148	150	50
16.73	218	3	100	9.9148	150	50
16.55	218	3	100	9.9148	150	50
18.54	218	3	125	9.9148	150	50
18.04	218	3	125	9.9148	150	50
18.01	218	3	125	9.9148	150	50
18.17	218	3	125	9.9148	150	50
18.91	218	3	125	9.9148	150	50
8.67	218	0	22	4.40128	150	50
9.58	218	0	22	4.40128	150	50
9.19	218	0	22	4.40128	150	50
10.67	218	0	22	4.40128	150	50
9.01	218	0	22	4.40128	150	50
12.64	218	0	22	9.9148	150	50
13.27	218	0	22	9.9148	150	50
12.8	218	0	22	9.9148	150	50
15.77	218	0	22	9.9148	150	50
13.92	218	0	22	9.9148	150	50
14.55	218	0	22	12.791	150	50
15.36	218	0	22	12.791	150	50

13.64	218	0	22	12.791	150	50
14.2	218	0	22	12.791	150	50
14	218	0	22	12.791	150	50
13.12	218	0	22	9.9148	60	50
15.84	218	0	22	9.9148	60	50
14.3	218	0	22	9.9148	60	50
12.38	218	0	22	9.9148	60	50
15.02	218	0	22	9.9148	60	50
13.53	218	0	22	9.9148	150	50
13.27	218	0	22	9.9148	150	50
12.74	218	0	22	9.9148	150	50
15.77	218	0	22	9.9148	150	50
13.92	218	0	22	9.9148	150	50
14.56	218	0	22	9.9148	265	50
13.24	218	0	22	9.9148	265	50
13.8	218	0	22	9.9148	265	50
11.18	218	0	22	9.9148	265	50
12.08	218	0	22	9.9148	265	50
13.61	218	0	22	9.9148	150	60
14.94	218	0	22	9.9148	150	60
14.78	218	0	22	9.9148	150	60
14.27	218	0	22	9.9148	150	60
14.13	218	0	22	9.9148	150	60
15.01	218	0	22	9.9148	150	120
14.8	218	0	22	9.9148	150	120
15.02	218	0	22	9.9148	150	120
15.36	218	0	22	9.9148	150	120
14.78	218	0	22	9.9148	150	120
15.28	218	0	22	9.9148	150	180
15.12	218	0	22	9.9148	150	180
14.54	218	0	22	9.9148	150	180
14.91	218	0	22	9.9148	150	180
15.15	218	0	22	9.9148	150	180
15.76	218	0	22	9.9148	150	240
15.66	218	0	22	9.9148	150	240
15.26	218	0	22	9.9148	150	240
15.88	218	0	22	9.9148	150	240
16.17	218	0	22	9.9148	150	240

Table 12: Input data for regression analysis with 125 data sets

## D. FIBRE DISTRIBUTION PLOTS FOR EACH SAMPLE

---

This appendix presents a microstructural investigation of all the samples generated. Each sample of spread tow was captured between two spreader bars in the spreading unit to visualise the evolution of fibre orientation/distribution in tow as its width increases.

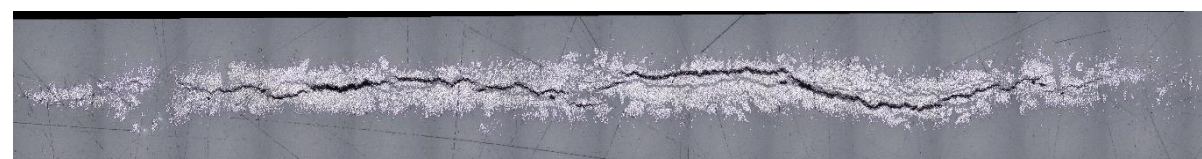
Figures D.1 to D.5 show the microstructure investigation of each sample. In each figure, the first image displayed (top) is the original image captured from the confocal microscope. It is followed by the threshold image where the fibres and matrix are represented by green and purple respectively. The fibre distribution plot that is presented below the threshold image, shows the approximate shape of the tow. The fourth image from the top is the heatmap displaying the fibre volume fraction in the tow across the width. The last image is the corresponding histogram of the heatmap which display the frequency of occurrence of the fibre volume fraction in the tow.

Given below are the specifications of the samples for which the microscopic images were taken in figures D.1 to D.5:

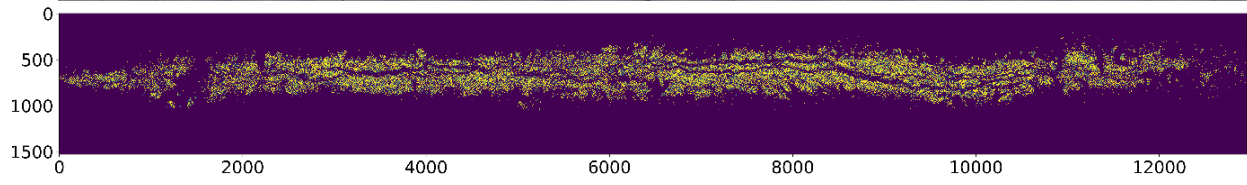
- Figure D.1: Unspread tow / Tow from the spool with a width of 8mm.
- Figure D.2: Spread tow with a width of 10 mm captured between 1<sup>st</sup> and 2<sup>nd</sup> spreader bar.
- Figure D.3: Spread tow with a width of 12.5 mm captured between 2<sup>nd</sup> and 3<sup>rd</sup> spreader bar.
- Figure D.4: Spread tow with a width of 13.5 mm captured between 3<sup>rd</sup> and 4<sup>th</sup> spreader bar.
- Figure D.5: Spread tow with a width of 14.2 mm captured between 4<sup>th</sup> and 5<sup>th</sup> spreader bar.

UNSPREAD TOW - 8 mm

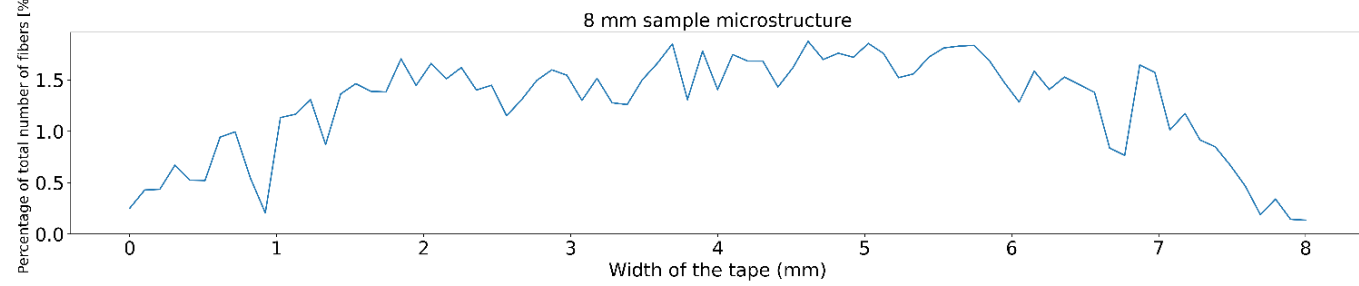
Original image



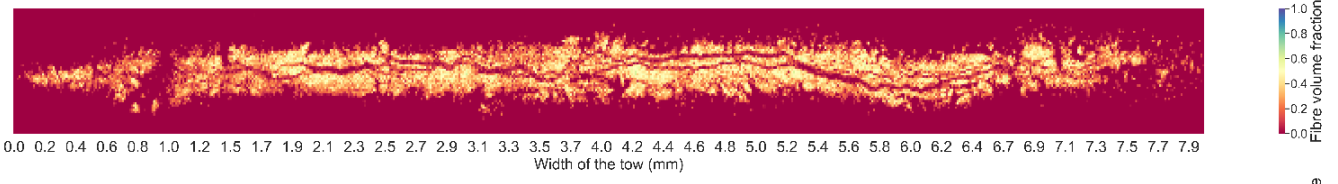
Threshold image



Fibre distribution plot



Fibre volume content heatmap



Fibre volume content histogram

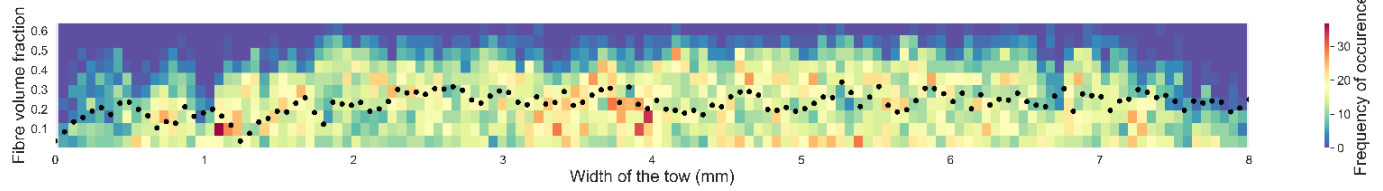


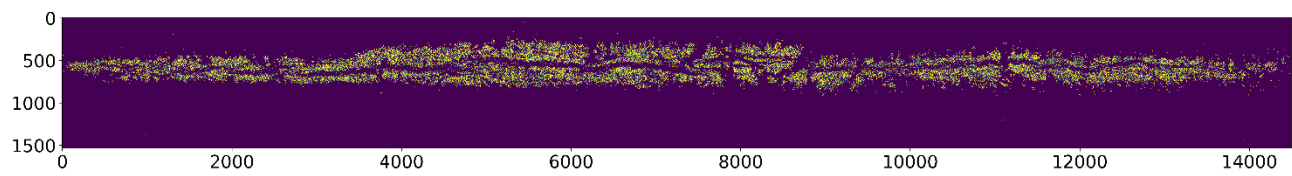
Figure D.1: 8 mm unspread tow microstructure

SPREAD TOW – 10 mm

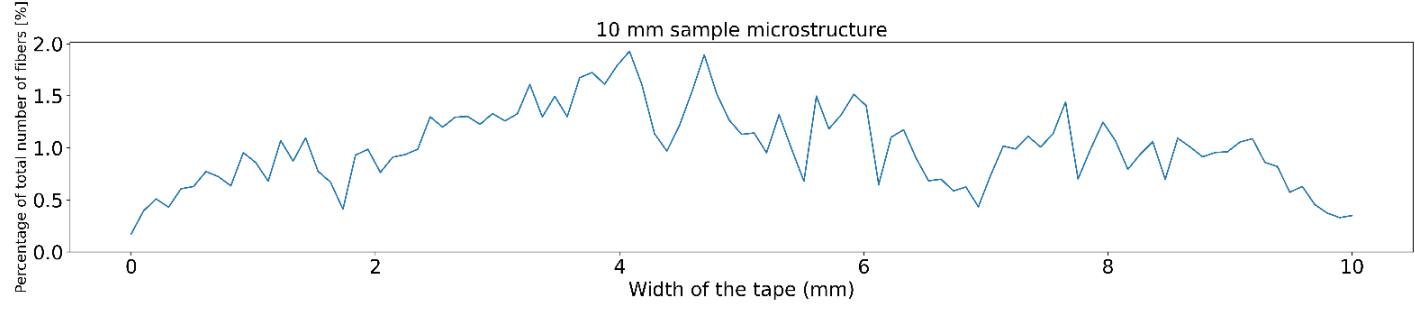
Original image



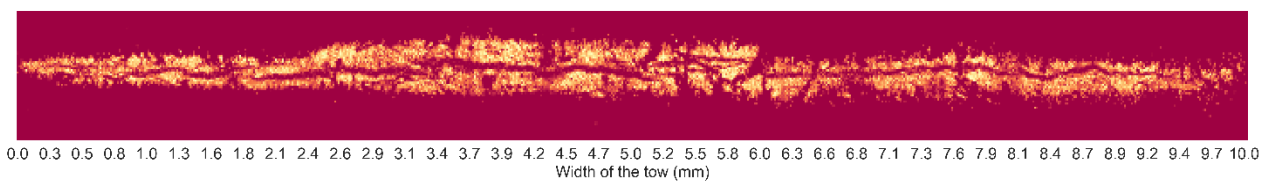
Threshold image



Fibre distribution plot



Fibre volume content heatmap



Fibre volume content histogram

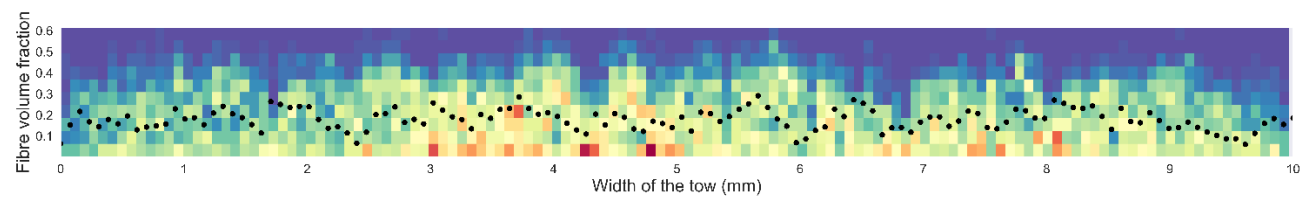
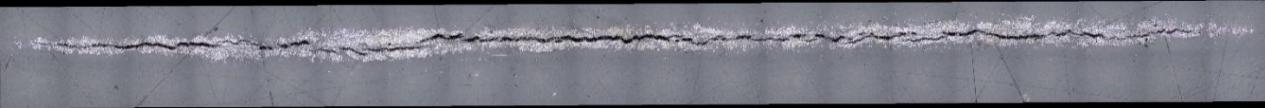


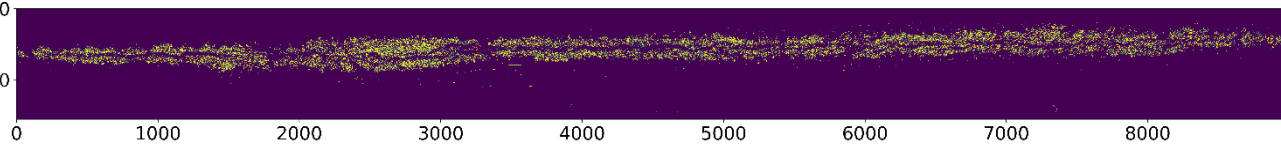
Figure D.2: 10 mm spread tow microstructure

SPREAD TOW – 12.5 mm

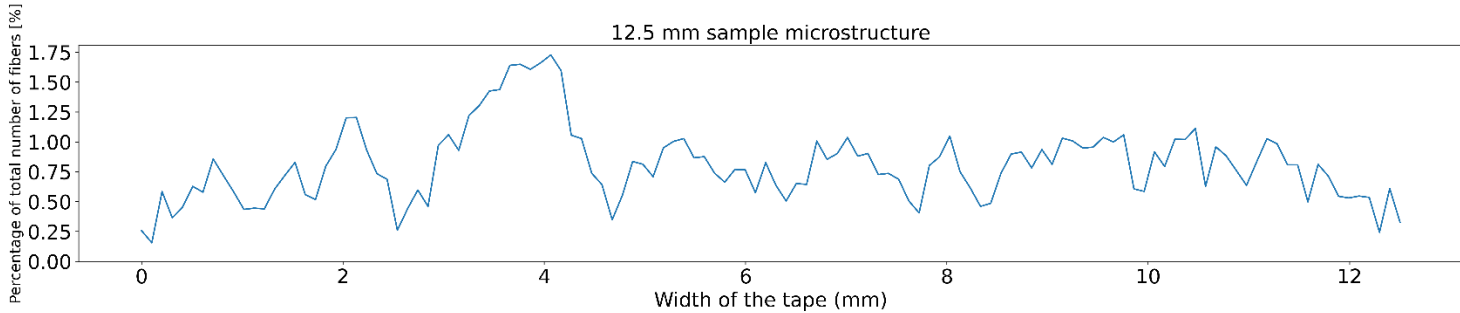
Original image



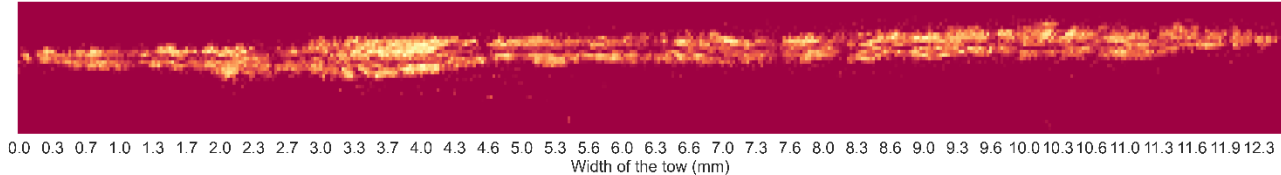
Threshold image



Fibre distribution plot



Fibre volume content heatmap



Fibre volume content histogram

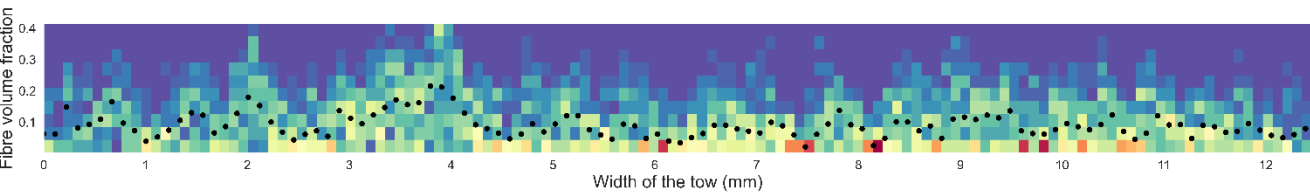
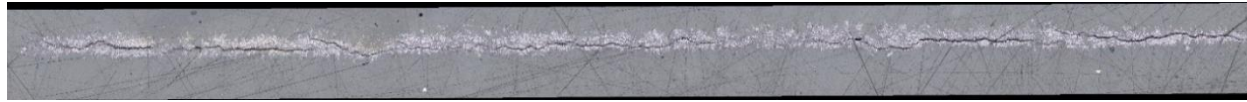


Figure D.3: 12.5 mm spread tow microstructure

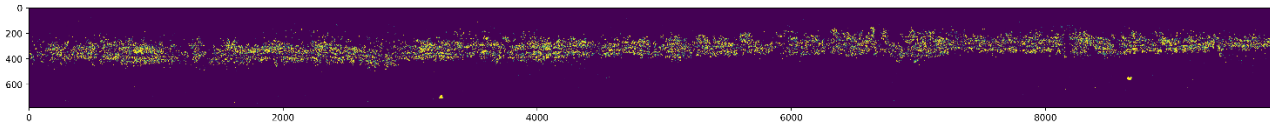


SPREAD TOW – 13.5 mm

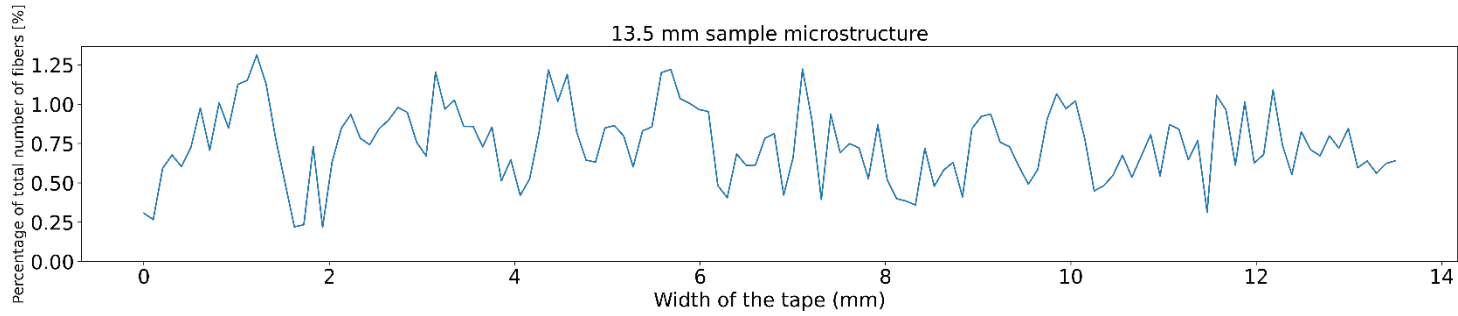
Original image



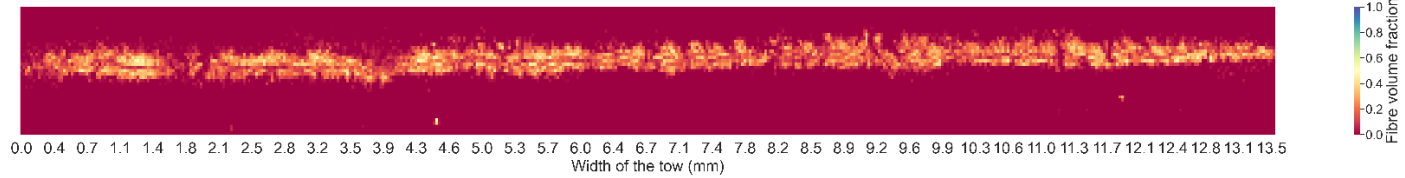
Threshold image



Fibre distribution plot



Fibre volume content heatmap



Fibre volume content histogram

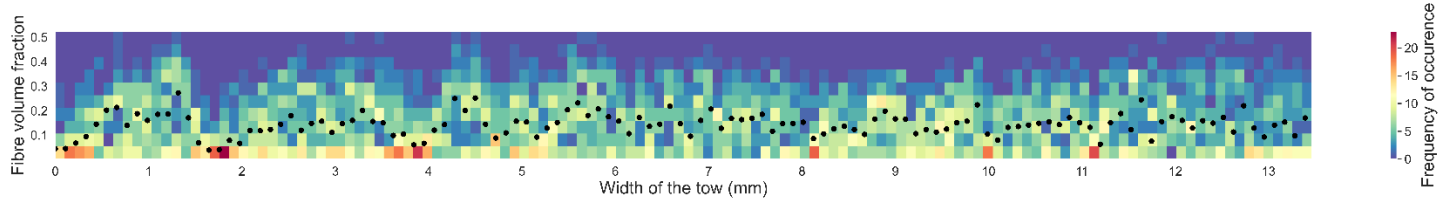
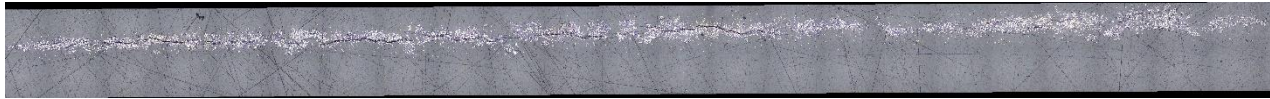


Figure D.4: 13.5 mm spread tow microstructure

Spread tow – 14.2 mm

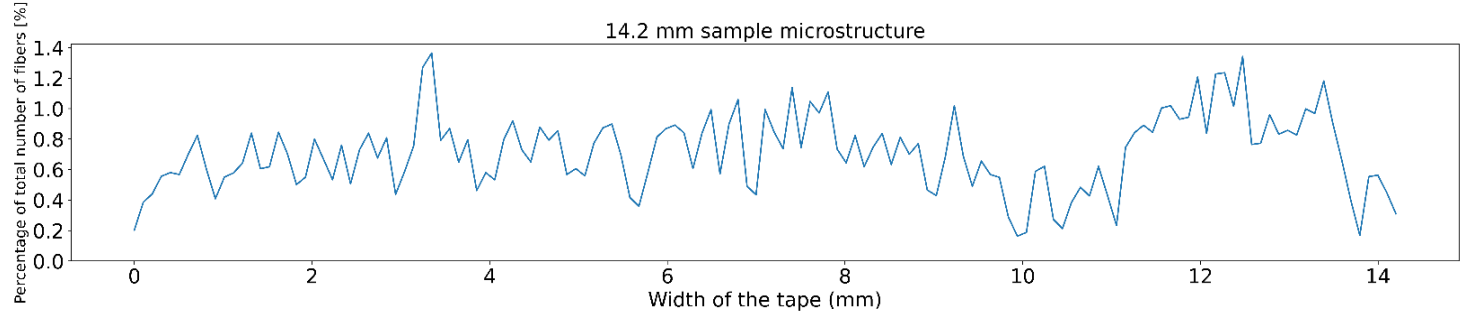
Original image



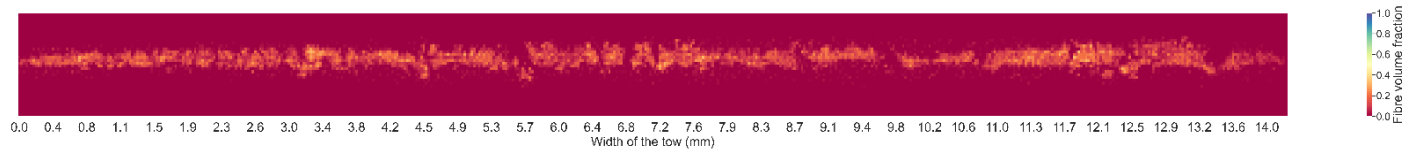
Threshold image



Fibre distribution plot



Fibre volume content heatmap



Fibre volume content histogram

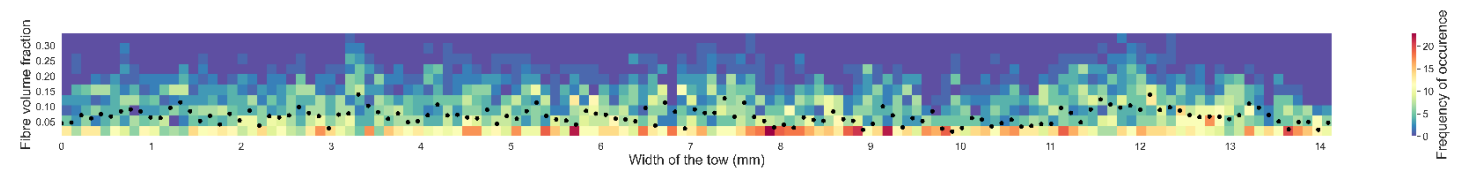


Figure D.5: 14.2 mm spread tow microstructure

## E. POST-PROCESSING CODES IN PYTHON

---

This appendix presents the python codes written for processing the data and images acquired during this research. The first code analyses the image of spread tow over the 5<sup>th</sup> spreader bar and generates the RGB values for it. This information is then used by the second code to recognise the shifts in colours and by extension the shifts in objects in the image which outputs an array of pixels representing the spread tow. This array is then used to calculate the width of the tow. It is followed by a code to calculate the fibre distribution along the width of the tow from an image of the microstructure sample. Lastly, the final code plots the heatmap and histograms of fibre volume fraction over the cross-section of the tow in the microstructural images.

### Colour recognition code for spread width on 5<sup>th</sup> bar

```
from PIL import Image

width = 0
height = 0
maxval = 0

#Reads image file and store RGB values in a 2-d array

def readImage(filename):
    img = Image.open(filename, 'r')
    w, h = img.size
    pix = list(img.getdata())
    return [pix[n:n+w] for n in range(0, w*h, w)]

# The following code uses the data from the above function.
# Establishes a 5x5 kernal
# This kernal sweeps the complete image, analysing the central pixel and
the ones around it.

def multiply(pixel, kernel, i, j):
    R = 0
    G = 0
    B = 0
    if i<2 or j<2 or i>=height-2 or j>=width-2:
        R = int(pixel[i][j][0])
        G = int(pixel[i][j][1])
        B = int(pixel[i][j][2])
    else:
        R = (
```

```

    pixel[i-2][j-2][0] * kernel[0][0] + pixel[i-2][j -1][0] *
kernel[0][1] + pixel[i-2][j ][0] * kernel[0][2] + pixel[i-2][j+1][0] *
kernel[0][3] + pixel[i-2][j+2][0] * kernel[0][4] +
    pixel[i-1][j-2][0] * kernel[1][0] + pixel[i-1][j -1][0] *
kernel[1][1] + pixel[i-1][j ][0] * kernel[1][2] + pixel[i-1][j+1][0] *
kernel[1][3] + pixel[i-1][j+2][0] * kernel[1][4] +
    pixel[i ][j-2][0] * kernel[2][0] + pixel[i ][j -1][0] *
kernel[2][1] + pixel[i ][j ][0] * kernel[2][2] + pixel[i ][j+1][0] *
kernel[2][3] + pixel[i ][j+2][0] * kernel[2][4] +
    pixel[i+1][j-2][0] * kernel[3][0] + pixel[i+1][j -1][0] *
kernel[3][1] + pixel[i+1][j ][0] * kernel[3][2] + pixel[i+1][j+1][0] *
kernel[3][3] + pixel[i-2][j+2][0] * kernel[3][4] +
    pixel[i+2][j-2][0] * kernel[4][0] + pixel[i+2][j -1][0] *
kernel[4][1] + pixel[i+2][j ][0] * kernel[4][2] + pixel[i+2][j+1][0] *
kernel[4][3] + pixel[i-2][j+2][0] * kernel[4][4]
)

```

```

G = (
    pixel[i-2][j-2][1] * kernel[0][0] + pixel[i-2][j -1][1] *
kernel[0][1] + pixel[i-2][j ][1] * kernel[0][2] + pixel[i-2][j+1][1] *
kernel[0][3] + pixel[i-2][j+2][1] * kernel[0][4] +
    pixel[i-1][j-2][1] * kernel[1][0] + pixel[i-1][j -1][1] *
kernel[1][1] + pixel[i-1][j ][1] * kernel[1][2] + pixel[i-1][j+1][1] *
kernel[1][3] + pixel[i-1][j+2][1] * kernel[1][4] +
    pixel[i ][j-2][1] * kernel[2][0] + pixel[i ][j -1][1] *
kernel[2][1] + pixel[i ][j ][1] * kernel[2][2] + pixel[i ][j+1][1] *
kernel[2][3] + pixel[i ][j+2][1] * kernel[2][4] +
    pixel[i+1][j-2][1] * kernel[3][0] + pixel[i+1][j -1][1] *
kernel[3][1] + pixel[i+1][j ][1] * kernel[3][2] + pixel[i+1][j+1][1] *
kernel[3][3] + pixel[i+1][j+2][1] * kernel[3][4] +
    pixel[i+2][j-2][1] * kernel[4][0] + pixel[i+2][j -1][1] *
kernel[4][1] + pixel[i+2][j ][1] * kernel[4][2] + pixel[i+2][j+1][1] *
kernel[4][3] + pixel[i+2][j+2][1] * kernel[4][4]
)

```

```

B = (
    pixel[i-2][j-1][2] * kernel[0][0] + pixel[i-2][j ][2] *
kernel[0][1] + pixel[i-2][j+1][2] * kernel[0][2] + pixel[i-2][j+1][2] *
kernel[0][3] + pixel[i-2][j+2][2] * kernel[0][4] +
    pixel[i-1][j-1][2] * kernel[1][0] + pixel[i-1][j ][2] *
kernel[1][1] + pixel[i-1][j+1][2] * kernel[1][2] + pixel[i-1][j+1][2] *
kernel[1][3] + pixel[i-1][j+2][2] * kernel[1][4] +
    pixel[i ][j-1][2] * kernel[2][0] + pixel[i ][j ][2] *
kernel[2][1] + pixel[i ][j+1][2] * kernel[2][2] + pixel[i ][j+1][2] *
kernel[2][3] + pixel[i ][j+2][2] * kernel[2][4] +

```

```

        pixel[i+1][j-1][2] * kernel[3][0] + pixel[i+1][j ][2] *
kernel[3][1] + pixel[i+1][j+1][2] * kernel[3][2] + pixel[i+1][j+1][2] *
kernel[3][3] + pixel[i+1][j+2][2] * kernel[3][4] +
        pixel[i+2][j-1][2] * kernel[4][0] + pixel[i+2][j ][2] *
kernel[4][1] + pixel[i+2][j+1][2] * kernel[4][2] + pixel[i+2][j+1][2] *
kernel[4][3] + pixel[i+2][j+2][2] * kernel[4][4]
    )

```

```

# if <0, then 0
R = int(R*(R>0))
G = int(G*(G>0))
B = int(B*(B>0))

```

```

R = R if R<256 else 255
G = G if G<256 else 255
B = B if B<256 else 255

```

```

# if >255, then 255
if R<0 or R>255 or G<0 or G>255 or B<0 or B>255:
    print(R, G, B)
return (R,G,B)

```

```

#=====

```

```

#The following function outputs an image in a JPEG format.

```

```

def writeImage(image_out,filename):

    #Array to store pixel values
    pix = []
    height = len(image_out)
    width = len(image_out[0])

    # Write pixel values to the array
    for i in range(height):
        for j in range(width):
            pix += [(image_out[i][j][0], image_out[i][j][1],
image_out[i][j][2])]

    outputIm = Image.new("RGB", (width, height))
    outputIm.putdata(pix)
    outputIm.save(filename, "JPEG")

```

## Spread width on 5<sup>th</sup> bar calculator

```
import cv2
import numpy as np
from PIL import Image, ImageEnhance
from images_fcp import *
import os
import glob

#=====
# The Function widthfinder accepts an image as a parameter and calculates
# the width of the tape in mm.
# This function works on the basis of colour recognition.
# It calculates the length of the tape in pixels.
# It calculates the width of a reference object, in this case a blue
block.
# The size of the reference object is known.
# Using ratio and proportion, the size of the tape is determined.
# The exposure and contrast of the image change the threshold defined in
the
# code below.
# This function requires a customised library called images_kernel.
#=====

def widthfinder(im):

    a = im
    w = len(a[0])
    # width - number of pixels in a row
    h = len(a)
    # height - number of pixels in a column

    pos = [0,0,0,0]
    # pos- position of [A, B, A', B']

#=====
# A - transition of silver to blue, the starting point of the block.
# B - transition of blue to silver, the ending point of the block.
# A' - transition of grey to black, the starting point of the tape.
# B' - transition of black to grey, the starting point of the tape.
#=====

# The for loop below is to establish X
# This runs from red to silver and finds the transition.
for i in range(1,int(h/2)):
    x = (a[i][int(w/4)])
```

```

    y = (a[i-1][int(w/4)])
# x and y define the point of transition.
    if ( x[0] < 100):
        if (y[0] >= 100):
            pos[0] = i

# The for loop below is to establish X'
for i in range(1, h):
    x = (a[i][int(w/4)])
    y = (a[i - 1][int(w/4)])
# x and y define the point of transition.
    if ( x[0] >= 100):
        if (y[0] <= 100):
            pos[1] = i

mid = int((pos[0] + pos[1])/2)
mid = mid - int(mid/10)

# This is to establish A
for i in range(1,w):
    x = (a[mid][i])
    y = (a[mid][i-1])
# x and y define the point of transition.
    if ( x[0] <= 25):
        if (y[0] >= 25):
            pos[0] = i
            break

# The for loop below is to establish B
for i in range(1, int(w/2)):
    x = (a[mid][i])
    y = (a[mid][i-1])
# x and y define the point of transition.
    if ( x[0] >= 25):
        if (y[0] <= 25):
            pos[1] = i
            break

temp = pos[1]

# The for loop below is to establish A'
for i in range(temp,w):
    x = (a[mid][i])
    y = (a[mid][i-1])
# x and y define the point of transition
    if ( x[1] <= 20):
        if (y[1] >= 20):

```

```

        pos[2] = i
        break

# The for loop below is to establish B'
for i in range(temp, w):
    x = (a[mid][i])
    y = (a[mid][i-1])
# x and y define the point of transition.
    if ( x[1] >= 20):
        if (y[1] <= 20):
            pos[3] = i

# Size of the tape detected in pixels

tape_size = pos[3] - pos[2]

# Size of the blue reference block in pixels

block_size = pos[1] - pos[0]

# Size of the blue reference block in mm

true_block = 13

# Width of the spread tow

spread = (tape_size * true_block ) / block_size

return spread

# Importing images for width detection

img_dir = "..." # Enter Directory of all images
data_path = os.path.join(img_dir, '*png')
files = glob.glob(data_path)
data = []

for f1 in files:
    im = readImage(f1)
    print(f1, data.append(widthfinder(im)) )
print(data)
im1 = readImage("(...).png")

```



## Fibre distribution along width – Microstructural images

```
import numpy as np
import cv2
import matplotlib.pyplot as plt
import seaborn as sns

#=====
# The code converts an image into a binary colour image representing
# fibres and matrix
# The image is split into vertical columns based on step size
# Pixels representing fibres are detected in each column
# Pixels in each column are compared to the total number of pixels
# representing fibres
# Fibre distribution along the width is represented through plots
#=====

# Detecting first fibre in image

def first_fiber(pic):
    pic = np.divide(pic, 255)
    check = True
    i = 0
    while check == True:
        if np.sum(pic[:, i]) > 10:
            check = False
            print(i, np.sum(pic[:, i]))
        else:
            i = i+1
            # print(i, np.sum(pic[:, i]))
    return(i)

# Detecting last fibre in image

def last_fiber(pic):
    pic = np.divide(pic, 255)
    check = True
    i = 0
    while check == True:
        if np.sum(pic[:, -i]) > 10:
            check = False
            print(i, np.sum(pic[:, -i]))
        else:
            i = i+1
    return(i)
```

```

tape_width = 8 # Enter width of tape
step_size = 0.1 # step size for calculation (decides size of column for
analysis)
N_blocks = int((tape_width-tape_width % step_size)/step_size) #Number of
blocks in image

# Import microstructure image

image = cv2.imread("sample 1.png")
images = cv2.cvtColor(image, cv2.COLOR_BGR2GRAY)

# Convert image into threshold binary image

_, thrash = cv2.threshold(images, 200, 255, cv2.THRESH_BINARY)

# Crop image from first to last fibre

ff = first_fiber(thrash)
lf = -last_fiber(thrash)

thrash = thrash[:, ff:lf]

column_width = int(np.shape(thrash)[1]/N_blocks)-1

[N, M] = np.shape(thrash)

thrash = thrash[:, :M-M % column_width]

thrash = thrash/255

vals = np.zeros((N_blocks))

# Detecting number of pixels representing fibres in each block across
width

for i in range(N_blocks):
    vals[i] = np.sum(thrash[:, column_width*i:column_width*(i+1)-1])

x_axis = np.linspace(0,tape_width, N_blocks)

#=====

# Plotting fibre distribution across width of tow

vals = 100*vals/np.sum(vals)
plt.figure(figsize=(25, 4), dpi=500)
x=np.linspace(-7.2,7.2,N_blocks)

```

```
plt.plot(x, vals)
plt.ylim(0)
plt.ylabel("Percentage of total number of fibers [%]", fontsize=15)
plt.xlabel("Width of the tape (mm)", fontsize=20)
plt.yticks(fontsize=20)
plt.xticks(fontsize=20)
plt.title('14.2 mm sample microstructure', fontsize=20)
plt.show()
```

```
# Displaying threshold image
```

```
plt.figure(figsize = (25,4),dpi=500)
plt.imshow(thrash)
plt.yticks([])
plt.xticks([])
plt.show()
```

## Heatmaps and histograms for fibre volume fraction – Microstructural image

```
import numpy as np
import cv2
import matplotlib.pyplot as plt
import seaborn as sns; sns.set_theme()

#=====
# The code converts an image into a binary colour image representing
# fibres and matrix
# The image is split into squared blocks based on step size
# Pixels representing fibres are detected in each block
# Fibre volume content is calculated for each block
# Heatmaps are plotted for the fibre volume content
# Corresponding histograms are plotted representing the fibre volume
# content and
# Frequency of occurrence
#=====

def to_matrix(l, n):
    return [l[i:i + n] for i in xrange(0, len(l), n)]

# Import microstructure image

image = cv2.imread("sample 2_crop.png", cv2.IMREAD_UNCHANGED)
print('Original Dimensions : ', image.shape)
AR = float(image.shape[1]) / image.shape[0]
print(AR)

images = cv2.cvtColor(image, cv2.COLOR_BGR2GRAY)

picturewidth = 10 # enter the width of the tape

samplesize = 20 # step size to split image into pixel blocks

# Splitting image by step size in x and y direction

yrange = int((image.shape[0] - image.shape[0] % samplesize) / samplesize)
xrange = int((image.shape[1] - image.shape[1] % samplesize) / samplesize)

test = np.empty((xrange,yrange))
histo_x = []
histo_y = []

# Number of pixels in 1 mm
```

```

px_per_mm = image.shape[1] / picturewidth

# Step size/ sample size in mm

sample_in_mm = samplesize / px_per_mm

print(xrange, px_per_mm, sample_in_mm)

i = 0
for y in range(yrange):
    for x in range(xrange):

        img =
images[y*samplesize:(y+1)*samplesize,x*samplesize:(x+1)*samplesize]
    _, thresh = cv2.threshold(img, 240, 255, cv2.THRESH_BINARY)

# Converting image into threshold binary image

    fibre = np.count_nonzero(thresh == 255)

# Finding pixels representing fibres

    matrix = thresh.size - fibre #finding pixels representing matrix
    Vf = fibre/thresh.size #fibre volume fraction
    kernal = np.ones((1,1),np.uint8);
    dilation = cv2.dilate(thresh, kernal, iterations=1)
    contours, hierarchy = cv2.findContours(dilation,
cv2.RETR_EXTERNAL, cv2.CHAIN_APPROX_SIMPLE)
    objects = str(len(contours))
    if Vf != 0:
        histo_x.append(x*sample_in_mm)
#Histogram for fibre content in x direction

        histo_y.append(Vf)
#Histogram for fibre content in y direction

        i = i + 1
        test[x,y] = Vf #array containing heatmap values

o = np.ma.masked_where(test == 0, test)
mediantrend = np.ma.median(o.T, axis=0).filled(0)

#median values of fibre volume content across width

#=====

```

```

# Heatmap plot based on step size

xticks =np.round(np.linspace(0,10,725),decimals=1)
plt.figure(figsize= (11.684*3,3),dpi=500)

# Heatmap plot function
ax = sns.heatmap(test.T, xticklabels=xticks,vmin = 0, vmax =
1,cmap='Spectral',cbar_kws={'label': 'Fibre volume fraction'})
ax.figure.axes[-1].yaxis.label.set_size(20)
ax.locator_params(nbins=40, axis='x')
ax.set_xticklabels(xticks, rotation = 0, fontsize=20)
ax.set_yticklabels([])
cbar = ax.collections[0].colorbar
cbar.ax.tick_params(labelsize=16, pad=1)
plt.xlabel('Width of the tow (mm)', fontsize=20)
plt.show()

#=====

# Corresponding histogram plot

x= np.arange(0,11,1)
fig = plt.figure(figsize=(11.684*3,3),dpi=500)
ax = fig.add_subplot(1, 1, 1)
m = ax.hist2d(histo_x,histo_y, bins=(130,10), cmap = 'Spectral_r' )
#histogram plot function

cbar = fig.colorbar(m[3], ax=ax)
cbar.ax.set_ylabel('Frequency of occurrence')
cbar.ax.tick_params(labelsize=16)
ax.figure.axes[-1].yaxis.label.set_size(22)
plt.xticks(x, fontsize = 16)
plt.yticks(fontsize = 16)
mediantrend = mediantrend[0:520]
x1 = np.linspace(0,10,130)
mediantrend = np.mean(mediantrend.reshape(-1, 4), axis=1)
plt.scatter(x1,mediantrend, color = 'black')
plt.xlabel('Width of the tow (mm)', fontsize=22)
plt.ylabel('Fibre volume fraction', fontsize=22)
plt.show()

```

## F. RAW DATA AND PROCESSING FILES

---

Raw data, post-processing files, LabVIEW programs, microscopic images electronically submitted to *Aerospace Manufacturing Technologies group, TU Delft*.

- [1] Y. K. Kumar and D. S. Lohchab, "Influence of Aviation Fuel on Mechanical properties of Glass Fiber-Reinforced Plastic Composite," *International Advanced Research Journal in Science, Engineering and Technology*, vol. 3, no. 4, 2016.
- [2] J. L. & V. M. A. Thomason, "Influence of fibre length and concentration on the properties of glass fibre-reinforced polypropylene: 1. Tensile and flexural modulus," *Composites Part A: Applied Science and Manufacturing*, pp. 27(6), 477–484. , 1996.
- [3] K. Friedrich and A. A. Almajid, "Manufacturing Aspects of Advanced Polymer Composites for Automotive Applications," *Applied Composite Materials*, p. 107–128, 2012.
- [4] IZUMI International. *Composite Manufacturing: Lab & Pilot Line Equipment: Mechanical Fiber Spreader*.
- [5] H. M. El-Dessouky and C. A. Lawrence, "Ultra-lightweight carbon fibre/thermoplastic composite material using spread tow technology," *Composites Part B: Engineering*, pp. 91-97, 2013.
- [6] R. Y. Kim and S. R. Soni, "Experimental and analytical studies on the onset of delamination in laminated composites," *Journal of composite materials*, pp. 70-80, 1984.
- [7] S. Shin, S. R. Soni, K. Kawabe and S. W. Tsai, "Experimental studies of thin-ply laminated composites," *Composites science and technology*, pp. 996-1008, 2007.
- [8] T. Morii, M. Shimaba and M. Mogi, "Development of fiber tow spreading system and its application for thin fiber reinforced materials," in *The 19th International Conference on Composite Materials*, Montréal, 2013.
- [9] D. Gizik, C. Metzner, C. Weimer and P. Middendorf, "Spreading of heavy tow carbon fibres for the use in aircraft structures," in *ECCM17 - 17th European Conference on Composite Materials* , Munich, 2016.
- [10] H. M. El-Dessouky, "Spread tow technology for ultra lightweight CFRP composites: Potential and possibilities," *Advanced Composite Materials: Properties and Applications*, pp. 323-348, 2017.
- [11] T. Ames, R. L. Kenley, E. J. Powers, W. West, W. T. Wygand and B. R. Lomax, "Method and apparatus for making an absorbent composite". United States of America Patent US7,181,817 B2, 2007.



- [12] T.-S. Chung, H. Furst, Z. Gurion, P. E. McMahon, R. D. Orwoll and D. Palangio, "Process for preparing tapes from thermoplastic polymers and carbon fibres". United States of America Patent US4,588,538, 1986.
- [13] R. M. Baucom, J. J. Snoha and J. M. Marchello, "Process for application of powder particles to filamentary materials". United States of America Patent US5,057,338, 1991.
- [14] K. Kawabe and S. Tomoda, "Multi-filament split-yarn sheet and method and device for the manufacture thereof". Japan Patent US6,032,342, 2000.
- [15] C. G. Daniels, "Pneumatic spreading of filaments". United States of America Patent US3,795,944, 1974.
- [16] T. B. Sager, "Method and apparatus for separating monofilaments forming a strand". United States of America Patent US4,959,895, 1990.
- [17] D. Akase, H. Matsumae, T. Hanano and T. Sekido, "Method and apparatus for opening reinforcing fiber bundle and method of manufacturing prepreg". Japan Patent US6,094,791, 2000.
- [18] K. Yamamoto, K. Yamatsuta and Y. Abe, "Spreading fibre bundle". Japan Patent EP0.292,266, 1988.
- [19] K. Tanaka, H. Ohtani, H. Matsumae, S. Tsuji and D. Akase, "Production device and method for opened fibre bundle and prepreg production method". Japan Patent US6,743,392B2, 2004.
- [20] S. Iyer and L. T. Drzal, "Method and system for spreading a tow of fibers". United States of America Patent US5,042,122, 1991.
- [21] J. N. Hall, "Apparatus for spreading a graphite fiber tow into a ribbon of graphite filaments". United States of America Patent US3,704,485, 1972.
- [22] G. Niina, Y. Sasaki and M. Takahashi, "Process for spreading and dividing textile materials". Japan Patent US3,358,436, 1967.
- [23] S. Uchiyama, E. Kaku, M. Kobayashi and T. Zoda, "Method and apparatus for spreading or dividing yarn, tow or the like". Japan Patent US3,657,871, 1972.
- [24] E. M. Sternberg, "Method and apparatus for charging a bundle of filaments". United States of America Patent US3,967,118, 1976.
- [25] J. M. Peritt, R. Everett and A. Edelstein, "Electrostatic fiber spreader including a corona discharge device". United States of America Patent 5200620, 1993.

- [26] M. S. Irfan, V. R. Machavaram, R. S. Mahendran, N. Shotton-Gale, C. F. Wait, M. A. Paget, M. Hudson and G. F. Fernando, "Lateral spreading of a fiber bundle via mechanical means," *Journal of composite materials*, pp. 311-330, 2012.
- [27] S. D. R. Wilson, "Lateral spreading of fibre tows," *Journal of engineering mathematics*, pp. 19-26, 1997.
- [28] R. W. Calkins, "Fiber impregnation process". United States of America Patent US4,994,303, 1991.
- [29] A. Davijani, "Experiments and prediction of the spreading behavior of fibrous tows by means of the Discrete Element Method," University of Twente, 2012.
- [30] R. C. Murray, "An investigation into fibre spreading (Unpublished master's thesis)," University of Birmingham.
- [31] J.-M. Guirman, B. Lecerf and A. Memphis, "Method and device for producing a textile web by spreading tows". France Patent US6,836,939B2, 2005.
- [32] N. Nakagawa and Y. Ohsora, "Fiber separator for producing fiber reinforced metallic or resin body". Japan Patent US5,101,542A, 1992.
- [33] R. Marissen, L. T. Van Der Drift and J. Sterk, "Technology for rapid impregnation of fibre bundles with a molten thermoplastic polymer.," *Composites Science and Technology*, pp. 2029-2034, 2000.
- [34] M. S. Irfan, V. R. Machavaram, R. C. Murray, F. N. Bogonez, C. F. Wait, S. D. Pandita, M. A. Paget, M. Hudson and G. Fernando, "The design and optimisation of a rig to enable the lateral spreading of fibre bundles," *Journal of Composite Materials*, pp. 1813-1831, 2014.
- [35] R. G. Krueger, "Apparatus and method for spreading fibrous tows into linear arrays of generally uniform density and products made thereby". United States of America Patent US6,311,377B1, 2001.
- [36] J. L. Lifke, L. D. Busselle and D. J. Finley, "Method and apparatus for spreading fibre bundles". United States of America Patent US006049956A, 2000.
- [37] G. Van Den Hoven, "Widening-Narrowing guide for textile filament bundle". Patent US4,301,579, 1981.
- [38] J. W. Jin, B. W. Jeon, C. W. Choi and K. W. (. Kang, "Multi-scale probabilistic analysis for the mechanical properties of plain weave carbon/epoxy composites using the homogenization technique," *Applied Sciences (Switzerland)*, pp. 1-14, 2020.

- [39] D. Hull and T. W. Clyne, *An introduction to composite materials.*, 2nd ed., Cambridge university press, 1996.
- [40] H. G. Howell and J. Mazur, "Amontons' law and fibre friction.," *Journal of the Textile Institute Transactions*, pp. T59-T69, 1953.
- [41] J. Y. Cai, J. McDonnell, C. Brackley, L. O'Brien, J. S. Church, K. Millington, S. Smith and N. Phair-Sorensen, "Polyacrylonitrile-based precursors and carbon fibers derived from advanced RAFT technology and conventional methods – The 1st comparative study," *Materials Today Communications*, pp. 22-29, 2016.
- [42] J. L. Thomason, "Glass fibre sizing: A review," *Composites Part A: Applied Science and Manufacturing*, vol. 127, 2019.
- [43] D. M. Mulvihill, O. Smerdova and M. P. F. Sutcliffe, "Friction of carbon fibre tows," *Composites Part A: Applied science and manufacturing*, pp. 185-198, 2017.
- [44] M. Suzuki, Y. Kubota and F. Hoshiai, "Mechanics of Fiber Entanglements," *Journal of the Textile Machinery Society of Japan*, pp. T678-T684, 1965.
- [45] D. Kastanis, H. Steiner, E. Fauster and R. Schledjewski, "Compaction behavior of continuous carbon fiber tows: an experimental analysis.," *Advanced Manufacturing: Polymer and Composites Science*, pp. 169-174, 2015.
- [46] M. Tonejc, H. Steiner, E. Fauster, S. Konstantopoulos and R. Schledjewski, "A study on geometrical parameters influencing the mechanical spreading of fibre bundles," *IICM International conferences on composite materials*, 2015.
- [47] D. Wiangyangkung, "The design and developement of a fibre tow spreading test setup," 2019.
- [48] "TEXMER GmbH & Co. KG," [Online]. Available: <https://www.texmer.de/>.
- [49] "Hans Schmidt & Co GmbH," [Online]. Available: <https://www.hans-schmidt.com/en/>.
- [50] Y. Kyosev, "Yarn winding operations in braiding," *Braiding Technology for Textiles*, p. 231–254, 2015.
- [51] B. Cornelissen, "The role of friction in tow mechanics," 2013.
- [52] N. D. Chakladar, P. Mandal and P. P, "Effects of inter-tow angle and tow size on carbon fibre friction," *Composites Part A: Applied Science and Manufacturing*, vol. 65, pp. 115-124, 2014.

- [53] "Reinforced plastic composites: Fibre sizing," Michelman, [Online]. Available: <https://www.michelman.com/markets/reinforced-plastic-composites/fiber->.
- [54] K. Mason, "Sizing Up Fiber Sizings," Composites World, 4 1 2006. [Online]. Available: <https://www.compositesworld.com/articles/sizing-up-fiber-sizings>. [Accessed 2 9 2021].
- [55] Prof. C. Dransfeld, TU Delft Aerospace Manufacturing Technologies research group.
- [56] S. M. Lee, Handbook of Composite Reinforcements, Wiley, 1996.